

**THERMODYNAMIC PROPERTIES OF HIGH TEMPERATURE
SUPERCONDUCTORS BASED ON THE t-J-d MODEL**

BY

RAPANDO WAKHU BERNARD

**A THESIS SUBMITTED TO THE SCHOOL OF SCIENCE IN PARTIAL
FULFILMENT OF THE REQUIREMENTS FOR THE DEGREE OF DOCTOR
OF PHILOSOPHY IN PHYSICS OF UNIVERSITY OF ELDORET, KENYA**

NOVEMBER, 2015

DECLARATION

Declaration by the candidate

This thesis is my original work and has not been presented for a degree in any other university. No part of this thesis may be reproduced without the prior written permission of the author and /or University of Eldoret.

RAPANDO WAKHU BERNARD

.....

Date.....

SC/PhD/P/002/12

Declaration by supervisors

This thesis has been submitted for examination with our approval as University Supervisors.

.....

Date.....

**Prof. K. M. Khanna,
University of Eldoret, Kenya**

.....

Date.....

**Prof. J. K. Tonui,
University of Eldoret, Kenya**

DEDICATION

I dedicate this thesis to my wife, Grace. She was of great inspiration to me in the whole process of research and compilation of this thesis.

ABSTRACT

Many theories that attempt to describe the superconducting state have suffered significant failures, leaving the t-J model as the only model which effectively captures the physics of the strong correlations inherent in this problem. However, many aspects of this model are quite complex and the thermodynamic properties of the superconducting state need to be analyzed carefully. In this thesis, second quantization techniques involving Bogliubov-Valatin transformation have been used to diagonalize the t-J model Hamiltonian so that the thermodynamic properties of high temperature superconductors can be studied. Formulae for ground state energy, E_0 , specific heat, c_v , and entropy, s , of high temperature superconductors have been derived in the framework of the t-J model. Additionally, the superconducting dipole Hamiltonian has been diagonalized and the sum of the t-J and dipole Hamiltonians obtained resulting in what is now referred to as the 't-J-d model'. Transition temperature for LSCO in the t-J formalism is obtained as $T_c = 102.5K$ and $T_c = 103.98K$ in the t-J-d system. Transition temperature for YBCO in the t-J formalism is obtained as $T_c = 111.8K$ and $T_c = 113.2K$ in the t-J-d model. Both models predict T_c that is higher than the experimental value of 90K but remarkably close to the known values. Highest heat capacity of the superconducting state of the t-J model is found to be $4.7 \times 10^{-3} eV/K$ while the highest entropy value is $3.15 \times 10^{-3} eV/K$ for high- T_c superconductors. The total energy of the system increases exponentially with the temperature.

TABLE OF CONTENTS

DECLARATION	i
DEDICATION	ii
ABSTRACT.....	iii
LIST OF TABLES.....	vii
LIST OF FIGURES	viii
LIST OF ABBREVIATIONS AND SYMBOLS USED.....	ix
ACKNOWLEDGEMENT	x
CHAPTER ONE	1
INTRODUCTION	1
1.1 Introduction to Superconductivity	1
1.2 The superconducting state and the thermal transport properties.....	3
1.3 Characteristics of the superconducting state	5
1.4 Basic properties of the superconducting state.....	12
1.5 High Temperature superconductivity.....	14
1.6 Characteristics of high temperature superconductors	17
1.7 Room Temperature superconductivity.....	18
1.8 The t-J model for High – T_c Superconductors	20
1.9 The t-J model and the basic electronic structure of high- T_c superconductors.....	22
1.10 Electron-phonon interaction- The breathing and buckling modes.....	26
1.11 The role of Coulomb interaction and hopping in high- T_c superconductors.....	27
1.12 Electronic dipoles.....	27
1.13 Crystal-Field generated Electronic Dipoles	29
Dipolon created electron-electron pair correlations in superconductivity	30
1.14 Statement of the problem	31
Objectives of the study.....	32
1.15 General Objective	32
1.16 Specific Objectives	32
1.17 Rationale/justification	33
1.18 Importance of the study	33
CHAPTER TWO	36
LITERATURE REVIEW	36
2.1 Introduction.....	36

2.2 The t - J_p - U model.....	36
2.3 The density function Theory	37
2.4 Resonating Valence Bond Theory for High T_c superconductors (RVB – theory)	40
2.5 Effects of Higher Hopping Terms on the Stripe states in the Hubbard Model	42
2.6 Polaronic Mechanism of superconductivity in cuprates	43
2.7 Thermodynamic properties of small superconductors with fixed number of particles.....	44
2.8 Collective modes in the superconducting ground states	46
2.9 Spin liquid states near the Mott transition	46
2.10 Effect of chalcogenides on critical temperature.....	47
2.11 The t - J model and Monte-Carlo calculations	49
CHAPTER THREE	50
METHODOLOGY	50
3.1 Introduction.....	50
3.2 The t - J model	50
3.3 The t - J - d model	51
3.4 Generation of Data.....	51
3.5 Data presentation	51
3.6 Approximations and assumptions used.....	52
CHAPTER FOUR.....	53
THE DIAGONALIZED t - J HAMILTONIAN AND THE THERMODYNAMIC PROPERTIES OF HIGH- T_c SUPERCONDUCTORS.....	53
4.1 Introduction.....	53
4.2 The canonical transformation	56
4.3 Inverse transformation	59
4.4 Thermodynamic properties of high- T_c superconductors	78
CHAPTER FIVE	81
THE DIPOLE MEDIATED t - J MODEL OF HIGH- T_c SUPERCONDUCTIVITY: “THE t - J - d MODEL”	81
5.1 Introduction.....	81
5.2 Diagonalization of the dipole Hamiltonian.....	82
5.3 Thermodynamic properties of high- T_c superconductors in the t - J - d model.....	89
CHAPTER SIX.....	92
RESULTS AND DISCUSSION	92
6.1 Numerical evaluation of the ground state energy	92

6.2 Graphical analysis of system energy.....	95
6.3 Numerical evaluation of the transition temperature.....	97
6.4 Variation of Heat capacity, C_v with Temperature, T	102
6.5 Numerical C_v of the t-J and the t-J-d models	106
6.6 Variation of entropy, s with Temperature, T	106
6.7 Numerical entropy of the t-J and the t-J-d models.....	109
CHAPTER SEVEN	110
CONCLUSIONS AND RECOMMENDATIONS	110
7.1 CONCLUSIONS.....	110
7.2 RECOMMENDATIONS	111
REFERENCES	113
Appendix I: CHRONOLOGICAL GROWTH OF T_c IN SUPERCONDUCTORS	121
Appendix II: VARIATION OF HOPING INTEGRAL tpd WITH ON-SITE COULOMB REPULSION ENERGY, Ud FOR TRANSITIONS FROM P TO D LEVELS	122
Appendix III: DIPOLE STATISTICS IN CUPRATES.....	123
Appendix IV: TABLES OF RESULTS FOR THE t-J-d MODEL	124
Appendix V: PREDICTIVE POWER OF FT-VAP	126
Appendix VI: MATHCAD RESULTS	127
Appendix VII: CRITICAL TEMPERATURE AND TRANSFER ENERGY FOR T-J-D MODEL	133

LIST OF TABLES

Table		Page
1.0	Characteristics of some selected superconductors in	12
2.0	Some of the superconducting Cuprates	16
3.0	A summary of transfer energy values of the t-J system for various high- T_c superconducting cuprates	99
4.0	A summary of transfer energy values of the t-J-d system for various high- T_c superconducting cuprates	101

LIST OF FIGURES

Figure		Page
Figure 1.1	Schematic diagram showing penetration depth of a superconductor	7
Figure 1.2a	A diagram showing temperature dependence of type I superconductors	10
Figure 1.2b	A diagram showing the temperature dependence of type II superconductors	10
Figure 1.3	Meissner effect	13
Figure 1.4	Spin alignment and matrix elements in the t-J model	22
Figure 1.5a	Atomic arrangement in La_2CuO_4	23
Figure 1.5b	Atomic arrangement in Hg1223	23
Figure 1.6	The copper d and oxygen p orbitals in the hole picture	24
Figure 1.7a	Electronic dipole	28
Figure 1.7b	Polarized atom	28
Figure 2.1	Electronic structure of cuprates for a 2-dimensional copper layer for a one band model	38
Figure 2.2a	A cartoon representation of RVB liquid or singlets	41
Figure 2.2b	An electron removed from the plane	41
Figure 2.3	Structural lattice of $\text{Y}_1\text{Ba}_2\text{Cu}_3\text{O}_7$	48
Figure 6.1(a)	Variation of system energy with temperature for the t-J model	95
Figure 6.1 (b)	Variation of system energy with temperature for the t-J-d model	96
Figure 6.2 (a)	Variation of heat capacity with temperature of the t-J model	102
Figure 6.2 (b)	Variation of heat capacity with temperature of the t-J-d model	103
Figure 6.3	Evolution of specific heat with temperature obtained with FT-PAV	105
Figure 6.4 (a)	Variation of entropy with temperature for the t-J model	107
Figure 6.4 (b)	Variation of entropy with temperature for the t-J-d model	107

LIST OF ABBREVIATIONS AND SYMBOLS USED

Abbreviation/ symbol	Name
\hbar	Reduced Planck's constant
h_p	Holes in the copper-oxygen bonds
θ_D	Debye temperature
$\langle \omega \rangle$	Average phonon frequency
C_{es}	Electronic specific heat
η	Electron-phonon coupling strength
BCS	Berdeen-Cooper-Schrieffer
Bi2201	Bismuth-Strontium-Copper-Oxide
FT-PAV	Finite Temperature Projection After Variation
FT-VAP	Finite Temperature Variation After Projection
H	Dipole interaction energy
H_c	Critical magnetic field
Hg1223	Mercury-Barium-Calcium-Copper-Oxide
HTS	High temperature superconductors
J	Exchange energy
LSCO	Lanthanum-Strontium-Copper-Oxide
T	Hopping energy
T_c	Transition/Critical temperature
t-J model	Model based on electron hopping and exchange energy
t-J-d model	Model based on electron hopping, exchange & dipole energy
Tl2212	Thallium-Barium-Calcium-Copper-Oxide
U	On-site Coulomb energy
YBCO	Yttrium-Barium-Copper-Oxide

ACKNOWLEDGEMENT

Quote: Christ is the mystery of God in whom are hidden all the treasures of wisdom and knowledge-Col 2:3.

My first gratitude goes to the Almighty God who is the very source of all knowledge-revealed and yet to be revealed. He gave me divine understanding and health that I desperately needed in the research period. My first supervisor, Prof. K.M Khanna is a man to whom I owe a lot not only for the success of this work but also in my academic life. He is selfless, kind and pure in the heart, a man dedicated to serving humanity. He has taught me to be humble even as I climbed my academic ladder right from undergraduate level to PhD. He facilitated the acquisition of most of the research papers I used in this research. May God bless him with long life and good health.

My second supervisor, Prof. J.K Tonui was a great inspiration to me. With his busy schedule as the head of department of physics, University of Eldoret, he spared time to guide me in every step I took in this research. I pray that he prospers in all his endeavors. The University of Eldoret at which this research was conducted deserves accolades. The conducive academic environment and the professionalism by which I was handled as a PhD student led to the success of this work in the minimum possible time.

Finally, I wish to appreciate the contribution of my friends, Dr. Mugambi of Karatina University and Ms. Sarai Antoinette of Masinde Muliro University of Science and Technology. They lend me their computers that could handle the softwares that were used in the analysis of my work. May God bless them

CHAPTER ONE

INTRODUCTION

1.1 Introduction to Superconductivity

Superconductivity is the disappearance of d.c electrical resistance of a conductor when the conductor is cooled to a certain characteristic temperature called critical temperature, T_c . It was discovered in 1911 by Onnes Kamerlingh (Kamerlingh, 1911) who worked on mercury at very low temperatures using Helium as a refrigerant (Andrei, 2004). At the temperature of 4.2K, the electrical resistance of mercury abruptly disappeared and mercury became a superconductor.

This phenomenon was not well understood until 1957 when an acceptable microscopic theory (Bardeen, *et al.*, 1957) based on the concept of pairing of electrons of opposite spins and momenta near the Fermi surface was given by Bardeen, Cooper and Schriffer. The theory was named after the three scientists as Bardeen-Cooper-Schriffer theory (BCS theory). In this theory, superconductivity was explained as a phenomenon which originates from the effective interaction between a pair of electrons called Cooper pair. The pair of electrons exchange a phonon through virtual means leading to a virtual attraction between them, specifically when the energy difference between the electronic states involved $\Delta\varepsilon$ is less than the phonon energy, $\hbar\omega$. The strength of this electron – phonon interaction is maximum when the electrons are in the states of equal and opposite momenta and spins. The importance of the role played by electron-phonon interaction was emphasized by the discovery of the fact that the critical temperature of the transition

from normal to the superconducting state depends on isotopic mass. In 1950, *H. Fröhlich* (Fröhlich, 1950) proposed that vibrating atoms of a material play an important role causing it to superconduct. Following his proposal, the isotope effect was introduced by E. Maxwell and C.A Raynolds. They studied different superconducting isotopes of mercury and established a relationship between the critical temperature, T_c and the isotope mass, M as;

$$T_c M^{\frac{1}{2}} = \text{constant} \quad (1.0)$$

This pointed to the understanding that the superconducting transition must be involving some kind of interaction with the crystal lattice.

Superconducting state is described as a diamagnetic state. In 1933, W. Meissner and R.Ochsenfeld (Meissner, 1933) discovered that superconductors exhibit one fundamental property called perfect diamagnetism. They found that magnetic flux is expelled from the interior of the sample that is cooled below its critical temperature in weak external magnetic field, a phenomenon called Meissner effect. The relationship between the magnetic flux B and the magnetic field H (Qiang, *et al.*, 1992) is given by;

$$B = H(1 + 4\pi\chi) \quad (1.1)$$

where $\chi = \frac{M}{H}$ is magnetic susceptibility and M is magnetic intensity. When $B=0$, magnetic susceptibility is negative ($\chi = -\frac{1}{4\pi}$), a condition for diamagnetism.

Similarly, electric field, E inside the superconductor is expected to be zero. In 1935, two brothers, F. London and H. London came up with two equations which govern the microscopic electric and magnetic fields in the superconductor. The London equations explained Meissner effect and also provided an expression for the first characteristic

length of superconductivity called the London penetration depth, λ_L . When the superconductor is cooled to temperatures below the critical temperature, current density, J is found to be very large as the conductivity σ approaches infinity. From the relation;

$$\sigma = \frac{J}{E} \quad (1.2)$$

it is very clear that for infinite σ , the electric field, E must be equal to zero, thus we expect the exclusion of electric field from the inside of a superconductor. We further note that for infinite current flow, Maxwell's relation stipulate that the rate of change of magnetic flux must be equal to zero, i.e;

$$\frac{\partial B}{\partial t} = (-c)\nabla \times E = 0 \quad (1.3)$$

Eq. (1.3) implies that B is constant inside the material. This constant, according to Meissner is zero. In 1950, V. Ginzburg and L. Landau proposed an intuitive theory of superconductivity called the Ginzburg-Landau theory which helped in understanding the behavior of superconductors in strong magnetic fields. The theory confirmed the London equations and provided an expression for the second characteristic length, called the Ginzburg-landau coherence length, ξ_{GL} .

1.2 The superconducting state and the thermal transport properties

The onset of the superconducting state is accompanied by drastic changes in the thermodynamic equilibrium and thermal transport properties of a superconductor. The heat capacity of a normal conductor is determined by the normal electrons with a small contribution from the thermal vibrations of the crystal lattice and is nearly proportional to the temperature. At the transition temperature, there appears a discontinuity in heat capacity which then decreases more rapidly with decreasing temperature. At temperatures well below critical temperature, heat capacity varies exponentially as $\exp(-\frac{\Delta}{kT})$ where Δ

is the energy gap and k is Boltzmann constant. Such exponential temperature dependence is a hallmark of a system with an energy gap in the spectrum of allowed energy states.

The thermal conductivity of a superconductor is less than that of the normal conductor and approaches zero at very low temperatures. This is because the transport of heat requires transport of disorder or entropy and the superconducting state being one of perfect order or zero entropy we expect very low or no thermal conductivity.

Most of the superconducting electrons are located either on the Fermi surface or very close to the Fermi surface (Bardeen et al, 1957). This is because the Fermi energy is much larger than the phonon energy and two electrons deep inside the Fermi sea cannot form a Cooper pair as they are constrained by Pauli Exclusion Principle. When these electrons are on or close to the Fermi surface they form a bound pair as phonon energy here is now larger.

To obtain the superconducting state of the conventional superconductors, liquid helium 4, which is costly, has to be used. For this reason large scale production of superconducting materials becomes too expensive. A great breakthrough was realized in 1986 when high temperature superconductivity was discovered in La-Ba-Cu-O. This will be discussed later in this thesis. Research is still on-going to discover materials with transition temperature greater than 77K which is the temperature at which liquid nitrogen can be used as a coolant. Liquid nitrogen is much cheaper than helium 4.

1.3 Characteristics of the superconducting state

The features discussed below characterize the superconducting state of high- T_c superconductors. They describe why superconducting state occurs and what causes it (Andrei, 2004).

i. Critical temperature

This is the temperature at which the second order phase transition from normal into the superconducting state occurs. Critical temperature is a macroscopic quantity and at the time of this research there is no consensus on the rule for predicting critical temperature in high temperature superconductors.

ii. Cooper pair wave function

In quantum mechanics, any particle is characterized by a wave function. Similarly, a Cooper pair is also characterized by a wave function $\psi(r_1-r_2)$ where r_1, r_2 are the positions of the electrons in the real space. The attraction between two electrons in a superconductor leads to the coupling of the pair forming a composite boson called Cooper pair. The wave function of this pair is a complex scalar having an amplitude and a phase. The probability to find a Cooper pair in real space is given by $\psi^*\psi$, where ψ^* is a complex conjugate of ψ .

iii. Order parameter ($\psi(r)$)

This is the wave function of the superconducting condensate. The superconducting state is characterized by a single wave function;

$$\psi(r) = \psi(r)e^{i\theta} \tag{1.4}$$

where θ is the phase. The order parameter has the following properties;

- a) It is a complex scalar which is continuous in real space.
 - b) It is a single-valued function.
 - c) In the absence of magnetic field, $\psi(r) \neq 0$ at $T < T_c$ and $\psi(r) = 0$ at $T \geq T_c$
 - d) $\psi(r) = 0$ outside the superconductor
 - e) It is usually normalized so that $|\psi(r)|^2$ gives the density of the Cooper pairs at point r .
 - f) In the momentum space, the variations of $|\psi(r)|$ are proportional to the energy gap, Δ
 - g) The phase of the order parameter is a periodic function in the real space. If the order parameter is known explicitly, then almost complete information about the superconducting condensate is known too.
- iv. Penetration depth, λ

This is a very thin layer from the surface of a superconductor in which surface current that sets up a magnetic field which cancels the applied field flows. It can also be defined as the length in which the applied magnetic field is exponentially screened from the interior of the superconducting sample. It was first predicted by the London brothers.

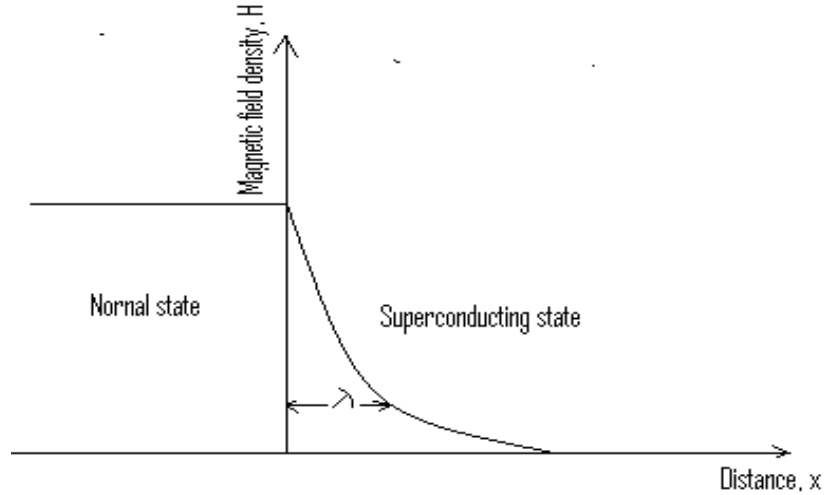


Fig.1.1: Schematic diagram showing penetration depth of a superconductor.

(Source: Andrei, 2004)

Penetration depth is temperature- dependent and it can be expressed in terms of critical temperature, T_c as;

$$\lambda(T) = \frac{\lambda(0)}{\left[1 - \left(\frac{T}{T_c}\right)^4\right]^{\frac{1}{2}}} \quad (1.5)$$

where $\lambda(0)$ is penetration depth at 0K and T is the temperature of the system. In metals the London penetration depth (Andrei, 2004) is $\lambda_L \approx 530 \text{ \AA}$.

v. Coherence length, ξ

This is the characteristic length or scale over which the variations of the order parameter occur in a spatially-varying magnetic field (Andrei, 2004). Coherence length defines variations of order parameter of the superconducting condensate and it is temperature-dependent. It was first predicted by Ginzburg and Landau. It diverges as temperature approaches critical temperature.

In conventional superconductors, at zero Kelvin temperature, the Ginzburg- Landau coherence length, ξ_{GL} , is equal to the size of the Cooper pair. In the framework of the BCS theory for conventional superconductors, coherence length determined by the energy gap at zero Kelvin temperature, $\Delta(T = 0)$, is called intrinsic coherence length, ξ_0 , and it can be expressed in terms of Fermi-velocity and reduced Planck's constant, \hbar as;

$$\xi_0 = \frac{\hbar v_F}{\pi \Delta(0)} \quad (1.6)$$

In metal superconductors the value of intrinsic coherence length is $\xi_0 = 3 \times 10^3 \text{Å}$.

In 'dirty' superconductors i.e. superconductors in which electron mean free path (approximate width of the path of the electron), ℓ , is much less than the intrinsic coherence length, the Ginzburg- Landau temperature dependence of coherence length at temperatures close to T_c is given by;

$$\xi_{GL}(T) = 0.85(\xi_0 \ell)^{\frac{1}{2}} \left(1 - \frac{T}{T_c}\right)^{-\frac{1}{2}} \quad (1.7)$$

vi. Type I and type II superconductors

Type I superconductors are those that expel magnetic flux completely from their interior while type II superconductors are those that expel magnetic flux completely only in a small magnetic field but partially in higher external fields. This is because the surface energy of the interface between the normal and the superconducting region is positive for type I superconductors and negative for type II superconductors.

The ratio of the penetration depth to the Ginsburg –Landau coherence length is called the Ginzburg-Landau parameter, κ . Hence;

$$\kappa = \frac{\lambda}{\xi_{GL}} \quad (1.8)$$

This parameter characterizes the superconducting material and allows one to distinguish between type I and type II superconductors. A superconductor is type I if $\kappa < \frac{1}{\sqrt{2}}$ and if $\kappa > \frac{1}{\sqrt{2}}$ then the superconductor is type II. In unconventional superconductors (most high- T_c superconductors), $\kappa \gg 1$ hence they are of type II. Most metallic superconductors are type I superconductors.

vii. Critical magnetic field, H_c

The superconducting state can be destroyed by applying sufficiently strong magnetic field. In type I superconductors, superconductivity is destroyed when the applied field reaches a single critical field value, H_c . For type II superconductors there are two critical fields (Qiang Du et al, 1992), the lower critical field, H_{c1} and the upper critical field H_{c2} . If the applied field is less than H_{c1} , the superconductor completely expels the field but at fields just above H_{c1} , flux begins to penetrate the superconductor in microscopic filaments called vortices which form a regular lattice surrounded by a superconducting region.

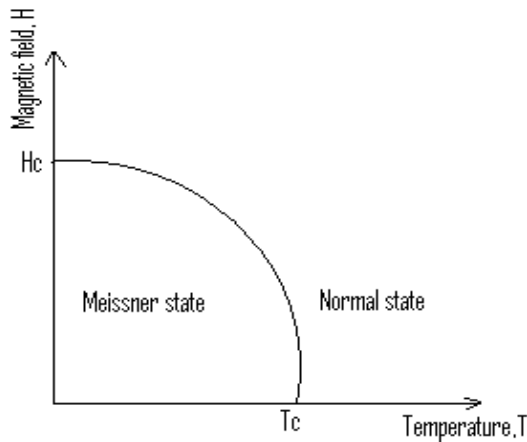


Figure 1.2a: A diagram showing temperature dependence of type I superconductors

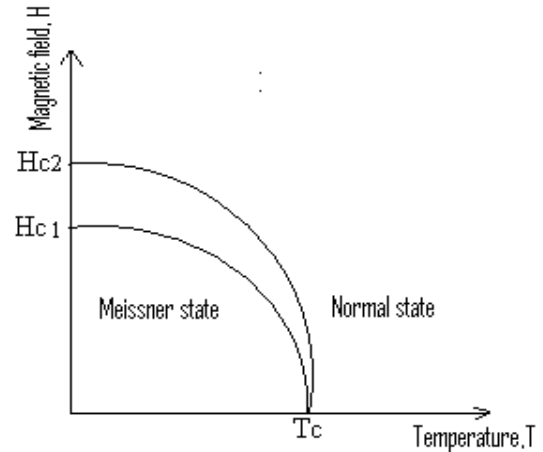


Figure 1.2b: A diagram showing temperature dependence of type II superconductors

i. Critical current, J_c

Superconductivity can also be destroyed by a d.c electrical current. The critical current, J_c is the maximum current that a superconductor can support. Above J_c , the current breaks the Cooper pairs and thus destroys the superconducting state. Thus, any superconductor is characterized by a critical d.c current density, j_c . At $T=0$ K, the critical current density can be estimated using the superfluid density, n_s , and the velocity of the Cooper pair V_c as; $j_c = n_s e V_c$. The maximum current density that can theoretically be sustained in a superconductor is of the order of $j_c \approx 10^6 \text{ A/cm}^2$.

ii. Energy scales

The superconducting state is characterized by a few energy scales namely; pairing energy gap, phase coherence gap, phases stiffness and condensation energy.

a. Pairing energy gap, $2\Delta_p$

The pairing energy gap measures the strength of the binding of the electrons or quasi-particles into the Cooper pairs. The value of this gap corresponds to the binding energy that holds the electrons together. The pairing energy gap is directly proportional to the pairing temperature such that;

$$2\Delta_p = k_B T_{pair} \quad (1.9)$$

b. Phase coherence energy gap, $2\Delta_c$

This is the condensation energy of a Cooper pair when the long-range phase coherence appears. Its magnitude is temperature dependent and it is highly anisotropic in high- T_c superconductors

c. Phase stiffness

This is the energy scale that measures the ability of the superconductor to carry a supercurrent.

d. Condensation energy

This is the free energy difference between the normal and the superconducting state given as;

$$F_n(T) - F_s(T) = \frac{8H_c^2(T)}{8\pi} \quad (1.10)$$

where symbols carry their usual meaning. The condensation energy in a conventional superconductor is of the order of $10^{-7} - 10^{-8} eV/atom$.

NB. Values of some of the characteristic features of high-temperature superconducting cuprates are given in the table 1.0;

Table 1.0: Characteristics of some selected superconductors(Source: Puri *et al.*, 2001)

YEAR	Critical Temp. T_c (K)	MATERIAL	CLASS	CRYSTAL STRUCTURE	TYPE	Critical field, H_c (MA/M)
1911	4.2	Hg	Metal	Tetragonal	I	0.033
1913	6.2	Pb	Metal	f.c.c	I	0.064
1930	9.25	Nb	Metal	b.c.c	II	0.164
1940	15	NbN	Interstitial Compound	NaCl	II	12.2
1950	17	V_3Si	Intermetallic Compound	B-Tungsten W_3O	II	12.4
1954	18	Nb_3Sn	Intermetallic Compound	W_3O	II	18.5
1960	10	Nb-Ti	Alloy	B.c.c	II	11.9
1964	0.7	$SrTiO_3$	Ceramic	Perovskite	II	Small
1970	20.7	$Nb_3(Al, Ge)$	Intermetallic	W_3O	II	34.0
1977	23	Nb_3Ge	Intermetallic	W_3O	II	29.6
1986	34	$La_{1.85}Ba_{0.15}CuO_4$	Ceramic	Tetragonal	II	43
1987	90	$YBa_2Cu_3O_7$	Ceramic	Orthorhombic	II	111
1988	108	Bicuprates	Ceramic	Orthorhombic	II	-
1988	125	Ticuprates	Ceramic	Orthorhombic	II	-

1.4 Basic properties of the superconducting state

The main basic properties of the superconducting state are; zero d.c electrical resistance, meissner effect, magnetic flux quantization and the Josephson effect.

a. Zero d.c electrical resistance

Every superconductor has zero resistivity or infinite conductivity (Timusk et al, 1996) for a small-amplitude direct current (d.c) at any temperature below T_c . In essence, the resistivity of a superconductor is smaller than $10^{-23}\Omega$ which is 18 times smaller than the resistivity of copper at room temperature. Such a value of resistivity implies that the current lifetime in a superconducting ring in zero magnetic field is not less than 10^5 years (Andrei, 2004). However, the resistivity of a superconductor to an alternating current (a.c) is not zero. Alternating current flows on the surface of a superconductor within a thin layer of the order of the London penetration depth.

b. Meissner effect

This is the exclusion of weak magnetic field from the inside of a superconductor. Every superconductor exhibits perfect diamagnetism. The applied magnetic field penetrates into the superconductor within a very thin surface layer of thickness, λ_L . To cancel the applied field, a superconductor creates a direct current on the surface which gives rise to a magnetization, M that cancels the applied field.

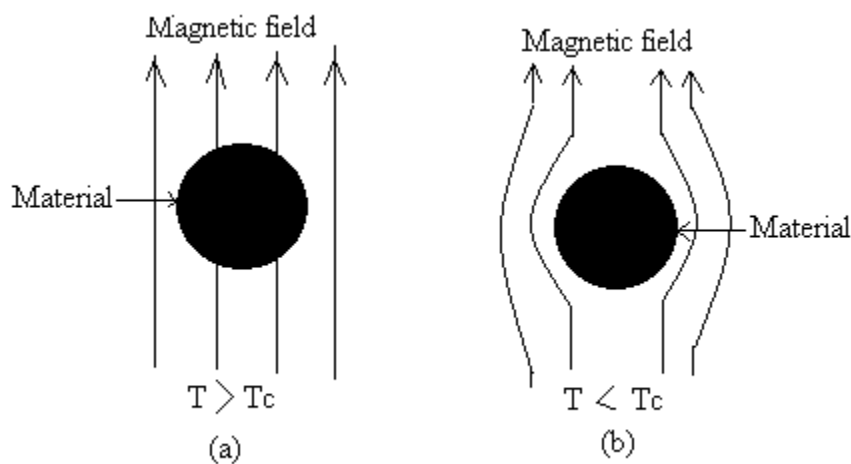


Figure 1.3: Meissner effect

In figure 1.3(a), Magnetic field penetrates the material in normal state ($T > T_c$), while part (b) shows exclusion of magnetic field from the inside of the material in the superconducting state ($T < T_c$).

c. Flux quantization

Since the superconducting state is a quantum state occurring on a macroscopic scale, the magnetic flux characterizing the state can also be quantized. If a superconductor with a hole inside is cooled to $T < T_c$, the magnetic field trapped inside the hole is found to exist only in discrete values, a proof of the fact that magnetic field in a superconductor can be quantized.

d. Josephson effect

An oscillating current of Cooper pairs flows when a steady voltage is maintained across the tunnel barrier between two superconductors. This effect is called a.c Josephson effect and it plays an important role in superconducting applications like SQUIDS (Superconducting Quantum Interference Devices)

1.5 High Temperature superconductivity

The real history of high- T_c superconductivity begun in 1986 when Bednorz and *Müller* found evidence for superconductivity at $T_c = 30$ K in La-Ba-Cu-O ceramic (Rapando et al, 2013). In 1987, the groups at the universities of Alabama and Houston under the direction of M.K Wu and P.W Chu jointly announced the discovery of the superconductor, YBaCuO whose T_c was 93K. This discovery was very important since liquid nitrogen which has a high boiling point of 77K could now be used as a coolant instead of the expensive liquid helium. A high- T_c superconductor is defined (Khanna, 2008) as one

whose critical temperature is greater than 90K and the superconducting state can be reached by cooling in liquid nitrogen.

In 1988, Bismuth and Thallium-based superconducting cuprates were discovered (Andrei, 2004) having $T_c=110\text{K}$ and $T_c=125\text{K}$ respectively. In 1993, the highest critical temperature of 135K was discovered in mercury-based cuprates. At high pressure this T_c increased to 164K. The four main families of mixed oxides that have shown high- T_c superconducting properties are;

- a) Yttrium-Barium-Copper-Oxide (YBa-Cu-O)
- b) Bismuth-Strontium-Calcium-Copper-Oxide (Bi-Si-Ca-Cu-O)
- c) Thallium-Barium-Calcium-Copper-Oxide (Tl-Ba-Ca-Cu-O)
- d) Mercury-Barium-Calcium-Copper-Oxide (Hg-Ba-Ca-Cu-O)

Some of the superconducting Cuprates with their corresponding T_c values are shown in table 2.0.

Table 2.0: Some of the superconducting cuprates**(Source: Marouchkine, 2004.)**

Cuprate	CuO ₂ planes	T _c (K)	Abbreviation
La _{2-x} Sr _x CuO ₄	1	38	LSCO
Nd _{2-x} Ce _x CuO ₄	1	24	NCCO
YBa ₂ Cu ₃ O _{6+x}	2	93	YBCO
Bi ₂ Sr ₂ CuO ₆	1	12	Bi2201
Bi ₂ Sr ₂ CaCu ₂ O ₈	2	95	Bi2212
Bi ₂ Sr ₂ Ca ₂ Cu ₃ O ₁₀	3	110	Bi2223
Tl ₂ Ba ₂ CuO ₆	1	95	Tl2201
Tl ₂ Ba ₂ CaCu ₂ O ₈	2	105	Tl2212
Tl ₂ Ba ₂ Ca ₂ Cu ₃ O ₁₀	3	125	Tl2223
TlBa ₂ Ca ₂ Cu ₄ O ₁₁	3	128	Tl1224
HgBa ₂ CuO ₄	1	98	Hg1201
HgBa ₂ CaCu ₂ O ₈	2	128	Hg1212
HgBa ₂ Ca ₂ Cu ₃ O ₁₀	3	135	Hg1223

With the discovery of high- T_c superconductivity in copper oxides which are very bad electrical conductors, the first reaction of most scientists was to think of another mechanism of superconductivity since phonon-mediated mechanism was impossible at so high a temperature. In 1988, A.S Davydov suggested that high- T_c superconductivity occurs due to the formation of bisolitons (Andrei, 2004). Bisolitons are electron or hole pairs coupled in a singlet state due to local deformation of copper oxide planes.

In 1994, A.S Alexandrov and N.F. Mott pointed out that in cuprates it is necessary to distinguish the internal wave function of a Cooper pair and the order parameter of a Bose- Einstein condensate which may have different symmetries. In 1995, V.J Emery and S.A Kivelson emphasized that superconductivity requires pairing and long-range phase coherence (Emery et al, 1987). They demonstrated that in cuprates the pairing may occur above T_c without the onset of long-range phase coherence

In 1997, V.J Emery, S.A Kivelson and O. Zachar presented a theoretical model of high- T_c superconductivity based on the presence of charge stripes and in 1999 the analysis of tunneling and neutron scattering measurements showed that in $\text{Bi}_2\text{Sr}_2\text{CaCu}_2\text{O}_{8+z}$ and $\text{YBa}_2\text{Cu}_3\text{O}_{6+x}$ the phase coherence is established due to spin fluctuations.

1.6 Characteristics of high temperature superconductors

Three main features characterize high- T_c superconducting cuprates;

(a) Strong correlations on copper

In cuprates, copper ions are the main sources of electrons while oxygen ions are the main donors of holes. The valence state of copper is Cu^{2+} . The only hole of the copper ion is localized since the energy barrier prevents transfer of the hole to the neighboring oxygen ion. The magnetic moments associated with spin-1/2 of the copper ion are coupled by the super-exchange interaction to a given anti-ferromagnetic ground state with Neel temperature greater than 300K. When the oxygen content is increased, additional holes mainly from oxygen are transferred into O (2P) states in the copper planes. These holes form a band of states within energy gap for the copper charge excitations. When the

number of holes increases, they tend to align adjacent spins in a parallel configuration that leads to a Mott insulator and the material becomes a superconductor.

b) **Profound Anisotropy**

High- T_c superconductors exhibit strong anisotropic behavior due to their quasi-two-dimensional structure. Superconducting currents flow in copper oxide planes implying that the coupling between adjacent layers is in the form of a tunneling process.

c) **Large electron-phonon coupling**

The critical temperature of superconductors is given in the BCS formalism as;

$$kT_c = 1.134\hbar\omega_D \exp\left(-\frac{1}{V\rho(\epsilon_F)}\right) \quad (1.11)$$

where k is Boltzmann constant, V is the coupling constant and $\rho(\epsilon_F)$ is the density of states at Fermi surface. This equation shows that for T_c to be large the electron-phonon coupling constant V should be large.

1.7 Room Temperature superconductivity

It is necessary to note that the expression “a room-temperature superconductor” inherently contains an ambiguity. Some perceive this expression as a superconductor having a critical temperature $T_c \sim 300$ K, others as a superconductor functioning at 300 K. There is a huge difference between these two cases. From a technical point of view, superconductors only become useful when they are operated well below their critical temperature—one-half to two-third of that temperature provides a rule of thumb. Therefore, for the technologist, a room-temperature superconductor (Andrei, 2004) would be a substance whose resistance disappears somewhere above 450 K. Such a material could actually be used at room temperature for large-scale applications. A room

temperature superconductor can also be considered as a substance whose critical temperature is approximately equal to 350K.

In 1992, T.H Geballe summarized some guidelines that can give insight into the possibility of developing a room temperature superconductor.

- ❖ The room temperature superconducting materials should be multi-component structures with more than two sites per unit cell where one or more sites not involved in the conduction band can be used to introduce itinerant charge carriers.
- ❖ Composition of the material should be near metal-insulator, Mott transition.
- ❖ On the insulating side of the Mott transition the localized states should have spin-1/2 ground states and anti-ferromagnetic ordering of the parent compound.
- ❖ The conduction band should be formed from anti-bonding tight-binding states that have a high degree of cation-anion hybridization near the Fermi level. There should be no extended metal-metal bonds.
- ❖ Structural features that are desirable include two- dimensional extended sheets or clusters with controllable linkage or both.

All these hints are based on the working experience with cuprates. These hints are correct but, not complete. This thesis sets out to give more conditions necessary for high- T_c superconductivity. If we suppose that, one day, a room-temperature superconductor will be available, and that in time, scientists and engineers synthesize it in useful forms and build devices out of it then we expect a technological revolution in the world never witnessed before.

- ❖ First of all, all devices made from the room-temperature superconductor will be reasonably cheap since its use would not involve cooling cost. The benefits would range from minor improvements in existing technology to revolutionary upheavals in the way we live our lives. Energy savings from many sources would add up to a reduced dependence on conventional power plants.
- ❖ Compact superconducting cables would replace unsightly power lines and revolutionize the electrical power industry. A world with room-temperature superconductivity would unquestionably be a cleaner world and a quieter world.
- ❖ Compact superconducting motors would replace many noisy, polluting engines.
- ❖ Advance transportation systems would lessen our demands on the automobile.
- ❖ Superconducting magnetic energy storage would become commonplace.
- ❖ Computers would be based on compact Josephson junctions.
- ❖ High-frequency, high-sensitivity operation of superconductive electronics, mobile phones would be so compact that could be made in the form of an earring.

1.8 The t-J model for High – T_c Superconductors

The t-J model was first proposed in 1977 from the Hubbard model by Józef Spalek (Wikipedia free encyclopedia, 2015). The model describes strongly correlated electron systems. It is used to calculate high temperature superconductivity states in doped anti-ferromagnets. The Hubbard model, as the beginning point of the t-J model, based on the electron- electron interaction alone to explain superconductivity on a two- dimensional square lattice of copper oxide since the phonon mediation could not explain the

occurrence of superconductivity in high- T_c superconducting systems which have very large electron correlations. The Hubbard model considered strong repulsive Coulomb interaction, U , on lattice sites and gave the Hamiltonian of the interacting electrons (K. Park, 2005) in terms of hopping energy matrix, t , electron creation and annihilation operators on neighbor sites, (i and j), $C_{i\sigma}^+$ and $C_{j\sigma}$ respectively, onsite Coulomb energy, U and electron occupation number operators, n_i as,

$$H_{Hub} = -t \sum_{(i,j)} (C_{i\sigma}^+ C_{j\sigma} + h.c) + U \sum_i n_{i\uparrow} n_{i\downarrow} \quad (1.12)$$

While working on the Hubbard model, Heisenberg found that when copper oxide is doped to half-filling level and the onsite Coulomb energy is increased to large values, the cuprate system becomes anti-ferromagnetic with neighboring electrons acquiring opposite spins; hence an electron would gain energy in hopping to the neighbor site where the other electron has opposite spin. This leads to pairing of electrons forming Cooper pairs that facilitate the process of superconductivity. The pairing electrons were found to exchange spins and as a result there exists exchange energy, J .

From Hubbard model, the Heisenberg model was developed. The Heisenberg Hamiltonian was expressed in terms of spin exchange integral, J , the electron spin operators in the neighboring sites, S_i and S_j , and the number operators, n_i and n_j as:

$$H_{Heisenberg} = J \sum_{(i,j)} (S_i S_j - \frac{n_i n_j}{4}) \quad (1.13)$$

Combining the Hubbard model and the Heisenberg model in the strong Coulomb repulsion or in the limit of large U resulted into the t - J model whose Hamiltonian is expressed in both the hopping integral t and spin transfer integral, J , and electron creation and annihilation operators in the neighboring sites (i, j) $C_{i\sigma}^+$ and $C_{j\sigma}$ respectively as:

$$H = \sum_{ij} J \left(S_i S_j - \frac{1}{4} n_i n_j \right) - \sum_{ij,\sigma} t_{ij} (C_{i\sigma}^+ C_{j\sigma} + H.C) \quad (1.14)$$

The t-J model therefore, describes an anti-ferromagnetic system in which if in the initial and final states, alignment of electrons is such that they have like spins for closest neighbor electrons, both t and J will be zero, while opposite spin pairing will give rise to energy gain in the magnitude of $\pm \frac{J}{2}$ or $\pm \frac{2t^2}{U}$ (K. Park, 2005) as shown in t figure 1.4.

initial	final	matrix element	initial	intermediate	final	matrix element
$\uparrow \uparrow$	$\uparrow \uparrow$	0	$\uparrow \uparrow$	$\uparrow \uparrow$		0
$\uparrow \downarrow$	$\uparrow \downarrow$	$-J/2$	$\uparrow \downarrow$	$\uparrow \downarrow$	$\uparrow \downarrow$	$-2t^2/U$
	$\downarrow \uparrow$	$J/2$		$\downarrow \uparrow$	$\downarrow \uparrow$	$2t^2/U$
$\downarrow \uparrow$	$\downarrow \uparrow$	$-J/2$	$\downarrow \uparrow$	$\downarrow \uparrow$	$\downarrow \uparrow$	$-2t^2/U$
	$\uparrow \downarrow$	$J/2$		$\uparrow \downarrow$	$\uparrow \downarrow$	$2t^2/U$
$\downarrow \downarrow$	$\downarrow \downarrow$	0	$\downarrow \downarrow$	$\downarrow \downarrow$		0

Figure 1.4: Spin alignment and matrix elements in the t-J model

(Source: Park, 2005)

1.9 The t-J model and the basic electronic structure of high- T_c superconductors

By now it is well established that the physics of High temperature Superconductivity is that of the Copper-Oxygen layers. Superconducting currents flow in the CuO_2 planes. The essential aspects of the electronic structure of CuO_2 planes may be described by the two-dimensional t-J model. There are copper and oxygen sites where electrons can interact with each other by hopping, exchange and Coulomb interaction. The hopping is represented by the hopping integral t for the nearest neighbor hopping between two lattice points. The on-site repulsion could be the Coulomb interaction, U, and the exchange

between the nearest neighbors is represented by the integral, J . The t - J model basically describes interacting electrons on a lattice. In general, three energies are involved, i.e., U , t , and J and they are related through the equation;

$$J = \frac{4t^2}{U} \quad (1.15)$$

In the parent compound of cuprates such as La_2CuO_4 , the formal valence of Cu is 2+, which means that its electronic state is in the d^9 configuration. The Copper is surrounded by six oxygen atoms in the octahedral environment (the apical Oxygen lying above and below the copper atoms) as shown in figure 1.5 (a)

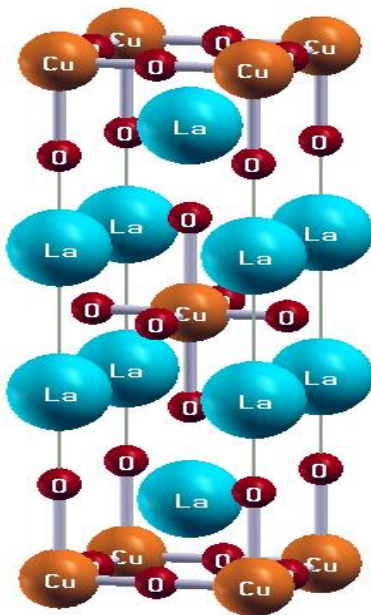


Figure 1.5 (a): Atomic arrangement in La_2CuO_4 (Source: Kazuhiko, 2011)

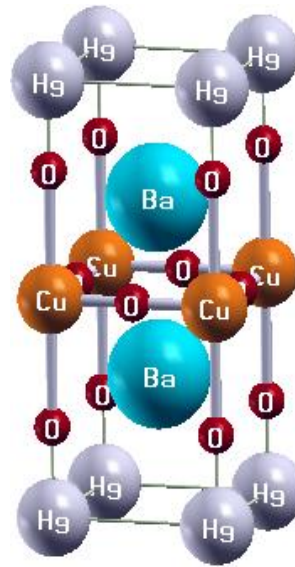


Figure 1.5 (b): Atomic arrangement in Hg_{1223} (Source: Kazuhiko, 2011)

Figure 1.6 shows an energy level diagram for the arrangement. The Copper d^9 configuration is represented by the energy level E_d occupied by a single hole with $s = \frac{1}{2}$. The Oxygen p orbital is empty of holes and it lies at energy E_p , which is higher than E_d

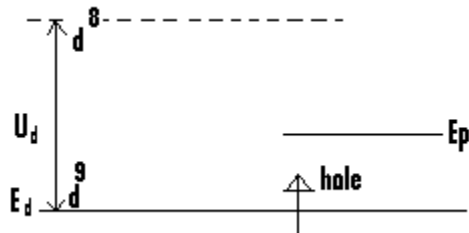


Figure 1.6 – The copper d and oxygen p orbitals in the hole picture.

A single hole with $S = \frac{1}{2}$ occupies the copper of orbital in the insulator. The energy to doubly occupy E_d (leading to a d^8 configuration) is U_d , and this is quite large, can be taken as infinity.

The lowest energy excitation is the charge – transfer excitation in which the hole hops from d to p with amplitude – t_{pd} . If $E_p - E_d$ is sufficiently large compared with t_{pd} , the hole will form a local moment on Cu. Experimentally an energy gap of 2.0eV is observed, and is interpreted as the charge-transfer excitation (Kastner et al, 1998).

In the one band Mott- Hubbard insulator, virtual hopping to doubly occupied states leads to an exchange interaction J_{S_1, S_2} , where;

$$J = \frac{4t^2}{U} \quad (1.16)$$

In the Mott-transfer insulator the local moments on the nearest neighbor Cu prefer anti – ferromagnetic alignment because both the spins can virtually hop to the E_p orbital. Ignoring the U_p for doubly occupying the “p” orbital with holes, the exchange integral is given by;

$$J = \frac{t_{pd}^4}{(E_p - E_d)^3} \quad (1.17)$$

Experimentally, the insulator is found to be in an anti ferromagnetic ground state. By fitting Raman scattering to two magnon excitations, the exchange energy is found to be $J = 0.13$ eV, for La_2CuO_4 (Sulewsley et al. Al, 1990). This is one of the largest exchange energies known.

By substituting divalent Sr for trivalent La, the electron count on the Cu-O layer can be changed in a process called doping. For instance, in $\text{La}_{2-x}\text{Sr}_x\text{CuO}_4$, x holes per Cu are added to the layer. As can be seen in Fig, 1.5, due to the U_d , the hole will reside on the oxygen p orbital. The hole can hop via t_{pd} , due to translational symmetry. The holes are mobile and form a metal, unless localization due to disorder or some other phase transition intervenes. The full description of hole hopping in the three-band model is complicated, and a number of theories^{4,5} considered this essential to the understanding of high T_c superconductivity (Emery, 1987). However, there is strong evidence that the low energy physics (on a scale small compared with t_{pd} and $E_p - E_d$) can be understood in terms of an effective one –band model. The essential insight is that the doped hole resonates on the four oxygen sites surrounding a Cu and the spin of the doped hole combines with the spin on the Cu to form a spin singlet. This is known as the Zhang –

Rice singlet (Zhang and Rice, 1988). The state is split off by energy of order, $\frac{(t_{pd})^2}{(E_p - E_d)}$ since the singlet gains energy by virtual hopping. However, the Zhang-Rice singlet can also hop from site to site. Since the hopping is a two-step process, the effective hopping integral t is also of the order of $\frac{(t_{pd})^2}{(E_p - E_d)}$. Parametrically, t is the same as the bonding energy of the singlet.

By focusing on the low lying singlet, the hole -doped three-band model simplifies to a one-band tight-binding model on the square lattice, with an effective nearest -neighbor hopping integral t , with $(E_p - E_d)$ playing a role analogous to U . In the large $(E_p - E_d)$ limit, this maps onto the t - J model. It is also possible to dope with electrons instead of holes. The typical electron-doped system is $\text{Nd}_{2-x}\text{Ce}_x\text{CuO}_{4+\delta}$ (NCCO). The added electron correspond to the removal of a hole from the Cu site in the hole picture, i.e. the Cu ion is in the d^{10} configuration. This vacancy can hop with a t_{eff} and the mapping to the one - band model is more direct than the hole doped case.

It is well known that the electron correlation is strong enough to produce a Mott insulation at half-filling. Furthermore, the one-band t - J model captures the essence of the low-energy electronic excitations of the cuprates. Particle-hole asymmetry may be accounted for by including further-neighbor hopping t' .

1.10 Electron-phonon interaction- The breathing and buckling modes.

Breathing phonons are high frequency phonons that run parallel to the CU-O planes while buckling phonons are low frequency phonons that run perpendicular to the Co-O planes. Breathing phonons may have a strong coupling. This may be understood by

noticing that the formation of the Zhang-Rice singlet in the t-J model involves a large energy of several electron Volts. In the breathing mode, O atoms in the CU-O plane move in the direction of the Copper atoms thereby changing the bond-lengths. This directly modulates the CU-O hopping integral, t_{pd} determining the Zhang-Rice singlet energy and leads to substantial coupling.

1.11 The role of Coulomb interaction and hopping in high- T_c superconductors

Coulomb interactions play an important role in superconducting process in the cuprates. A frequently used model for describing this is the three-band model. The model includes the Cu-O hopping integrals and the Coulomb interaction between two electrons on the Cu orbital. From this model, the t-J model can be derived such that each site corresponds to a copper atom in the copper-oxide plane. In the undoped system, corresponding to all copper atoms being in the d^9 configurations, each site is occupied by one hole. In a hole-doped system the holes go primarily on to the O sites. Such an O hole forms a Zhang-Rice singlet with a Cu hole. A Zhang-Rice singlet is described by an empty site in the t-J model

1.12 Electronic dipoles

Superconductivity occurs when two electrons pair up to form a composite boson leading to resistance-free flow of charges in the crystal. Thus, superconductivity could be explained in terms of phonon-mediated electron-electron pairing, electron-hole pairing, hole-hole pairing or any other hitherto unknown mechanism. The electrons in cuprates are generated by the copper ions (electron reservoirs) and they flow to the electron-deficient oxygen ions (hole reservoirs)

By definition, a dipole is a pair constituting an equal negative and a positive charge interacting by their electric fields.

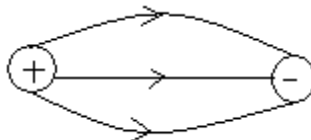


Figure 1.7a: Electronic dipole

In high- T_c superconductors the broken symmetry, lattice distortion and oxygen vacancies lead to local polarization of highly polarizable ions (Heebok Lee et al, 1991). The absence of the inversion symmetry at an oxygen site in the multilayered high- T_c superconductors causes electronic polarization of oxygens such that the valency electrons are displaced on one end leaving the other end effectively positive. This polarized oxygen ion form a dipole.

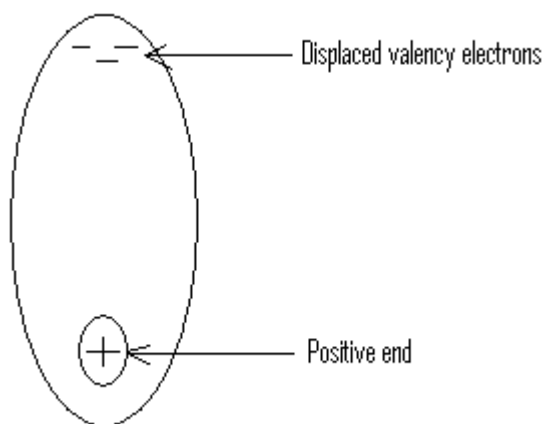


Figure 1.7b: Polarized atom

Once induced dipoles are present in the system they oscillate in a self-sustained and collective manner. When an electron flows through the crystal, it causes dynamic perturbations on the crystal field-generated electronic dipoles changing the dipoles in magnitude and direction and provides the time-dependent changing electric fields on the other dipoles. These dipoles, influenced by the changing electric fields on the other dipoles thus form a system of dipoles oscillating collectively generating lattice vibration. Quantized lattice vibrations are called phonons, responsible for electron pairing which lead to superconductivity.

1.13 Crystal-Field generated Electronic Dipoles

The crystal fields that can induce dipoles on highly polarizable ions are present on the oxygen-ion sites in high- T_c superconductors. The local electric field E_i acting on the i th ion can be written as;

$$E_i = E_i^m + \sum_j (F_{ij}) \cdot P_j \quad (1.18)$$

In eq. 1.18, P_j is the electronic dipole of the j th ion; E_i^m is the electric field at the i th ion produced by the monopoles (ionic charges) on the surrounding ions and $(F_{ij}) \cdot P_j$ represents the electric field at the i th site due to a dipole P_j at the j th site. E_i^m , in general, is not zero where a sub lattice point does not have inversion symmetry and is expressed as;

$$E_i^m = \sum_k \frac{q_k^*}{r_{ik}^3} \cdot r_{ik} \quad (1.19)$$

In eq. 1.19, q_k^* is the (effective) charge (monopole) of the k -th ion and r_{ik} is the position vector directed from the k -th ion to the i -th ion; (F_{ij}) is the Lorentz tensor.

The dipoles in high- T_c superconductors depend strongly on the oxygen deficiency parameter δ , and in this study the effects of monopoles as well as dipoles should be taken into account. Most of the high- T_c superconductors have layered structure. In some single-layered crystals, the oxygen sites in the CuO_2 planes contain inversion symmetry, and consequently, there are no oxygen dipoles in the planes. Because of the absence of dipoles in the conducting planes of these systems, the superconductivity is not expected to occur due to the collective dipole mechanism, and hence such systems are not found to be high- T_c superconductors.

However, there are multi-layered pure crystals that do not have inversion symmetry at the oxygen sites in CuO_2 planes and thereby possess induced dipoles. Since such systems have induced dipoles in the superconducting CuO_2 planes, they are expected to be the high- T_c superconductors under the collective dipole mechanism, consistent with the experimental observations.

Dipolon created electron-electron pair correlations in superconductivity

In general, the electron energy, ϵ_k , is determined experimentally and it includes necessary electron correlations. Thus the dipolon theory considers necessary electron correlations in the band energy.

Dipolons are cooperative oscillations of crystal-field generated dipoles. They have inherent electronic correlations present in their formation. Quantum mechanical dipoles refer to transitions with probabilities of electrons from the occupied orbitals of the ion to the higher unoccupied orbitals due to the electric field (Corson et al, 2000, Curro et al, 2000). The dipoles on the oxygen ions are formed by the transition of electrons from

the 1s, 2s and 2p orbitals to 3s, 3p and 3d and higher orbitals due to the electric field with different probabilities. Similarly, the dipoles on the copper ion are formed by the transition of electrons from 1s, 2s, 3s, 2p, 3p, 3d to 4s, 4p and 4d and higher orbitals with different probabilities under the action of electric field. Thus the strong correlations between the orbitals on all and every ion in the crystal constitute a strongly correlated system in the dipolons created electron-electron pair-correlations which lead to superconductivity. Since the crystal fields change due to doping in the crystal, such considerations (effects of the electric field and dipolon created electron-electron pair correlations) inherently include changes in the electronic correlations due to doping.

Out of a large number of electronic correlations present in the superconductors (under the dipolon theory), two types of correlations may be very significant;

(i) Electron- or hole-on-site Coulomb correlations (called U parameter)

(ii) The correlation between the d-electron of copper and the p-electron of oxygen called the charge transfer correlation generally represented by t_{pd} parameter. This is similar to the t-J model.

1.14 Statement of the problem

Most high temperature superconductors with practical applications are Mott insulators. It is now a widely accepted view that the problem of high- T_c superconductivity (Patrick Lee et al, 2003) is how to achieve the Mott insulator state and its working principles that lead to high- T_c superconduction. Many theories that attempt to describe this state have suffered significant failures as discussed in chapter two of this thesis, leaving the t-J model as the only model which captures the physics of the strong correlations inherent in

this problem effectively. However, the t-J model ignores the effect of electronic interaction with the lattice. Furthermore, thermodynamic properties of the superconducting state can only be obtained using this model if its Hamiltonian is diagonalized. This thesis provides solutions to these inefficiencies of the t-J model.

Objectives of the study

1.15 General Objective

This research aims at considering an in-depth study of the structure of High- T_c superconductors, the existing theories and the equations involved with an intention of developing a high temperature Superconductivity theory of t-J model and electronic dipoles.

1.16 Specific Objectives

- (i) To diagonalize the t-J model Hamiltonian using Bogliubov-Valatin transformation and hence obtain expressions for the thermodynamic properties of high- T_c superconductivity namely; system energy, specific heat capacity, entropy and transition temperature.
- (ii) To develop a dipole mediated t-J Hamiltonian (The t-J-d model) that can lead to high-temperature superconductivity and hence obtain expressions for the thermodynamic properties of high- T_c superconductivity namely; system energy, specific heat capacity, entropy and transition temperature based on the t-J-d model.
- (iii) To analyze the effect of varying the temperature and the electronic transfer energy on the thermodynamic properties of high- T_c superconductors.

1.17 Rationale/justification

Experimental evidence has shown that charge carriers in high temperature superconductors are strongly correlated but also coupled with lattice vibrations or phonons (Alexandrov, 2012). This signals the idea that the true origin of high- T_c superconductivity can only be found in proper combination of Coulomb and electron-phonon interactions. As such, this study which describes a model that strongly considers on-site Coulomb repulsion energy, U , electron hopping, t , and exchange energy J , is quite appropriate in the analysis of the phenomenon of high- T_c superconductivity. Further, there is need for the Hamiltonian of the t - J model which captures the physics of strong correlations of high- T_c superconductivity to be diagonalized in order to get the energy of a system of independent fermions so as to obtain thermodynamic properties of the system.

1.18 Importance of the study

Knowledge generated in this thesis will help in building High- T_c superconductors that can work at room temperature in order to avoid costs spent on coolants to achieve critical temperature. With this knowledge we expect transformation in number of technologies connected with computers, energy sector, electronics and electrical engineering, medical diagnostics, power generation and transportation. Successful applications of high-temperature superconductors (Ayodo, 2011) include;

- i. Magnetic levitation

Transport vehicles such as trains can be made to ‘float’ on strong superconducting magnets virtually eliminating friction between the train and its tracks. Such trains are called magnetically levitated trains or MAGLEVS. A MAGLEV runs using

superconducting levitation (floating) electromagnets and propulsion electromagnets. To achieve levitation, electromagnets are mounted on arms that extend around and under the guide-way. When a current is sent to an electromagnet, the resulting magnetic field creates induced magnetism in a rail mounted in the guide-way. The upward attraction force from the induced magnetism is balanced by the weight of the train so that the train moves without touching the rail or the guide-way. By controlling the direction of the currents in the train and guide-way electromagnets it is possible to create unlike poles in the guide-way just a head of each electromagnet on the train and a like pole just behind. Each electromagnet on the train is thus pushed forward by electromagnets on the guide-way. By adjusting the timing of the like and unlike poles, the speed of the train can be adjusted. A landmark for the commercial use of MAGLEV technology occurred in 1990 when it gained the status of a nationally-funded project in Japan. Yamanashi MAGLEV Test line opened in April 3, 1997 and in 1999, the MLX01 test vehicle attained a speed of 343 miles per hour.

ii. Magnetic Resonance Imaging

By impinging a strong superconductor-derived magnetic field into the body, the hydrogen nuclei that exist in the water inside the body and fat molecules are forced to accept energy from the magnetic field. They then release this energy at a frequency that can be detected and displayed graphically by a computer. This technique is used by doctors as a non-invasive means of determining what is going on in the body of a human being. It is applied in Magnetic Resonance Imaging (MRI).

Very sensitive devices called Superconducting Quantum Interference Devices (SQUIDS) can detect minute changes in magnetic fields. They are used in biomagnetic applications to monitor accurately heart and brain activity non-invasively.

iii. Petaflop computers

A petaflop is a thousand-trillion floating point operations per second. It has been conjectured that devices of the order of 50 nanometers in size along with unconventional switching mechanisms such as the Josephson junctions associated with superconductors will be necessary to achieve petaflop speeds that will be applied in the manufacture of very high speed computers called petaflop computers.

iv. Ultra-high-performance filters

Sine superconducting wire has near-zero resistance, it can be used to build Ultra-high-performance filters which are devices that have the ability to pass desired frequencies and block undesired frequencies in high-congestion radio-frequency applications such as cellular telephone systems. ISCO International and Superconductor Technologies are companies currently offering such filters.

CHAPTER TWO

LITERATURE REVIEW

2.1 Introduction

The problem of the nature of charge carriers and the elementary excitations which lead to superconductivity in the doped copper oxides can be studied in the two-dimensional Hubbard model, and its strong coupling limit, the t-J model (Anderson P.W, 1987), (Zhang et al, 1988). This model is generally assumed to be the simplest model possibly able to describe some essential features of these materials, an important feature being the metal-insulator transition with doping. However, in spite of many years of theoretical efforts, many properties of this model are not well understood. In this chapter, a study of the research done on the t-J model and related work by various authors is carried out. In this study, the strong points and weaknesses of the proposed models are pointed out with an intention of coming up with a better explanation of the features of the t-J model and another new model that best describes the phenomenon of high- T_c superconductivity.

2.2 The t- J_p -U model

As an essential generalization of the t-J model, the t- J_p -U model (Alexandrov, 2012) was introduced. The model discussed electron-electron and electron-phonon correlations providing a microscopic explanation of the high- T_c superconductivity phenomenon. It showed that the inclusion of the residual on-site interaction \tilde{U} which was neglected in the t-J model drives the system to a Bose-Einstein Condensation/ Berdeen-Cooper-Schrieffer cross over that reconciles the polaron-bipolaron theory of superconductivity with the observation of large Fermi surface in overdoped cuprate conductors. It was found that the polaron (an electron surrounded by a cloud of phonons) exchange energy, J_p , is attractive

for polarons in the singlet channel and repulsive for triplet channel. The explanation for this is that if two polarons with opposite spins occupy nearest-neighbor sites, they can exchange sites without any potential barrier between them, which lowers their energy by J_p proportional to the un-renormalized hopping integral squared.

Further, it was found that if the polaronic hopping, t , was ignored ($t=0$), the ground and the highest energy states become bipolaronic spin-singlet and spin-triplet, respectively, made up of two polarons on neighboring sites. For t not equal to zero, the probability to find nearest neighbor bipolarons fall as the hopping is increased or the strength of on-site repulsion \tilde{U} for 100x100 square lattice is increased. Importantly, although small bipolaronic configurations persist for any values of the hopping at $\tilde{U} = 0$, for $\tilde{U} \neq 0$ and large values of t up to a critical value;

$$t_c = \tilde{U}J_p(u)/(2\tilde{U} - 8J_p(u)) \quad (2.0),$$

the presence of a finite onsite interaction leads to the crossover from small to large bipolaronic configuration. Further increasing t , the system undergoes a phase transition to an unbound state at $t = t_c$.

2.3 The density function Theory

The local -density function Theory (Hybertson et. al, 1990) was used to calculate the value of J and a value of $128 \pm 5meV$ was obtained for cuprates. This was in excellent agreement with the experimental values. Also, $t \approx 0.41ev$ was obtained for electron doping and $t= 0.44ev$ for hole doping. Based on their results, the commonly used

parameter $\frac{J}{t}$ for t - J model is $\frac{1}{3}$. However, in view of the fact that the on-site repulsion

is the largest energy scale in the problem, it would be appropriate to begin the modeling of the Cuprates with the t-J model.

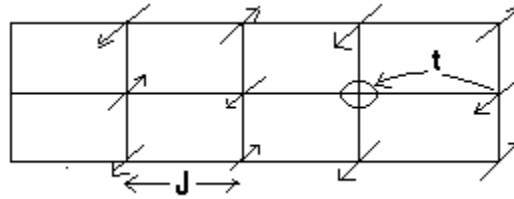


Fig. 2.1: Electronic structure of cuprates for a two-dimensional copper-oxygen layer for a one band model.

The essence of the problem is that doping can be understood from Fig. 2.1 when a vacancy is introduced into an anti-ferromagnetic spin background, it would like to hop with amplitude t to lower its kinetic energy. However, after one hop, its neighboring spin finds itself in a Ferro-magnetic environment, at an energy cost of $\frac{3}{2} J$ if the spins are treated as classical $S = \frac{1}{2}$. It is clear that the holes are very effective in destroying the anti-Ferro magnetic background. This is particularly so at $t \gg J$ when the hole is strongly delocalized. The basic physics is the competition between the exchange J and the kinetic energy which is of the order t per hole or kinetic energy which is of order, xt per unit area. When $xt \gg J$, we expect the kinetic energy to win and the system would be a Fermi-liquid metal with a weak residual anti-ferromagnetism correlation. When $xt \leq J$, however, the outcome is much less clear since the system would like to maintain the anti-ferromagnetic correction while allowing the hole to move as freely as possible. Experimentally it is known (Lee, Patrick, 2006) that the Neel order is destroyed with 3% hole doping, after which the d-wave superconducting state emerges as the ground state up

to 30% doping. Exactly how and why superconductivity emerges as the best compromise is the central problem of the high $-T_c$ puzzle. However, the competition between J and xt sets the correct scale such that $x = \frac{J}{t} = \frac{1}{3}$. It is well known experimentally that the normal state above the superconducting T_c behaves differently from any other metallic state that may be known up to now.

After knowing the properties and structure of the High T_c superconductors, it is clear that the high $-T_c$ superconductors are different from the BCS or conventional superconductor. Another difference comes from the measurement of the change in kinetic energy through the transition. In conventional BCS theory, pairing between quasi-particles leads to the gain in the attractive potential energy since the Fermi-distribution is smeared by the creation of the energy gap. There are two major differences between high- T_c superconductors and convectional BCS superconductors. The first being due to the super fluid density of the superconductor which is small and vanishes with decreasing hole concentration.

Second when the pairing is d-wave, the gap vanishes at four points on the Fermi surface (called gap nodes) so that the quasi particle excitations are gapless and affect the physical properties even at the lowest temperatures.

The physical properties to which the nodal quasi particles clearly contribute are the thermo- dynamical quantities such as the specific heat. Because their density of states vanishes linearly in energy they give rise to a T^2 term, which dominates the low temperature specific heat. In practice, disorder rounds off the linear density of states, giving instead a $(\delta T + \beta T^3)$ behavior. It should be noted that since the BCS quasi-

particle is a superposition of a particle and a hole, the charge is a good quantum number. However, the particle component with momentum P and the hole component with momentum $-k$ each carry the same electrical current $-e\left(\frac{\partial E_k}{\partial k}\right)$, and it would be proper to consider this to be the current carried by the quasi-particle. It should be noted that the velocity, $V(j_k/e)$, of the quasi-particles is very different from the group velocity $\left(\frac{\partial E_k}{\partial k}\right)$. The quasi-particles also contribute to the low $-$ temperature transport properties (Lee, 1993).

2.4 Resonating Valence Bond Theory for High T_c superconductors (RVB – theory)

It is well understood that the Neel spin order is incompatible with hole doping. Thus could there be another arrangement of the spin which achieves a better compromise between the exchange energy and the kinetic energy of the hole?

Soon after the discovery of high $-T_c$ superconductors, Anderson (Anderson, 1987) revived the RVB idea and proposed that with the introduction of holes, the Neel state is destroyed and the spins form a superposition of singlets. The vacancy can hop in the background of what he envisioned as a liquid of singlet and a better compromise between the hole kinetic energy and the spin exchange energy may be achieved. The vacancies are responsible for the transport in the plane. The conductivity spectral weight in the plane is in the form of hole concentration 'x' and is unaffected between planes conductivity, an electron is transported between planes. In this picture, the superconductivity is driven by the phase coherence of holes, which lowers the kinetic energy of the holes.

A second concept associated with RVB idea is the notion of spinons and holons and the spin-charge separations. Anderson postulated that spin excitations in a RVB state are $S = \frac{1}{2}$ fermions, which he called spinons. This is in contrast with excitations in a Neel state which are $S = 1$ magnons or $S = 0$ gapped singlet excitations.

The concept of spinons is a familiar one in one-dimensional spin chains where they are well understood to be domain walls. In two dimensions';

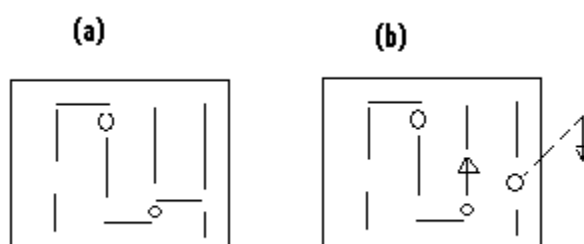


Fig. 2.2: A cartoon representation of the RVB liquid or singlets.(a) Solid bonds and vacancies,(b) An electron removed from the plane.

In Fig. 2.2(a) the solid bond represents a spin-singlet configuration and the circles represent a vacancy (b) When an electron is removed from the plane in photoemission on a C- axis conductivity experiment. This requires the breaking of a pair. The concept is a novel one which does not involve domain walls. Instead, a rough physical picture is as follows:-

If we assume a background of short range singlet bond, forming the so called short-range RVB state, a cartoon of the spinon is shown in fig. 2.2 If the singlet bond are liquid, two $S = \frac{1}{2}$ spins formed by breaking a single bond can drift apart with the liquid of singlet bond, filling in the space between them. They behave as free particles and are called

spinons. The vacancy left over by removing a spinon is called a holon. The holon carries charge 'e' but no spin.

2.5 Effects of Higher Hopping Terms on the Stripe states in the Hubbard Model

The purpose of the two-dimensional Hubbard model was to investigate whether the stripe states exist in the electron doped cuprate NCCO or the bilayer system such as $YBa_2Cu_3O_{6+y}$. Using the variational Monte Carlo method for the two – dimensional $t - t' - t''$ Hubbard model (Mitake Miyazaki, 2005), it was found that while stripe states with the periodicity consistent with experiments for $La_{2-x}Sr_xCuO_4$ are stabilized in the case of $t'/t < 0$, the positive t'/t makes the stripe state unstable with the lowest energy state being the commensurate AF state which is consistent with experiments on the electron doping system such as $Nd_{2-x}Ce_xCuO_4$. In this model, it was also shown that the stripe state is sensitive to the value of t'/t and the results indicated that the nesting condition is a critical factor to the stripe instability. To study this for the 2D Hubbard model on a square lattice, the Hamiltonian given in eq.1.12 was used. The transfer energy for the nearest neighbor hopping, $t_{ij} = t, t', t''$, if sites i and j are nearest, second nearest, third-nearest neighbor pairs, t was taken as unit energy, $C_{i\sigma}^+(C_{i\sigma})$ is the creation (annihilation) operator of the electron with spin σ (\uparrow or \downarrow) at site i and $n_{i\sigma} = C_{i\sigma}^l C_{i\sigma}$. U is the on-site Coulomb energy.

The Variational total energy was calculated as;

$$E_{coexist} = \frac{\langle \Psi | H | \Psi \rangle}{\langle \Psi | \Psi \rangle} \quad (2.1),$$

where the trial wave function was defined as;

$$\Psi = P_{N_e} P_G I \Psi_{coexist}^{MF} \rangle \quad (2.2)$$

In eq.2.2, P_G is the Gutzwiller projection operator and P_{N_e} is a projection operator which extracts only the states with fixed total electron number, N_e .

However, this model does not give the nature of pairing mechanism that leads to the phenomenon of superconductivity. The physical properties of the superconducting state e.g. electronic specific heat, Gibb's free energy and entropy were not discussed. In this thesis, the physical properties of the superconducting state will be discussed in detail.

2.6 Polaronic Mechanism of superconductivity in cuprates

In order to comprehend the nature of the superconducting state, it was found necessary to construct a consistent microscopic theory which could describe superconductive and normal properties of HTSCs. The Polaronic model of charge carriers in cuprates (Pradeep et al, 2013) was proposed. A Hamiltonian that governs electron- phonon and electron-electron correlations was developed. A one particle temperature-dependent Greens function with an anomalous component was developed disregarding electronic spins. The Greens function was used to obtain the correlation functions which were used in calculating the superconducting order parameter, Δ and hence the physical properties namely critical field H_c , free energy, F and electronic specific heat, C_{cs} . The superconducting order parameter was found to drop exponentially with rise in temperature from 2.6 eV at 4 K to 0.9 eV at 90 K for phonon and polaron interaction. The same trend was observed for phonon interaction but at a lower level ranging from 2.5 eV at 4 K to 0.8 eV at 90 K for YBCUO. Temperature rise did not have effect on order parameter for Polaron-Polaron interaction, the order parameter remained constant (0.1eV)

at all temperatures. The electronic specific heat was virtually zero from 0 K to 25 K, and beyond 25 K, it increased linearly with rise in temperature. Free energy increased non-linearly with temperature reaching peak of 0.22 eV at around 58 K before it dropped to approximately 0.11 eV at 90 K. The same trend was observed in the variation of specific heat with temperature having a peak at the same temperature, 58 K. It must be noted that in this model the hopping mechanism for the charge carriers was not considered and no attempt was made to analyze the transition temperature of the superconductors in this model, gaps of which this thesis sets out to fill.

2.7 Thermodynamic properties of small superconductors with fixed number of particles

Recent progress in single-electron tunneling spectroscopy has revealed the persistence of a pairing effect even at very small number of particles. By varying the number of particles, careful analysis has been made of thermal excitations or of the action of external magnetic field. The variation-after- projection approach (Danilo et al, 2012) was applied to the Richardson pairing Hamiltonian and used to describe the thermodynamics of small superconductors with a fixed number of particles. The canonical description of the quantum finite system was obtained by minimizing Helmholtz free energy and the pairing Hamiltonian used was;

$$\hat{H} = \sum_{i,\sigma=\pm} (\varepsilon_i - \sigma\mu_B B) \hat{c}_{i\sigma}^+ \hat{c}_{i\sigma} - G \sum_{i,j} \hat{c}_{i,+}^+ \hat{c}_{i,-}^+ \hat{c}_{i,-} \hat{c}_{i,+} \quad (2.3),$$

where B is the external magnetic field, G is the pairing strength, ε_i is the level energy, σ is spin state and $\hat{c}_{i\sigma}^+, \hat{c}_{i\sigma}$ are creation and destruction operators. In this model, free energy was found to rise from around -27 eV at 0 K reaching an approximately constant value of -10 eV at 5 K for the finite- temperature projection- after- variation (FT-PAV) approach,

while specific heat rose from 0 J/Keg at 0 K to a peak value of 6 J/Keg at 1K, there after dropped non-linearly for the same system. The same trends were observed for the finite-temperature variation-after-projection (FT-VAP) approach for energy and specific heat. In addition, entropy was found to rise non-linearly with temperature reaching a constant value of 10J/K for the temperature range of 0-5 K. Energy gap dropped non-linearly with rise in temperature reaching an almost constant value of 0.1eV for the temperature range of 0 - 5 K. While a good comparison was made for the FT-PAV, FT-BCS and FT-VAP approaches in describing the thermodynamic properties, it must be noted that this model has only been applied for low temperature, 1-5 K. It is well known that the FT-BCS theory suffers from sharp superfluid- to- normal phase transition as the temperature increases hence the results obtained differ from the exact solution. Better results are anticipated while using VAP approach. However, this approach requires that the variation be minimized by both varying the components of quasiparticle creation operators u_k and v_k and the energy E_k consistently. In principle, such minimization has never been performed because the BCS Hamiltonian and projector operator do not commute and therefore cannot be diagonalized simultaneously. When a projector operator does not commute with the Hamiltonian, no phase transition takes place. The minimization in this model was done via quadratic programming method not attested. Calculations were done for a very small number of particles, $N=10$. This thesis aims at coming up with a theory applicable to bulk high temperature systems for practical purposes through t-J model. Suitable values of u_k and v_k are chosen to minimize variations.

2.8 Collective modes in the superconducting ground states

Applying the gauge theory approach to the t-J model (Patrick Lee et al, 2003), the question as to whether the superconducting ground state that emerges out of the gauge theory is completely conventional or not was addressed. It was found that the gauge theory predicts collective modes in the superconducting ground state which have experimental consequences. Unlike the conventional BCS theory where the only order parameter is the complex pairing order parameter Δ , here, the hopping matrix element was also considered as an order parameter. In this model, collective modes appear at fairly high energy, approximately equal to the exchange energy, J , thereby confirming unconventional/ high- T_c superconductivity and the effectiveness of the t-J model in the analysis of high- T_c superconductivity. In this thesis we now proceed to employ the t-J model and electronic dipoles in obtaining transition temperature and the thermodynamic properties of high- T_c superconductors.

2.9 Spin liquid states near the Mott transition

In the large Coulomb repulsion limit, the Hubbard Hamiltonian model reduce to the t-J model which has an insulating and spin order at half filling. Using a U(1) gauge theory of the Hubbard model in the slave-rotor representation (Sung-Sik et al, 2005), it was argued that the spin liquid phases may exist near the Mott transition in the Hubbard model on triangular and honeycomb lattices at half filling. The spin liquid is a state in which the charges exhibit no spin order and it is important to this study in that it is the state that is just on the insulating side of the Mott transition. It has also been shown that a spin liquid state with spinon Fermi surface may be stable if the t-J model is extended to include higher order virtual hopping, a realization of the resonating Valence Bond (RVB) theory.

This extension is hereby provided for in this thesis so that the parameters under study will conveniently be analyzed in the proper Mott insulation state of high- T_c superconductivity.

2.10 Effect of chalcogenides on critical temperature

Tsendin and Denisov proposed that the replacement in large amount of Oxygen with Chalcogenides e.g. sulphur in YBaCuO will significantly increase critical temperature (Tsendin et al, 2001).

In this model, attention is given to localized pairs of electrons and negative-U centres. Negative-U centres are centres of localized electrons that neighbor one another or simply the copper ion centres in the lattice with energy U. Transition of electrons from one centre to another in the process of forming Cooper pairs is guided by a matrix element t_{ij} .

It is considered that where energy of electrons $U > 0$ and $t_{ij} \ll U$, negative values of U lead to attraction between electrons with opposite spins on the same negative U centre. At temperature, $T = 0$ K, all electrons are localized in pairs on the negative U centers. At $T \neq 0$ K, the system represents an assembly of empty centers, centers occupied with one electron and centers occupied with two electrons. The number of negative U centers occupied with one electron is proportional to $ne^{-\frac{u}{T}}$, where n is concentration of electrons. When $t \ll U$, the amount of single electrons is very little in comparison with the number of pairs and hence, the concentration of single electrons can be neglected. Thus, the formula of superconducting transition temperature is obtained as;

$$T_c = \frac{w(1-2v)}{\ln(v^{-1}-1)} \quad (2.4)$$

where w is the width of the pair's band and $w = \frac{2zt^2}{u}$; z is the number of the nearest neighbours of the given centre, and $\nu = \frac{n}{2}N$ where N is the concentration of negative U centres. Analyzing the eq. 2.4, it is seen that to increase T_c , it is necessary to increase the matrix element of electron transition from one negative U centre to another.

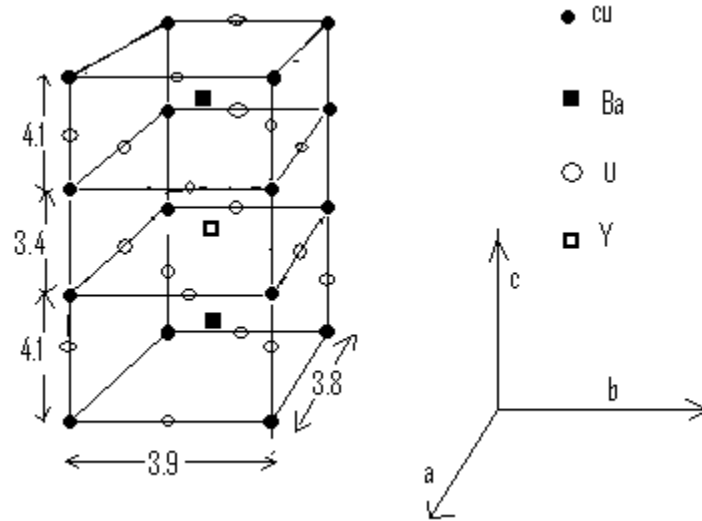


Figure. 2.3 Structural lattice of $Y_1Ba_2Cu_3O_7$ (Tsendin, 2001)

A possible way of increasing the matrix element t_y is by replacing the atoms of oxygen with those of the elements of the same group e.g. sulphur. For a separation distance of more than 1.5\AA , the matrix element for sulphur, t_{cus} will be greater than the matrix element for oxygen, t_{cuo} . In the same lattice of $YBaCuO$, the distance between atoms of Cu and O is 1.95\AA and t_{cuo} is $-0.609R_y$ where R_y is the distance between atoms in y-direction. If in the same lattice some atoms of Oxygen are replaced by those of sulphur, T_c will increase because the matrix element of transition of Cu-S on distance 1.95\AA is $-0.929R_y$. Ideally if all atoms of Oxygen are replaced, the T_c would be increased 2.3 times.

However, the constants of a structural lattice for full replacement of atoms of Oxygen by atoms of Sulphur are not known. Secondly, expressing the matrix element for electron transfer, t_{CuO} , which has units of energy as a function of inter-atomic distance ($t_{\text{CuO}} = -0.609\text{Ry}$) brings about dimensional problem because the right hand side has units of length.

2.11 The t-J model and Monte-Carlo calculations

Mishchenko and Nagaosa (Mishchenko et al, 2004) studied an undoped infinite Holstein-t-J model using a diagrammatic Monte-Carlo variation method. They used diagrams with crossing phonon propagators but neglected diagrams with magnon propagators crossed by phonon or other magnon propagators. They used electron phonon frequency ω_{ph} to hopping integral t ratio parameter as $\omega_{ph}/t = 0.1\text{Hz}/eV$ and the exchange integral to hopping integral ratio $J/t = 0.3$. They found self-trapping for electron- phonon strength $\lambda \approx 0.4$ for an electron at the bottom of the band for this system. It was concluded that the anti-ferromagnetic ground state and the coupling to magnons help the formation of polarons.

CHAPTER THREE

METHODOLOGY

3.1 Introduction

This chapter presents a detailed description of the techniques used in the formulation of the theories. It also presents the methods of data generation and data analysis. The assumptions and the approximations used are enlisted.

3.2 The t-J model

In order to obtain the quasi-particle Hamiltonian, the t-J model Hamiltonian, $H = \sum_{ij} J \left(S_i S_j - \frac{1}{4} n_i n_j \right) - \sum_{ij, \sigma} t_{ij} (C_{i\sigma}^+ C_{j\sigma} + H.C)$ was diagonalized by carrying out conversion of operators from the old to the new operators using second quantization techniques. Proper choice of conversion constants was done which made the elimination of the off-diagonal terms possible.

Neglecting the effect of the fourth-order terms, the diagonalized Hamiltonian was obtained. This gave the ground state energy of the t-J system, E_0 , and the expression of system energy at any temperature, E , was obtained by multiplying the ground state energy by the thermal activation factor. The derivative of energy with respect to temperature gave the expression of specific heat. Solving the integral of the quotient of specific heat and system temperature, entropy was obtained. The formula for critical temperature was found by equating the temperature derivative of heat capacity to zero.

3.3 The t-J-d model

As already stated in the introduction, the t-J model very well captures the physics of electronic correlations on a lattice site but does not account for the interaction of the electron with the lattice as a whole. In order to include the aspect of electronic interaction with the lattice in the t-J model, the dipole oscillation Hamiltonian was diagonalized and added to the diagonalized t-J Hamiltonian to obtain the t-J-d Hamiltonian. The contribution of electronic dipoles to the superconducting energy, heat capacity, entropy and critical temperature was considered. Research Variables

The following variables were considered;

- a. Energy of the superconducting state
- b. Specific heat
- c. Entropy
- d. Temperature of transition

3.4 Generation of Data

The data tables were obtained when the values of the constants were substituted in equations derived. Using MathCAD Application software, the resulting expressions were simplified and the tables of values generated.

3.5 Data presentation

Data generated was presented in tabular form. Graphs showing the variation of T_c and the independent variables were plotted and interpreted. Conclusions are drawn.

3.6 Approximations and assumptions used

In this thesis, the following approximations and assumptions were made;

- i. The lowest energy state described by the derived Hamiltonian was assumed to have occupation numbers equal to zero, a condition that befits high- T_c superconductivity. This is because at high temperature most of the electrons are thermally excited to higher states. Thus, all the occupation numbers m_k, n_k, η_k were equal to zero.
- ii. The contribution of the fourth order terms in the derived Hamiltonian to the energy of the system was too small and could be neglected, thus all fourth order terms were dropped.
- iii. All the off-diagonal terms in the Hamiltonian were eliminated so that we could be left with a Hamiltonian of a system of independent fermions and bosons that lead to the formation of quasi-particles responsible for high- T_c superconductivity.
- iv. In the conversion of operators from the old to the new operators, a choice of conversion constants U_k and V_k was made such that the constants were real and would obey the condition that $U_k^2 + V_k^2 = 1$ for fermions and $U_k^2 - V_k^2 = 1$ for bosons. This condition was necessary for the complete elimination of the off-diagonal terms.

CHAPTER FOUR

THE DIAGONALIZED t-J HAMILTONIAN AND THE THERMODYNAMIC PROPERTIES OF HIGH-T_c SUPERCONDUCTORS

4.1 Introduction

The spin fluctuation of superconductivity was first proposed as an explanation of superconductivity in heavy fermions (Miyage et al, 1986). This model is based on short range Coulomb interaction leading to an exchange coupling $J \times S_i S_j$ between near-neighbor copper spins S_i and S_j and strong spin fluctuations. The super-exchange constant is denoted by J . In cuprates it has an extremely high magnitude, $J \approx 125 \text{meV}$. The underlying microscopic physics can be described by the t-J model. In this chapter, we proceed to diagonalize the t-J model Hamiltonian in order to obtain the ground state energy of the quasi- particles and hence, the thermodynamic properties of the superconducting state. The t-J Hamiltonian is given by (Lee and Nagaosa, 2003);

$$H = \sum_{ij} J \left(S_i S_j - \frac{1}{4} n_i n_j \right) - \sum_{ij, \sigma} t_{ij} (C_{i\sigma}^+ C_{j\sigma} + H.C) \quad (4.1)$$

Here, transfer energy, $t_{ij} = t, t', t''$ for the nearest, second nearest, and third-nearest-neighbor pairs, respectively, and it is the electron transfer energy from i th location to the j th location, S_i and S_j are the electron spin operators in the i th and j th locations respectively, n_i and n_j are electron occupation number operators, J is the spin exchange energy while $H.C$ stands for the Hermitian conjugate of the electron creation operator, $C_{i\sigma}^+$ and annihilation operator, $C_{j\sigma}$. The effect of the strong Coulomb repulsion is

represented by the fact that the electron operators $C_{i\sigma}^+$ and $C_{j\sigma}$ are the projected ones in which double occupation is forbidden.

High- T_c superconductivity is obtained in the strong Coulomb repulsion regime. The effect of strong Coulomb repulsion is represented by the fact that the electron operators $C_{i\sigma}^+$ and $C_{j\sigma}$ are the projected ones in which double occupancy is prohibited. The constraint for the operators is written as an inequality;

$$\sum_{\sigma} C_{i\sigma}^+ C_{i\sigma} \leq 1 \quad (4.2)$$

This constraint can only be handled by the slave-boson method ³³(Barnes, 1976) by representing the electron operator as;

$$C_{i\sigma}^+ = f_{i\sigma}^+ b_i + \epsilon_{\sigma\sigma'} f_{i\sigma'} d_i^+ \quad (4.3)$$

where $\epsilon_{\uparrow\downarrow} = -\epsilon_{\downarrow\uparrow} = 1$ is the anti-symmetric tensor and $f_{i\sigma}^+$ and $f_{i\sigma'}$ are the fermion operators, b_i and d_i^+ , are the slave- boson operators. To produce all the algebra of the fermion operators, we impose another constraint;

$$f_{i\uparrow}^+ f_{i\uparrow} + f_{i\downarrow}^+ f_{i\downarrow} + b_i^+ b_i + d_i^+ d_i = 1 \quad (4.4)$$

In eq. (4.4), $f_{i\uparrow}^+$ is the creation operator for a fermion in spin up mode at the i-th site, $f_{i\uparrow}$ is the annihilation operator for a fermion in spin down mode at the i-th site. As such, $f_{i\uparrow}^+ f_{i\uparrow}$ represents the number operator for fermions in spin up and $f_{i\downarrow}^+ f_{i\downarrow}$ represents number operator for fermions in spin down mode while $b_i^+ b_i$ stands for the boson number operator in the same state and $d_i^+ d_i$ is the number operator for doubly occupied states.

The sum of occupation numbers is one showing that there exists a particle on the site. We exclude double occupancy following Pauli exclusion principle. Eq. (4.3) now becomes;

$$C_{i\sigma}^+ = \not{c}_{i\sigma}^+ b_i \quad (4.5)$$

The Heisenberg exchange term written in terms of fermion operators is given by

(Baskaran et al, 1987);

$$S_i \cdot S_j = -\frac{1}{4} \not{c}_{i\sigma}^+ \not{c}_{j\sigma} \not{c}_{j\beta}^+ \not{c}_{i\beta} - \frac{1}{4} (\not{c}_{i\uparrow}^+ \not{c}_{j\downarrow}^+ - \not{c}_{i\downarrow}^+ \not{c}_{j\uparrow}^+) (\not{c}_{j\downarrow} \not{c}_{i\uparrow} - \not{c}_{j\uparrow} \not{c}_{i\downarrow}) + \frac{1}{4} (\not{c}_{i\sigma}^+ \not{c}_{i\sigma}) \quad (4.6)$$

The number operators n_i and n_j are given by;

$$n_i = (1 - b_i^+ b_i) \quad (4.7)$$

And

$$n_j = (1 - b_j^+ b_j) \quad (4.8)$$

Thus, their product is;

$$n_i n_j = (1 - b_i^+ b_i)(1 - b_j^+ b_j) \quad (4.9)$$

Substituting eqn. 4.5 and its Hermitian conjugate, eqns. 4.6 and 4.9 in eqn. 4.1 we obtain the t-J Hamiltonian as;

$$\begin{aligned}
H_{t-J} = \sum_{ij} J \left\{ -\frac{1}{4} \psi_{i\sigma}^+ \psi_{j\sigma} \psi_{j\beta}^+ \psi_{i\beta} - \frac{1}{4} (\psi_{i\uparrow}^+ \psi_{j\downarrow}^+ - \psi_{i\downarrow}^+ \psi_{j\uparrow}^+) (\psi_{j\downarrow} \psi_{i\uparrow} - \psi_{j\uparrow} \psi_{i\downarrow}) + \frac{1}{4} (\psi_{i\sigma}^+ \psi_{i\sigma}) \right. \\
\left. - \frac{1}{4} (1 - b_i^+ b_i) (1 - b_j^+ b_j) \right\} \\
- \sum_{ij,\sigma} t_{ij} (\psi_{i\sigma}^+ b_i \psi_{j\sigma} b_j^+ + \psi_{i\sigma} b_i^+ \psi_{j\sigma}^+ b_j) \quad (4.10)
\end{aligned}$$

4.2 The canonical transformation

In order to obtain the quasi particles of the Hamiltonian given in eqn. 4.10, we have to diagonalize the Hamiltonian, by performing a canonical transformation that will convert the old operators into new operators that obey the same commutation laws. The most convenient way to do this is by use of the Bogoliubov- Volatin transformation (Khanna, 2008). This approach allows us to convert fermion $\psi_{i\sigma}$ or boson b_i operators into quasi-particle operators $\gamma_{i\sigma}$ that govern the superconducting state in such a way that the quasi-particle operators obey the same commutation laws of the fermions or bosons.

In eqn. 4.10, we single out the following operators;

- i. $\psi_{i\sigma} = \psi_{i\uparrow}$
- ii. $\psi_{j\sigma} = \psi_{j\uparrow}$
- iii. $\psi_{i\beta} = \psi_{i\downarrow}$
- iv. $\psi_{j\beta} = \psi_{j\downarrow}$
- v. b_i

vi. b_j

These operators together with their conjugates can be classified into two categories

(a) Electron operators, $f_{i\beta j\uparrow\downarrow\sigma}$

(b) Boson operators b_{ij}

In the canonical transformation, we define new operators for each category as follows;

(a) **Electron operators**

Let the new operators, $\gamma_{i\sigma}$ be defined in terms of the old operators, $f_{i\sigma}$ as;

$$i. \quad \gamma_{i\sigma} = U_{i\sigma} f_{i\sigma} - V_{i\sigma} f_{i\sigma}^+ \quad \text{and} \quad \gamma_{i\sigma'} = U_{i\sigma} f_{i\sigma'} + V_{i\sigma} f_{i\sigma}^+ \quad (4.11)$$

The complex conjugates of the operators in eq. 4.11 are;

$$\gamma_{i\sigma}^+ = U_{i\sigma} f_{i\sigma}^+ - V_{i\sigma} f_{i\sigma'} \quad \text{and} \quad \gamma_{i\sigma'}^+ = U_{i\sigma} f_{i\sigma'}^+ + V_{i\sigma} f_{i\sigma} \quad (4.12)$$

$$ii. \quad \gamma_{j\sigma} = U_{j\sigma} f_{j\sigma} - V_{j\sigma} f_{j\sigma'}^+ \quad \text{and} \quad \gamma_{j\sigma'} = U_{j\sigma} f_{j\sigma'} + V_{j\sigma} f_{j\sigma}^+ \quad (4.13)$$

Their complex conjugates are;

$$\gamma_{j\sigma}^+ = U_{j\sigma} f_{j\sigma}^+ - V_{j\sigma} f_{j\sigma'} \quad \text{and} \quad \gamma_{j\sigma'}^+ = U_{j\sigma} f_{j\sigma'}^+ + V_{j\sigma} f_{j\sigma} \quad (4.14)$$

The constants U_k and V_k are screened Coulomb repulsion term and the electron interaction term respectively (Khanna, 2008). A positive value of V_k corresponds to a net attractive interaction between electrons, a condition that is necessary for superconductivity to occur. A suitable choice of these constants will enable us to

eliminate the off-diagonal terms of the Hamiltonian. They are chosen to be real and positive constants and for fermions, they obey the condition that;

$$U_k^2 + V_k^2 = 1 \quad (4.15)$$

With this condition, the new and old operators obey the same fermion anti-commutation relations such that;

$$\{\gamma_k, \gamma_{k'}\} = \{\gamma_k, \gamma_{-k}\} = \{\gamma_k^+, \gamma_{-k}^+\} = 0 \quad (4.16)$$

And

$$\{\gamma_k^+, \gamma_{k'}\} = \{\gamma_{-k}^+, \gamma_{-k'}\} = \delta_{kk'} = \begin{cases} 1, & k = k' \\ 0, & k \neq k' \end{cases} \quad (4.17)$$

(b) Boson operators

Let the new boson operators \mathcal{b}_i be defined in terms of the old operators b_i as;

$$\text{i. } \mathcal{b}_i = U_i b_i - V_i b_i^+ \quad (4.18)$$

The complex conjugate of the boson operator in eq. 4.18 is;

$$\mathcal{b}_i^+ = U_i b_i^+ - V_i b_i \quad (4.19)$$

$$\text{ii. } \mathcal{b}_j = U_j b_j - V_j b_j^+ \quad (4.20)$$

The complex conjugate is;

$$\mathcal{b}_j^+ = U_j b_j^+ - V_j b_j \quad (4.21)$$

For this canonical transformation, the new and old boson operators obey the same commutation relations such that;

$$[\mathcal{b}_k^+, \mathcal{b}_{k'}^+] = [\mathcal{b}_k, \mathcal{b}_{-k}] = [\mathcal{b}_k, \mathcal{b}_{k'}] = 0 \quad (4.22)$$

And

$$[\mathcal{b}_k, \mathcal{b}_{k'}^+] = [\mathcal{b}_k, \mathcal{b}_{-k}^+] = \delta_{kk'} = \begin{cases} 0, k \neq k' \\ 1, k = k' \end{cases} \quad (4.23)$$

The constants U_k and V_k are real and for bosons, they obey the condition that;

$$\begin{aligned} U_k^2 - V_k^2 \\ = 1 \end{aligned} \quad (4.24)$$

4.3 Inverse transformation

The inverse transformation of the electron and boson operators in eqs. 4.11 to 4.21 is obtained as follows;

We multiply eq. 4.11 by $U_{i\sigma}$ and eq. 4.12 by $V_{i\sigma}$ to obtain;

$$U_{i\sigma}\gamma_{i\sigma} = U_{i\sigma}^2\mathcal{f}_{i\sigma} - U_{i\sigma}V_{i\sigma}\mathcal{f}_{i\sigma}^+ \quad (4.25)$$

And

$$U_{i\sigma}\gamma_{i\sigma'} = U_{i\sigma}^2\mathcal{f}_{i\sigma'} + U_{i\sigma}V_{i\sigma}\mathcal{f}_{i\sigma}^+ \quad (4.26)$$

$$V_{i\sigma}\gamma_{i\sigma}^+ = U_{i\sigma}V_{i\sigma}\mathcal{f}_{i\sigma}^+ - V_{i\sigma}^2\mathcal{f}_{i\sigma'} \quad (4.27)$$

And

$$V_{i\sigma}\gamma_{i\sigma'}^+ = U_{i\sigma}V_{i\sigma}\mathcal{f}_{i\sigma'}^+ + V_{i\sigma}^2\mathcal{f}_{i\sigma} \quad (4.28)$$

Adding eq. (4.25) and eq. (4.28), we obtain;

$$U_{i\sigma}\gamma_{i\sigma} + V_{i\sigma}\gamma_{i\sigma}^+ = (U_{i\sigma}^2 + V_{i\sigma}^2)\mathcal{f}_{i\sigma} \quad (4.29)$$

Substituting eq. (4.15) in eq. (4.29) we get;

$$\mathcal{f}_{i\sigma} = U_{i\sigma}\gamma_{i\sigma} + V_{i\sigma}\gamma_{i\sigma}^+ \quad (4.30)$$

Eq.(4.30) gives the inverse transformation of the electron operator. To obtain the inverse transformation of boson operator, we multiply eq. (4.18) by U_i and eq. (4.19) by V_i to get;

$$U_i\mathcal{b}_i = U_i^2b_i - U_iV_ib_i^+ \quad (4.31)$$

And

$$V_i\mathcal{b}_i^+ = U_iV_ib_i^+ - V_i^2b_i \quad (4.32)$$

Adding eq. (4.31) to eq. (4.32) and using eq. (4.24) we get;

$$b_i = U_i\mathcal{b}_i + V_i\mathcal{b}_i^+ \quad (4.32a)$$

Eq. (4.32a) is the inverse transformation of boson operator.

Using the above information we now obtain the inverse transformations of all the electron and boson operators as enlisted below;

$$i. \quad \mathcal{f}_{i\sigma} = U_{i\sigma}\gamma_{i\sigma} + V_{i\sigma}\gamma_{i\sigma}^+ \quad \text{and} \quad \mathcal{f}_{i\sigma'} = U_{i\sigma}\gamma_{i\sigma'} - V_{i\sigma}\gamma_{i\sigma}^+ \quad (4.33)$$

The complex conjugates of the operators are;

$$\mathcal{f}_{i\sigma}^+ = U_{i\sigma}\gamma_{i\sigma}^+ + V_{i\sigma}\gamma_{i\sigma'} \quad \text{and} \quad \mathcal{f}_{i\sigma'}^+ = U_{i\sigma}\gamma_{i\sigma'}^+ - V_{i\sigma}\gamma_{i\sigma} \quad (4.34)$$

$$ii. \quad \mathcal{f}_{j\sigma} = U_{j\sigma}\gamma_{j\sigma} + V_{j\sigma}\gamma_{j\sigma'}^+ \quad \text{and} \quad \mathcal{f}_{j\sigma'} = U_{j\sigma}\gamma_{j\sigma'} - V_{j\sigma}\gamma_{j\sigma}^+ \quad (4.35)$$

Their complex conjugates are;

$$f_{j\sigma}^+ = U_{j\sigma}\gamma_{j\sigma}^+ + V_{j\sigma}\gamma_{j\sigma'} \quad \text{and} \quad f_{j\sigma'}^+ = U_{j\sigma}\gamma_{j\sigma'}^+ - V_{j\sigma}\gamma_{j\sigma} \quad (4.36)$$

$$\text{iii.} \quad b_i = U_i\ell_i + V_i\ell_i^+ \quad (4.37)$$

The complex conjugate is;

$$b_i^+ = U_i\ell_i^+ + V_i\ell_i \quad (4.38)$$

$$\text{iv.} \quad b_j = U_j\ell_j + V_j\ell_j^+ \quad (4.39)$$

The complex conjugate is;

$$b_j^+ = U_j\ell_j^+ + V_j\ell_j \quad (4.40)$$

Using eqs. (4.33) – (4.40) in eq. (4.10), we obtain;

$$\begin{aligned}
H_{t-J} = \sum_{ij} J \left\{ -\frac{1}{4} \left[(U_{i\sigma}\gamma_{i\sigma}^+ + V_{i\sigma}\gamma_{i\sigma'}) (U_{j\sigma}\gamma_{j\sigma} + V_{j\sigma}\gamma_{j\sigma'}^+) (U_{j\sigma}\gamma_{j\sigma'}^+ - V_{j\sigma}\gamma_{j\sigma}) (U_{i\sigma}\gamma_{i\sigma'} \right. \right. \\
- V_{i\sigma}\gamma_{i\sigma}^+) \left. \right] \\
- \frac{1}{4} \left[(U_{i\sigma}\gamma_{i\sigma}^+ + V_{i\sigma}\gamma_{i\sigma'}) (U_{j\sigma}\gamma_{j\sigma'}^+ - V_{j\sigma}\gamma_{j\sigma}) \right. \\
- (U_{i\sigma}\gamma_{i\sigma'}^+ - V_{i\sigma}\gamma_{i\sigma}) (U_{j\sigma}\gamma_{j\sigma} + V_{j\sigma}\gamma_{j\sigma'}^+) \left. \right] \left[(U_{j\sigma}\gamma_{j\sigma'} - V_{j\sigma}\gamma_{j\sigma}^+) (U_{j\sigma}\gamma_{j\sigma} \right. \\
+ V_{j\sigma}\gamma_{j\sigma'}^+) - (U_{j\sigma}\gamma_{j\sigma} + V_{j\sigma}\gamma_{j\sigma'}^+) (U_{j\sigma}\gamma_{j\sigma'} - V_{j\sigma}\gamma_{j\sigma}^+) \left. \right] \\
+ \frac{1}{4} \left[(U_{i\sigma}\gamma_{i\sigma}^+ + V_{i\sigma}\gamma_{i\sigma'}) (U_{i\sigma}\gamma_{i\sigma} + V_{i\sigma}\gamma_{i\sigma}') \right] \\
- \frac{1}{4} \left[1 - (U_i\mathfrak{b}_i^+ + V_i\mathfrak{b}_i) (U_i\mathfrak{b}_i + V_i\mathfrak{b}_i^+) \right] \left[1 \right. \\
- (U_j\mathfrak{b}_j^+ + V_j\mathfrak{b}_j) (U_j\mathfrak{b}_j + V_j\mathfrak{b}_j^+) \left. \right] \left. \right\} \\
- \sum_{ij,\sigma} t_{ij} \left\{ (U_{i\sigma}\gamma_{i\sigma}^+ + V_{i\sigma}\gamma_{i\sigma'}) (U_i\mathfrak{b}_i + V_i\mathfrak{b}_i^+) (U_{j\sigma}\gamma_{j\sigma} + V_{j\sigma}\gamma_{j\sigma'}^+) (U_j\mathfrak{b}_j^+ \right. \\
+ V_j\mathfrak{b}_j) \\
+ (U_{i\sigma}\gamma_{i\sigma} + V_{i\sigma}\gamma_{i\sigma}') (U_i\mathfrak{b}_i^+ + V_i\mathfrak{b}_i) (U_{j\sigma}\gamma_{j\sigma}^+ + V_{j\sigma}\gamma_{j\sigma'}) (U_j\mathfrak{b}_j \\
+ V_j\mathfrak{b}_j^+) \left. \right\} \quad (4.41)
\end{aligned}$$

We now represent the particle spin up state with k and spin down with $-k$. The scattered particle spin states will be represented by k' and $-k'$ for spin up and spin down, respectively. It should also be noted that for the superconducting state, electrons in neighboring sites have opposite spins, thus while the electron in i -th state will be considered to be in spin up, the electron in j -th state will be in spin down mode. Applying this condition to eq. (4.41), we have;

$$\begin{aligned}
H_{t-J} = \sum_{k,-k} J \left\{ -\frac{1}{4} [(U_k \gamma_k^+ + V_{k'} \gamma_{k'}) (U_{-k} \gamma_{-k} + V_{-k'} \gamma_{-k}') (U_{-k'} \gamma_{-k'}^+ - V_{-k} \gamma_{-k}) (U_{k'} \gamma_{k'} \right. \\
- V_k \gamma_k^+)] \\
- \frac{1}{4} [(U_k \gamma_k^+ + V_{k'} \gamma_{k'}) (U_{-k'} \gamma_{-k'}^+ - V_{-k} \gamma_{-k}) \\
- (U_{k'} \gamma_{k'}^+ - V_k \gamma_k) (U_{-k} \gamma_{-k}^+ + V_{-k'} \gamma_{-k}')] [(U_{-k'} \gamma_{-k'} - V_{-k} \gamma_{-k}^+) (U_{-k} \gamma_{-k} \\
+ V_{-k'} \gamma_{-k}') - (U_{-k} \gamma_{-k} + V_{-k'} \gamma_{-k}') (U_{-k'} \gamma_{-k'} - V_{-k} \gamma_{-k}^+)] \\
+ \frac{1}{4} [(U_{k'} \gamma_{k'}^+ + V_{k'} \gamma_{k'}) (U_k \gamma_k + V_{k'} \gamma_{k'}^+)] \\
- \frac{1}{4} [1 - (U_k \mathfrak{b}_k^+ + V_k \mathfrak{b}_k) (U_k \mathfrak{b}_k + V_k \mathfrak{b}_k^+)] [1 \\
- (U_k \mathfrak{b}_k^+ + V_k \mathfrak{b}_k) (U_k \mathfrak{b}_k + V_k \mathfrak{b}_k^+)] \} \\
- \sum_{kk'} t_{kk'} \{ (U_k \gamma_k^+ + V_{k'} \gamma_{k'}) (U_k \mathfrak{b}_k + V_k \mathfrak{b}_k^+) (U_{-k} \gamma_{-k} + V_{-k'} \gamma_{-k}') (U_K \mathfrak{b}_K^+ \\
+ V_K \mathfrak{b}_K) \\
+ (U_k \gamma_k + V_{k'} \gamma_{k'}^+) (U_k \mathfrak{b}_k^+ + V_k \mathfrak{b}_k) (U_{-k} \gamma_{-k}^+ + V_{-k'} \gamma_{-k}') (U_K \mathfrak{b}_K \\
+ V_K \mathfrak{b}_K^+) \} \tag{4.42}
\end{aligned}$$

Eq. 4.42 has ten terms to be expanded in the process of diagonalization. We will progress step by step;

$$\begin{aligned}
\text{i. } & [(U_k \gamma_k^+ + V_{k'} \gamma_{k'}) (U_{-k} \gamma_{-k} + V_{-k'} \gamma_{-k'}^+) (U_{-k'} \gamma_{-k'}^+ - V_{-k} \gamma_{-k}) (U_{k'} \gamma_{k'} - \\
& V_k \gamma_k^+)] = (U_k U_{-k} \gamma_k^+ \gamma_{-k} + U_k V_{-k'} \gamma_k^+ \gamma_{-k'}^+ + V_{k'} U_{-k} \gamma_{k'} \gamma_{-k} + V_{k'} V_{-k'} \gamma_{k'} \gamma_{-k'}^+) \\
& (U_{-k'} U_{k'} \gamma_{-k'}^+ \gamma_{k'} - V_{-k} U_{k'} \gamma_{-k} \gamma_{k'} - U_{-k'} V_k \gamma_{-k'}^+ \gamma_k^+ \\
& + V_{-k} V_k \gamma_{-k} \gamma_k^+) \quad (4.43)
\end{aligned}$$

Equation 4.43 can be simplified using a new pair of number operators (Khanna, 2008)

$$m_k = \gamma_k^+ \gamma_k \text{ and } m_{-k} = \gamma_{-k}^+ \gamma_{-k} \quad (4.44)$$

$$\text{Such that } 1 - m_k = \gamma_k \gamma_k^+ \text{ and } 1 - m_{-k} = \gamma_{-k} \gamma_{-k}^+ \quad (4.45)$$

Substituting eqs. (4.44) and (4.45) in eq. (4.43) we obtain;

$$\begin{aligned}
& [U_k U_{-k} m_k + V_k U_{-k} \gamma_{k'} \gamma_{-k} + U_k V_{-k'} \gamma_k^+ \gamma_{-k'}^+ + V_{k'} V_{-k'} (1 - m_{k'})] \\
& [U_{-k'} U_{k'} m_{-k'} - U_{-k'} V_k \gamma_{-k'}^+ \gamma_k^+ - V_{-k} U_{k'} \gamma_{-k} \gamma_{k'} + V_{-k} V_k (1 - m_{-k})] \\
= & U_k U_{-k} U_{-k'} U_{k'} m_k m_{-k'} - U_k U_{-k} m_k U_{-k'} V_k \gamma_{-k'}^+ \gamma_k^+ - U_k U_{-k} m_k V_{-k} U_{k'} \gamma_{-k} \gamma_{k'} \\
& + U_k U_{-k} m_k V_{-k} V_k (1 - m_{-k}) + V_k U_{-k} U_{-k'} U_{k'} m_{-k'} \gamma_{k'} \gamma_{-k} \\
& - V_k U_{-k} U_{-k'} V_k \gamma_{k'} \gamma_{-k} \gamma_{-k'}^+ \gamma_k^+ - V_k U_{-k} V_{-k} U_{k'} \gamma_{k'} \gamma_{-k} \gamma_{-k} \gamma_{k'} \\
& + V_k U_{-k} V_{-k} V_k (1 - m_{-k}) \gamma_{k'} \gamma_{-k} + U_k V_{-k'} U_{-k'} U_{k'} m_{-k'} \gamma_k^+ \gamma_{-k'}^+ \\
& - U_k V_{-k'} U_{-k'} V_k \gamma_k^+ \gamma_{-k'}^+ \gamma_{-k'}^+ \gamma_k^+ - U_k V_{-k'} V_{-k} U_{k'} \gamma_k^+ \gamma_{-k'}^+ \gamma_{-k} \gamma_{k'} \\
& + U_k V_{-k'} V_{-k} V_k (1 - m_{-k}) \gamma_k^+ \gamma_{-k'}^+ + V_{k'} V_{-k'} (1 - m_{k'}) U_{-k'} U_{k'} m_{-k'} \\
& - V_{k'} V_{-k'} (1 - m_{k'}) U_{-k'} V_k \gamma_{-k'}^+ \gamma_k^+ - V_{k'} V_{-k'} (1 \\
& - m_{k'}) V_{-k} U_{k'} \gamma_{-k} \gamma_{k'} + V_{k'} V_{-k'} (1 - m_{k'}) V_{-k} V_k (1 - m_{-k}) \quad (4.46)
\end{aligned}$$

$$\begin{aligned}
\text{ii. } & (U_k \gamma_k^+ + V_{k'} \gamma_{k'}') (U_{-k'} \gamma_{-k'}^+ - V_{-k} \gamma_{-k}) \\
& = U_k U_{-k'} \gamma_k^+ \gamma_{-k'}^+ - U_k V_{-k} \gamma_k^+ \gamma_{-k} + V_{k'} U_{-k'} \gamma_{k'} \gamma_{-k'}^+ - V_{k'} V_{-k} \gamma_{k'} \gamma_{-k}
\end{aligned}$$

Substituting eqs. (4.44) and (4.45) we have;

$$\begin{aligned}
& (U_k \gamma_k^+ + V_{k'} \gamma_{k'}') (U_{-k'} \gamma_{-k'}^+ - V_{-k} \gamma_{-k}) \\
& = U_k U_{-k'} \gamma_k^+ \gamma_{-k'}^+ - U_k V_{-k} m_k + V_{k'} U_{-k'} (1 - m_{k'}) - V_{k'} V_{-k} \gamma_{k'} \gamma_{-k} \quad (4.47)
\end{aligned}$$

$$\begin{aligned}
\text{iii. } & (U_{k'} \gamma_{k'}^+ - V_k \gamma_k) (U_{-k} \gamma_{-k}^+ + V_{-k'} \gamma_{-k'}') \\
& = U_{k'} U_{-k} \gamma_{k'}^+ \gamma_{-k}^+ + U_{k'} V_{-k'} \gamma_{k'}^+ \gamma_{-k'}' - V_k U_{-k} \gamma_k \gamma_{-k}^+ - V_k V_{-k'} \gamma_k \gamma_{-k'}'
\end{aligned}$$

Substituting eqs. (4.44) and (4.46) we obtain;

$$\begin{aligned}
& (U_{k'} \gamma_{k'}^+ - V_k \gamma_k) (U_{-k} \gamma_{-k}^+ + V_{-k'} \gamma_{-k'}') \\
& = U_{k'} U_{-k} \gamma_{k'}^+ \gamma_{-k}^+ + U_{k'} V_{-k'} m_{k'} - V_k U_{-k} (1 - m_k) - V_k V_{-k'} \gamma_k \gamma_{-k'}' \quad (4.48)
\end{aligned}$$

$$\begin{aligned}
\text{iv. } & (U_{-k'} \gamma_{-k'}' - V_{-k} \gamma_{-k}^+) (U_{-k} \gamma_{-k} + V_{-k'} \gamma_{-k'}^+) \\
& = U_{-k'} U_{-k} \gamma_{-k'}' \gamma_{-k} + U_{-k'} V_{-k'} \gamma_{-k'}' \gamma_{-k'}^+ - V_{-k} U_{-k} \gamma_{-k}^+ \gamma_{-k} - V_{-k} V_{-k'} \gamma_{-k}^+ \gamma_{-k'}^+
\end{aligned}$$

Using eqs. (4.44) and (4.45),

$$\begin{aligned}
& (U_{-k'} \gamma_{-k'}' - V_{-k} \gamma_{-k}^+) (U_{-k} \gamma_{-k} + V_{-k'} \gamma_{-k'}^+) \\
& = U_{-k'} U_{-k} \gamma_{-k'}' \gamma_{-k} + U_{-k'} V_{-k'} (1 - m_{k'}) - V_{-k} U_{-k} m_{-k} - V_{-k} V_{-k'} \gamma_{-k}^+ \gamma_{-k'}^+ \quad (4.49)
\end{aligned}$$

$$\begin{aligned}
\text{v. } & (U_{-k} \gamma_{-k} + V_{-k'} \gamma_{-k'}^+) (U_{-k'} \gamma_{-k'}' - V_{-k} \gamma_{-k}^+) = \\
& U_{-k} U_{-k'} \gamma_{-k} \gamma_{-k'}' - U_{-k} V_{-k} \gamma_{-k} \gamma_{-k}^+ + V_{-k'} U_{-k'} \gamma_{-k'}^+ \gamma_{-k'}' - V_{-k'} V_{-k} \gamma_{-k'}^+ \gamma_{-k}^+
\end{aligned}$$

Substituting eqs. (4.44) and (4.45);

$$\begin{aligned}
& (U_{-k}\gamma_{-k} + V_{-k'}\gamma_{-k'}^+)(U_{-k'}\gamma_{-k'} - V_{-k}\gamma_{-k}^+) \\
&= U_{-k}U_{-k'}\gamma_{-k}\gamma_{-k'} - U_{-k}V_{-k}(1 - m_k) + V_{-k'}U_{-k'}m_{-k'} \\
& - V_{-k'}V_{-k}\gamma_{-k'}^+\gamma_{-k}^+ \tag{4.50}
\end{aligned}$$

$$\begin{aligned}
\text{vi. } & (U_{k'}\gamma_{k'}^+ + V_{k'}\gamma_{-k'}) (U_k\gamma_k + V_{k'}\gamma_{k'}^+) = U_{k'}U_k\gamma_{k'}^+\gamma_k + U_{k'}V_{k'}\gamma_{k'}^+\gamma_{k'}^+ + \\
& V_{k'}U_k\gamma_{-k'}\gamma_k + V_{k'}V_{k'}\gamma_{-k'}\gamma_{k'}^+
\end{aligned}$$

Substituting eqs. (4.44) and (4.45);

$$\begin{aligned}
& (U_{k'}\gamma_{k'}^+ + V_{k'}\gamma_{-k'}) (U_k\gamma_k + V_{k'}\gamma_{k'}^+) \\
&= U_{k'}U_k m_{k'} + U_{k'}V_{k'}\gamma_{k'}^+\gamma_{k'}^+ + V_{k'}U_k\gamma_{-k'}\gamma_k + V_{k'}V_{k'}(1 - m_{-k'}) \tag{4.51}
\end{aligned}$$

$$\begin{aligned}
\text{vii. } & (U_k\mathfrak{b}_k^+ + V_k\mathfrak{b}_k)(U_k\mathfrak{b}_k + V_k\mathfrak{b}_k^+) \\
&= U_k^2\mathfrak{b}_k^+\mathfrak{b}_k + U_kV_k\mathfrak{b}_k^+\mathfrak{b}_k^+ + V_kU_k\mathfrak{b}_k\mathfrak{b}_k + V_k^2\mathfrak{b}_k\mathfrak{b}_k^+ \tag{4.52}
\end{aligned}$$

Let the boson number operator n_k be defined as;

$$n_k = \mathfrak{b}_k^+\mathfrak{b}_k, \text{ such that } 1 - n_k = \mathfrak{b}_k\mathfrak{b}_k^+ \tag{4.53}$$

Using eq. (4.53) in eq. (4.52) we obtain;

$$(U_k\mathfrak{b}_k^+ + V_k\mathfrak{b}_k)(U_k\mathfrak{b}_k + V_k\mathfrak{b}_k^+) = V_k^2 + (U_k^2 - V_k^2)n_k + U_kV_k(\mathfrak{b}_k^+\mathfrak{b}_k^+ + \mathfrak{b}_k\mathfrak{b}_k) \tag{4.54}$$

viii. $(U_k \mathfrak{b}_k^+ + V_k \mathfrak{b}_k)(U_k \mathfrak{b}_k + V_k \mathfrak{b}_k^+) = V_k^2 + (U_k^2 - V_k^2)n_k + U_k V_k (\mathfrak{b}_k^+ \mathfrak{b}_k^+ + \mathfrak{b}_k \mathfrak{b}_k)$. This equation is the same as eq. (4.54).

ix. $(U_k \gamma_k^+ + V_{k'} \gamma_{k'}) (U_k \mathfrak{b}_k + V_k \mathfrak{b}_k^+) (U_{-K} \gamma_{-K} + V_{-k'} \gamma_{-k'}^+) (U_K \mathfrak{b}_K^+ + V_K \mathfrak{b}_K)$

$$= (U_k^2 \gamma_k^+ \mathfrak{b}_k + U_k V_k \gamma_k^+ \mathfrak{b}_k^+ + V_{k'} U_k \gamma_{k'} \mathfrak{b}_k + V_{k'} V_k \gamma_{k'} \mathfrak{b}_k^+)$$

$$(U_{-K} U_K \gamma_{-K} \mathfrak{b}_K^+ + U_{-K} V_K \gamma_{-K} \mathfrak{b}_K + V_{-k'} U_K \gamma_{-k'}^+ \mathfrak{b}_K^+ + V_{-k'} V_K \gamma_{-k'}^+ \mathfrak{b}_K) \quad (4.55)$$

We define new number operators for a mixture of fermions and bosons as;

$$\eta_k = \gamma_k^+ \mathfrak{b}_k, \quad \eta_{-k} = \gamma_{-k}^+ \mathfrak{b}_k, \quad \text{and} \quad 1 - \eta_k = \gamma_k \mathfrak{b}_k^+, \quad 1 - \eta_{-k} = \gamma_{-k} \mathfrak{b}_k^+ \quad (4.56)$$

$$\eta_{k'} = \gamma_{k'}^+ \mathfrak{b}_{k'}, \quad 1 - \eta_{k'} = \gamma_{k'} \mathfrak{b}_{k'}^+ \quad \text{and} \quad \eta_{-k'} = \gamma_{-k'}^+ \mathfrak{b}_{k'} \quad ,$$

$$1 - \eta_{-k'} = \gamma_{-k'} \mathfrak{b}_{k'}^+ \quad (4.57)$$

Using eqs. (4.56) and (4.57) in eq. (4.55), we obtain;

$$(U_k \gamma_k^+ + V_{k'} \gamma_{k'}) (U_k \mathfrak{b}_k + V_k \mathfrak{b}_k^+) (U_{-K} \gamma_{-K} + V_{-k'} \gamma_{-k'}^+) (U_K \mathfrak{b}_K^+ + V_K \mathfrak{b}_K)$$

$$= [U_k^2 \eta_k + U_k V_k \gamma_k^+ \mathfrak{b}_k^+ + V_{k'} U_k \gamma_{k'} \mathfrak{b}_k + V_{k'} V_k (1 - \eta_{k'})]$$

$$[U_{-K} U_K (1 - \eta_{-k}) + U_{-K} V_K \gamma_{-K} \mathfrak{b}_K + V_{-k'} U_K \gamma_{-k'}^+ \mathfrak{b}_K^+ + V_{-k'} V_K \eta_{-k'}]$$

$$\begin{aligned}
&= U_k^2 \eta_k U_{-K} U_K (1 - \eta_{-k}) + U_k^2 \eta_k U_{-K} V_K \gamma_{-K} \mathcal{B}_K + U_k^2 \eta_k V_{-k'} U_K \gamma_{-k'}^+ \mathcal{B}_K^+ \\
&\quad + U_k^2 \eta_k V_{-k'} V_K \eta_{-k'} + U_k V_k U_{-K} U_K (1 - \eta_{-k}) \gamma_k^+ \mathcal{B}_k^+ \\
&\quad + U_k V_k U_{-K} V_K \gamma_k^+ \mathcal{B}_k^+ \gamma_{-K} \mathcal{B}_K + U_k V_k V_{-k'} U_K \gamma_k^+ \mathcal{B}_k^+ \gamma_{-k'}^+ \mathcal{B}_K^+ \\
&\quad + U_k V_k V_{-k'} V_K \eta_{-k'} \gamma_k^+ \mathcal{B}_k^+ + V_{k'} U_k U_{-K} U_K (1 - \eta_{-k}) \gamma_{k'} \mathcal{B}_k \\
&\quad + V_{k'} U_k U_{-K} V_K \gamma_{k'} \mathcal{B}_k \gamma_{-K} \mathcal{B}_K + V_{k'} U_k V_{-k'} U_K \gamma_{k'} \mathcal{B}_k \gamma_{-k'}^+ \mathcal{B}_K^+ \\
&\quad + V_{k'} U_k V_{k'} V_k (\eta_{k'}) \gamma_{k'} \mathcal{B}_k + V_{k'} V_k (1 - \eta_{k'}) U_{-K} U_K (1 - \eta_{-k}) \\
&\quad + V_{k'} V_k (1 - \eta_{k'}) U_{-K} V_K \gamma_{-K} \mathcal{B}_K + V_{k'} V_k (1 - \eta_{k'}) V_{-k'} U_K \gamma_{-k'}^+ \mathcal{B}_K^+ \\
&\quad + V_{k'} V_k (1 - \eta_{k'}) V_{-k'} V_K \eta_{-k'} \tag{4.58}
\end{aligned}$$

$$\begin{aligned}
\text{x. } & (U_k \gamma_k + V_{k'} \gamma_{k'}^+) (U_k \mathcal{B}_k^+ + V_k \mathcal{B}_k) (U_{-K} \gamma_{-K}^+ + V_{-k'} \gamma_{-k'}) (U_K \mathcal{B}_K + V_K \mathcal{B}_K^+) \\
&= [U_k^2 \gamma_k \mathcal{B}_k^+ + U_k V_k \gamma_k \mathcal{B}_k + V_{k'} U_k \gamma_{k'}^+ \mathcal{B}_k^+ + V_{k'} V_k \gamma_{k'}^+ \mathcal{B}_k] \\
& [U_{-K} U_K \gamma_{-K}^+ \mathcal{B}_K + U_{-K} V_K \gamma_{-K}^+ \mathcal{B}_K^+ + V_{-k'} U_K \gamma_{-k'} \mathcal{B}_K + V_{-k'} V_K \gamma_{-k'} \mathcal{B}_K^+] \tag{4.59}
\end{aligned}$$

Substituting eqs. (4.56) and (4.57) in eq. (4.59), we get the following equation;

$$\begin{aligned}
& (U_k \gamma_k + V_{k'} \gamma_{k'}^+) (U_k \mathcal{B}_k^+ + V_k \mathcal{B}_k) (U_{-K} \gamma_{-K}^+ + V_{-k'} \gamma_{-k'}) (U_K \mathcal{B}_K + V_K \mathcal{B}_K^+) \\
&= [U_k^2 (1 - \eta_k) + U_k V_k \gamma_k \mathcal{B}_k + V_{k'} U_k \gamma_{k'}^+ \mathcal{B}_k^+ + V_{k'} V_k \eta_{k'}] \\
& [U_{-K} U_K \eta_{-k} + U_{-K} V_K \gamma_{-K}^+ \mathcal{B}_K^+ + V_{-k'} U_K \gamma_{-k'} \mathcal{B}_K + V_{-k'} V_K (1 - \eta_{-k'})]
\end{aligned}$$

$$\begin{aligned}
&= U_k^2(1 - \eta_k)U_{-K}U_K\eta_{-k} + U_k^2(1 - \eta_k)U_{-K}V_K\gamma_{-K}^+\mathcal{L}_K^+ + U_k^2(1 - \eta_k)V_{-k'}U_K\gamma_{-k'}\mathcal{L}_K \\
&\quad + U_k^2(1 - \eta_k)V_{-k'}V_K(1 - \eta_{-k'}) + U_kV_kU_{-K}U_K\eta_{-k}\gamma_k\mathcal{L}_k \\
&\quad + U_kV_kU_{-K}V_K\gamma_k\mathcal{L}_k\gamma_{-K}^+\mathcal{L}_K^+ + U_kV_kV_{-k'}U_K\gamma_k\mathcal{L}_k\gamma_{-k'}\mathcal{L}_K \\
&\quad + U_kV_kV_{-k'}V_K(1 - \eta_{-k'})\gamma_k\mathcal{L}_k + V_{k'}U_kU_{-K}U_K\eta_{-k}\gamma_{k'}^+\mathcal{L}_k^+ \\
&\quad + V_{k'}U_kU_{-K}V_K\gamma_{k'}^+\mathcal{L}_k^+\gamma_{-K}^+\mathcal{L}_K^+ + V_{k'}U_kV_{-k'}U_K\gamma_{k'}^+\mathcal{L}_k^+\gamma_{-k'}\mathcal{L}_K \\
&\quad + V_{k'}U_kV_{-k'}V_K(1 - \eta_{-k'})\gamma_{k'}^+\mathcal{L}_k^+ + V_{k'}V_K\eta_{k'}U_{-K}U_K\eta_{-k} \\
&\quad + V_{k'}V_K\eta_{k'}U_{-K}V_K\gamma_{-K}^+\mathcal{L}_K^+ + V_{k'}V_K\eta_{k'}V_{-k'}U_K\gamma_{-k'}\mathcal{L}_K \\
&\quad + V_{k'}V_K\eta_{k'}V_{-k'}V_K(1 - \eta_{-k'}) \tag{4.60}
\end{aligned}$$

Substituting the ten terms numbered i-x in the t-J Hamiltonian, we obtain;

$$\begin{aligned}
H_{t-J} = \sum_{k,-k} J \left\{ & -\frac{1}{4} [U_k U_{-k} U_{-k'} U_{k'} m_k m_{-k'} - U_k U_{-k} m_k U_{-k'} V_k \gamma_{-k'}^+ \gamma_k^+ \right. \\
& - U_k U_{-k} m_k V_{-k} U_{k'} \gamma_{-k} \gamma_{k'} + U_k U_{-k} m_k V_{-k} V_k (1 - m_{-k}) \\
& + V_k U_{-k} U_{-k'} U_{k'} m_{-k'} \gamma_{k'} \gamma_{-k} - V_k U_{-k} U_{-k'} V_k \gamma_{k'} \gamma_{-k} \gamma_{-k'}^+ \gamma_k^+ \\
& - V_k U_{-k} V_{-k} U_{k'} \gamma_{k'} \gamma_{-k} \gamma_{-k} \gamma_{k'} + V_k U_{-k} V_{-k} V_k (1 - m_{-k}) \gamma_{k'} \gamma_{-k} \\
& + U_k V_{-k'} U_{-k'} U_{k'} m_{-k'} \gamma_k^+ \gamma_{-k'}^+ - U_k V_{-k'} U_{-k'} V_k \gamma_k^+ \gamma_{-k'}^+ \gamma_{-k'}^+ \gamma_k^+ \\
& - U_k V_{-k'} V_{-k} U_{k'} \gamma_k^+ \gamma_{-k'}^+ \gamma_{-k} \gamma_{k'} \\
& + U_k V_{-k'} V_{-k} V_k (1 - m_{-k}) \gamma_k^+ \gamma_{-k'}^+ + V_{k'} V_{-k'} (1 - m_{k'}) U_{-k'} U_{k'} m_{-k'} \\
& - V_{k'} V_{-k'} (1 - m_{k'}) U_{-k'} V_k \gamma_{-k'}^+ \gamma_k^+ - V_{k'} V_{-k'} (1 \\
& - m_{k'}) V_{-k} U_{k'} \gamma_{-k} \gamma_{k'} + V_{k'} V_{-k'} (1 - m_{k'}) V_{-k} V_k (1 - m_{-k}) \left. \right] \\
& - \frac{1}{4} [(U_k U_{-k'} \gamma_k^+ \gamma_{-k'}^+ - U_k V_{-k} m_k + V_{k'} U_{-k'} (1 - m_{k'}) - V_{k'} V_{-k} \gamma_{k'} \gamma_{-k}) \\
& - (U_{k'} U_{-k} \gamma_{k'}^+ \gamma_{-k}^+ + U_{k'} V_{-k'} m_{k'} - V_k U_{-k} (1 - m_k) \\
& - V_k V_{-k'} \gamma_k \gamma_{-k'})] [(U_{-k'} U_{-k} \gamma_{-k'} \gamma_{-k} + U_{-k'} V_{-k'} (1 - m_{k'})) \\
& - V_{-k} U_{-k} m_{-k} - V_{-k} V_{-k'} \gamma_{-k}^+ \gamma_{-k'}^+] \\
& - (U_{-k} U_{-k'} \gamma_{-k} \gamma_{-k'} - U_{-k} V_{-k} (1 - m_k) + V_{-k'} U_{-k'} m_{-k'} \\
& - V_{-k'} V_{-k} \gamma_{-k'}^+ \gamma_{-k}^+) \left. \right] \\
& + \frac{1}{4} [U_{k'} U_k m_{k'} + U_{k'} V_{k'} \gamma_{k'}^+ \gamma_{k'}^+ + V_{k'} U_k \gamma_{-k'} \gamma_k + V_{k'} V_{k'} (1 - m_{-k'})] \\
& - \frac{1}{4} [1 - (V_k^2 + (U_k^2 - V_k^2) n_k + U_k V_k (\mathfrak{b}_k^+ \mathfrak{b}_k^+ + \mathfrak{b}_k \mathfrak{b}_k))] [1 - (V_k^2 \\
& + (U_k^2 - V_k^2) n_k + U_k V_k (\mathfrak{b}_k^+ \mathfrak{b}_k^+ + \mathfrak{b}_k \mathfrak{b}_k))] \left. \right\} \\
& - \sum_{kk'} t_{kk'} \{ (U_k^2 \eta_k U_{-k} U_k (1 - \eta_{-k}) + U_k^2 \eta_k U_{-k} V_k \gamma_{-k} \mathfrak{b}_k
\end{aligned}$$

$$\begin{aligned}
& + U_k^2 \eta_k V_{-k'} U_K \gamma_{-k'}^+ \mathcal{B}_K^+ + U_k^2 \eta_k V_{-k'} V_K \eta_{-k'} \\
& + U_k V_k U_{-K} U_K (1 - \eta_{-k}) \gamma_k^+ \mathcal{B}_k^+ + U_k V_k U_{-K} V_K \gamma_k^+ \mathcal{B}_k^+ \gamma_{-K} \mathcal{B}_K \\
& + U_k V_k V_{-k'} U_K \gamma_k^+ \mathcal{B}_k^+ \gamma_{-k'}^+ \mathcal{B}_K^+ + U_k V_k V_{-k'} V_K \eta_{-k'} \gamma_k^+ \mathcal{B}_k^+ \\
& + V_{k'} U_k U_{-K} U_K (1 - \eta_{-k}) \gamma_{k'} \mathcal{B}_k + V_{k'} U_k U_{-K} V_K \gamma_{k'} \mathcal{B}_k \gamma_{-K} \mathcal{B}_K \\
& + V_{k'} U_k V_{-k'} U_K \gamma_{k'} \mathcal{B}_k \gamma_{-k'}^+ \mathcal{B}_K^+ + V_{k'} U_k V_{k'} V_k (1 - \eta_{k'}) \gamma_{k'} \mathcal{B}_k \\
& + V_{k'} V_k (1 - \eta_{k'}) U_{-K} U_K (1 - \eta_{-k}) + V_{k'} V_k (1 - \eta_{k'}) U_{-K} V_K \gamma_{-K} \mathcal{B}_K \\
& + V_{k'} V_k (1 - \eta_{k'}) V_{-k'} U_K \gamma_{-k'}^+ \mathcal{B}_K^+ + V_{k'} V_k (1 - \eta_{k'}) V_{-k'} V_K \eta_{-k'} \\
& + (U_k^2 (1 - \eta_k) U_{-K} U_K \eta_{-k} + U_k^2 (1 - \eta_k) U_{-K} V_K \gamma_{-K}^+ \mathcal{B}_K^+ \\
& + U_k^2 (1 - \eta_k) V_{-k'} U_K \gamma_{-k'} \mathcal{B}_K + U_k^2 (1 - \eta_k) V_{-k'} V_K (1 - \eta_{-k'}) \\
& + U_k V_k U_{-K} U_K \eta_{-k} \gamma_k \mathcal{B}_k + U_k V_k U_{-K} V_K \gamma_k \mathcal{B}_k \gamma_{-K}^+ \mathcal{B}_K^+ \\
& + U_k V_k V_{-k'} U_K \gamma_k \mathcal{B}_k \gamma_{-k'} \mathcal{B}_K + U_k V_k V_{-k'} V_K (1 - \eta_{-k'}) \gamma_k \mathcal{B}_k \\
& + V_{k'} U_k U_{-K} U_K \eta_{-k} \gamma_{k'}^+ \mathcal{B}_k^+ + V_{k'} U_k U_{-K} V_K \gamma_{k'}^+ \mathcal{B}_k^+ \gamma_{-K}^+ \mathcal{B}_K^+ \\
& + V_{k'} U_k V_{-k'} U_K \gamma_{k'}^+ \mathcal{B}_k^+ \gamma_{-k'} \mathcal{B}_K + V_{k'} U_k V_{-k'} V_K (1 - \eta_{-k'}) \gamma_{k'}^+ \mathcal{B}_k^+ \\
& + V_{k'} V_K \eta_{k'} U_{-K} U_K \eta_{-k} + V_{k'} V_K \eta_{k'} U_{-K} V_K \gamma_{-K}^+ \mathcal{B}_K^+ \\
& + V_{k'} V_K \eta_{k'} V_{-k'} U_K \gamma_{-k'} \mathcal{B}_K \\
& + V_{k'} V_K \eta_{k'} V_{-k'} V_K (1 - \eta_{-k'}) \} \} \tag{4.61}
\end{aligned}$$

We can simplify the ten expressions belonging to the t-J Hamiltonian by making two assumptions. First, we assume that the lowest energy state of this system has all the occupation numbers m_k, n_k, η_k equal to zero. Secondly, we consider the effect of the fourth order terms as negligible. Thus the ten expressions reduce to;

$$\begin{aligned}
\text{i. } & [U_k U_{-k} m_k + V_k U_{-k} \gamma_{k'} \gamma_{-k} + U_k V_{-k'} \gamma_k^+ \gamma_{-k'}^+ + V_{k'} V_{-k'} (1 - m_{k'})] \\
& [U_{-k'} U_{k'} m_{-k'} - U_{-k'} V_k \gamma_{-k'}^+ \gamma_k^+ - V_{-k} U_{k'} \gamma_{-k} \gamma_{k'} + V_{-k} V_k (1 - m_{-k})] \\
& = V_k U_{-k} V_{-k} V_k \gamma_{k'} \gamma_{-k} + U_k V_{-k'} V_{-k} V_k \gamma_k^+ \gamma_{-k'}^+ \\
& - V_{k'} V_{-k'} U_{-k'} V_k \gamma_{-k'}^+ \gamma_k^+ - V_{k'} V_{-k'} V_{-k} U_{k'} \gamma_{-k} \gamma_{k'} + V_k V_{-k'} V_{-k} V_k \quad (4.62)
\end{aligned}$$

$$\begin{aligned}
\text{ii. } & (U_k \gamma_k^+ + V_{k'} \gamma_{k'}) (U_{-k'} \gamma_{-k'}^+ - V_{-k} \gamma_{-k}) \\
& = U_k U_{-k'} \gamma_k^+ \gamma_{-k'}^+ + V_{k'} U_{-k'} - V_{k'} V_{-k} \gamma_{k'} \gamma_{-k} \quad (4.63)
\end{aligned}$$

$$\begin{aligned}
\text{iii. } & (U_{k'} \gamma_{k'}^+ - V_k \gamma_k) (U_{-k} \gamma_{-k}^+ + V_{-k'} \gamma_{-k'}) \\
& = U_{k'} U_{-k} \gamma_{k'}^+ \gamma_{-k}^+ - V_k U_{-k} - V_k V_{-k'} \gamma_k \gamma_{-k'} \quad (4.64)
\end{aligned}$$

$$\begin{aligned}
\text{iv. } & (U_{-k'} \gamma_{-k'} - V_{-k} \gamma_{-k}^+) (U_{-k} \gamma_{-k} + V_{-k'} \gamma_{-k'}^+) \\
& = U_{-k'} U_{-k} \gamma_{-k'} \gamma_{-k} + U_{-k'} V_{-k'} - V_{-k} V_{-k'} \gamma_{-k}^+ \gamma_{-k'}^+ \quad (4.65)
\end{aligned}$$

$$\begin{aligned}
\text{v. } & (U_{-k} \gamma_{-k} + V_{-k'} \gamma_{-k'}^+) (U_{-k'} \gamma_{-k'} - V_{-k} \gamma_{-k}^+) \\
& = U_{-k} U_{-k'} \gamma_{-k} \gamma_{-k'} - U_{-k} V_{-k} - V_{-k'} V_{-k} \gamma_{-k'}^+ \gamma_{-k}^+ \quad (4.66)
\end{aligned}$$

$$\begin{aligned}
\text{vi. } & (U_{k'} \gamma_{k'}^+ + V_{k'} \gamma_{-k'}) (U_k \gamma_k + V_{k'} \gamma_{k'}^+) = U_{k'} V_{k'} \gamma_{k'}^+ \gamma_{k'}^+ + V_{k'} U_k \gamma_{-k'} \gamma_k + \\
& V_{k'} V_{k'} \quad (4.67)
\end{aligned}$$

$$\text{vii. } (U_k \mathfrak{b}_k^+ + V_k \mathfrak{b}_k) (U_k \mathfrak{b}_k + V_k \mathfrak{b}_k^+) = V_k^2 + U_k V_k (\mathfrak{b}_k^+ \mathfrak{b}_k^+ + \mathfrak{b}_k \mathfrak{b}_k) \quad (4.68)$$

$$\text{viii. } (U_k \mathfrak{b}_k^+ + V_k \mathfrak{b}_k) (U_k \mathfrak{b}_k + V_k \mathfrak{b}_k^+) = V_k^2 + U_k V_k (\mathfrak{b}_k^+ \mathfrak{b}_k^+ + \mathfrak{b}_k \mathfrak{b}_k)$$

$$\begin{aligned}
\text{ix. } & (U_k \gamma_k^+ + V_{k'} \gamma_{k'}^+) (U_k \mathfrak{b}_k + V_k \mathfrak{b}_k^+) (U_{-K} \gamma_{-K} + V_{-k'} \gamma_{-k'}^+) (U_K \mathfrak{b}_K^+ + V_K \mathfrak{b}_K) = \\
& U_k V_k U_{-K} U_K \gamma_k^+ \mathfrak{b}_k^+ + V_{k'} U_k U_{-K} U_K \gamma_{k'} \mathfrak{b}_k + V_{k'} V_k U_{-K} U_K + V_{k'} V_k U_{-K} V_K \gamma_{-K} \mathfrak{b}_K + \\
& V_{k'} V_k V_{-k'} U_K \gamma_{-k'}^+ \mathfrak{b}_K^+ \tag{4.69}
\end{aligned}$$

$$\begin{aligned}
\text{x. } & (U_k \gamma_k + V_{k'} \gamma_{k'}^+) (U_k \mathfrak{b}_k^+ + V_k \mathfrak{b}_k) (U_{-K} \gamma_{-K}^+ + V_{-k'} \gamma_{-k'}) (U_K \mathfrak{b}_K + V_K \mathfrak{b}_K^+) \\
& = U_k^2 U_{-K} V_K \gamma_{-K}^+ \mathfrak{b}_K^+ + U_k^2 V_{-k'} U_K \gamma_{-k'} \mathfrak{b}_K + U_k^2 V_{-k'} V_K + U_k V_k V_{-k'} V_K \gamma_k \mathfrak{b}_k \\
& + V_{k'} U_k V_{-k'} V_K \gamma_{k'}^+ \mathfrak{b}_k^+ \tag{4.70}
\end{aligned}$$

Using eqs. (4.62) – (4.70), the t-J model Hamiltonian can now be expressed as;

$$\begin{aligned}
H_{t-J} = \sum_{k,-k} J \left\{ -\frac{1}{4} [(V_k U_{-k} V_{-k} V_k \gamma_{k'} \gamma_{-k} + U_k V_{-k'} V_{-k} V_k \gamma_k^+ \gamma_{-k'}^+ \right. \\
- V_{k'} V_{-k'} U_{-k'} V_k \gamma_{-k'}^+ \gamma_k^+ - V_{k'} V_{-k'} V_{-k} U_{k'} \gamma_{-k} \gamma_{k'} + V_k V_{-k'} V_{-k} V_k)] \\
- \frac{1}{4} [(U_k U_{-k'} \gamma_k^+ \gamma_{-k'}^+ + V_{k'} U_{-k'} - V_{k'} V_{-k} \gamma_{k'} \gamma_{-k}) \\
- (U_{k'} U_{-k} \gamma_{k'}^+ \gamma_{-k}^+ - V_k U_{-k} - V_k V_{-k'} \gamma_k \gamma_{-k'})] [(U_{-k'} U_{-k} \gamma_{-k'} \gamma_{-k} \\
+ U_{-k'} V_{-k'} - V_{-k} V_{-k'} \gamma_{-k}^+ \gamma_{-k'}^+) \\
- (U_{-k} U_{-k'} \gamma_{-k} \gamma_{-k'} - U_{-k} V_{-k} - V_{-k'} V_{-k} \gamma_{-k}^+ \gamma_{-k}^+)] \\
+ \frac{1}{4} [(U_{k'} V_{k'} \gamma_{k'}^+ \gamma_{k'}^+ + V_{k'} U_{k'} \gamma_{-k'} \gamma_k + V_{k'} V_{k'})] \\
- \frac{1}{4} [1 - (V_k + U_k V_k (\mathcal{L}_k^+ \mathcal{L}_k^+ + \mathcal{L}_k \mathcal{L}_k))] [1 \\
- (V_k + U_k V_k (\mathcal{L}_k^+ \mathcal{L}_k^+ + \mathcal{L}_k \mathcal{L}_k))] \left. \right\} \\
- \sum_{kk'} t_{kk'} \{ (U_k V_k U_{-k} U_k \gamma_k^+ \mathcal{L}_k^+ + V_{k'} U_k U_{-k} U_k \gamma_{k'} \mathcal{L}_k + V_{k'} V_k U_{-k} U_k \\
+ V_{k'} V_k U_{-k} V_k \gamma_{-k} \mathcal{L}_k + V_{k'} V_k V_{-k'} U_k \gamma_{-k'}^+ \mathcal{L}_k^+) \\
- (U_k^2 U_{-k} V_k \gamma_{-k}^+ \mathcal{L}_k^+ + U_k^2 V_{-k'} U_k \gamma_{-k'} \mathcal{L}_k + U_k^2 V_{-k'} V_k \\
+ U_k V_k V_{-k'} V_k \gamma_k \mathcal{L}_k \\
+ V_{k'} U_k V_{-k'} V_k \gamma_{k'}^+ \mathcal{L}_k^+) \left. \right\} \tag{4.71}
\end{aligned}$$

Expanding further the factors in eq. (4.71) we obtain,

$$\begin{aligned}
H_{t-J} = \sum_{k,-k} J \left\{ -\frac{1}{4} \right. & \left[(V_k U_{-k} V_{-k} V_k \gamma_{k'} \gamma_{-k} + U_k V_{-k'} V_{-k} V_k \gamma_k^+ \gamma_{-k}^+ \right. \\
& \left. - V_{k'} V_{-k'} U_{-k'} V_k \gamma_{-k'}^+ \gamma_k^+ - V_{k'} V_{-k'} V_{-k} U_{k'} \gamma_{-k} \gamma_{k'} + V_k V_{-k'} V_{-k} V_k) \right] \\
& - \frac{1}{4} \left[U_k U_{-k'} U_{-k'} U_{-k} \gamma_k^+ \gamma_{-k}^+ \gamma_{-k'} \gamma_{-k} + U_k U_{-k'} U_{-k'} V_{-k'} \gamma_k^+ \gamma_{-k}^+ \right. \\
& - U_k U_{-k'} V_{-k} V_{-k'} \gamma_k^+ \gamma_{-k}^+ \gamma_{-k}^+ \gamma_{-k}^+ \\
& - U_k U_{-k'} U_{-k} U_{-k'} \gamma_k^+ \gamma_{-k}^+ \gamma_{-k} \gamma_{-k'} + U_k U_{-k'} U_{-k} V_{-k} \gamma_k^+ \gamma_{-k}^+ \\
& + U_k U_{-k'} V_{-k'} V_{-k} \gamma_k^+ \gamma_{-k}^+ \gamma_{-k}^+ \gamma_{-k}^+ + V_{k'} U_{-k'} U_{-k'} U_{-k} \gamma_{-k'} \gamma_{-k} \\
& + V_{k'} U_{-k'} U_{-k'} V_{-k'} \\
& - V_{k'} U_{-k'} V_{-k} V_{-k'} \gamma_{-k}^+ \gamma_{-k}^+ - V_{k'} U_{-k'} U_{-k} U_{-k'} \gamma_{-k} \gamma_{-k'} \\
& + V_{k'} U_{-k'} U_{-k} V_{-k} + V_{k'} U_{-k'} V_{-k'} V_{-k} \gamma_{-k'}^+ \gamma_{-k}^+ \\
& - V_{k'} V_{-k} U_{-k'} U_{-k} \gamma_{k'} \gamma_{-k} \gamma_{-k'} \gamma_{-k} - V_{k'} V_{-k} U_{-k'} V_{-k'} \gamma_k^+ \gamma_{-k} \\
& + V_{k'} V_{-k} V_{-k} V_{-k'} \gamma_{k'} \gamma_{-k} \gamma_{-k}^+ \gamma_{-k}^+ + V_{k'} V_{-k} U_{-k} U_{-k'} \gamma_{k'} \gamma_{-k} \gamma_{-k} \gamma_{-k'} \\
& - V_{k'} V_{-k} U_{-k} V_{-k} \gamma_{k'} \gamma_{-k} - V_{k'} V_{-k} V_{-k'} V_{-k} \gamma_{k'} \gamma_{-k} \gamma_{-k}^+ \gamma_{-k}^+ \\
& - U_{k'} U_{-k} U_{-k'} U_{-k} \gamma_k^+ \gamma_{-k}^+ \gamma_{-k'} \gamma_{-k} - U_{k'} U_{-k} U_{-k'} V_{-k'} \gamma_k^+ \gamma_{-k}^+ \\
& + U_{k'} U_{-k} V_{-k} V_{-k'} \gamma_k^+ \gamma_{-k}^+ \gamma_{-k}^+ \gamma_{-k}^+ \\
& + U_{k'} U_{-k} U_{-k} U_{-k'} \gamma_k^+ \gamma_{-k}^+ \gamma_{-k} \gamma_{-k'} - U_{k'} U_{-k} U_{-k} V_{-k} \gamma_k^+ \gamma_{-k}^+ \\
& - U_{k'} U_{-k} V_{-k'} V_{-k} \gamma_k^+ \gamma_{-k}^+ \gamma_{-k}^+ \gamma_{-k}^+ + U_{-k'} U_{-k} V_k U_{-k} \gamma_{-k'} \gamma_{-k} \\
& + V_k U_{-k} U_{-k'} V_{-k'} \\
& - V_k U_{-k} V_{-k} V_{-k'} \gamma_{-k}^+ \gamma_{-k}^+ - V_k U_{-k} U_{-k} U_{-k'} \gamma_{-k} \gamma_{-k'} \\
& + V_k U_{-k} U_{-k} V_{-k} + V_k U_{-k} V_{-k'} V_{-k} \gamma_{-k'}^+ \gamma_{-k}^+ \\
& + V_k V_{-k'} U_{-k'} U_{-k} \gamma_k \gamma_{-k'} \gamma_{-k'} \gamma_{-k} + U_{-k'} V_{-k'} V_k V_{-k'} \gamma_k \gamma_{-k'} \\
& \left. - V_k V_{-k'} V_{-k} V_{-k'} \gamma_k \gamma_{-k'} \gamma_{-k}^+ \gamma_{-k}^+ - V_k V_{-k'} U_{-k} U_{-k'} \gamma_k \gamma_{-k'} \gamma_{-k} \gamma_{-k'} \right\}
\end{aligned}$$

$$\begin{aligned}
& + U_{-k}V_{-k}V_kV_{-k'}\gamma_k\gamma_{-k'} + V_kV_{-k'}V_{-k'}V_{-k}\gamma_k\gamma_{-k'}\gamma_{-k'}^+\gamma_{-k}^+ \\
& + \frac{1}{4}[(U_{k'}V_{k'}\gamma_{k'}^+\gamma_{k'}^+ + V_{k'}U_k\gamma_{-k'}\gamma_k + V_{k'}V_{k'})] \\
& - \frac{1}{4}[[1 - (V_k + U_kV_k(\mathcal{B}_k^+\mathcal{B}_k^+ + \mathcal{B}_k\mathcal{B}_k))][1 \\
& - (V_k + U_kV_k(\mathcal{B}_k^+\mathcal{B}_k^+ + \mathcal{B}_k\mathcal{B}_k))]]\} \\
& - \sum_{kk'} t_{kk'}\{(U_kV_kU_{-K}U_K\gamma_k^+\mathcal{B}_k^+ + V_{k'}U_kU_{-K}U_K\gamma_{k'}\mathcal{B}_k \\
& + V_{k'}V_kU_{-K}U_K + V_{k'}V_kU_{-K}V_K\gamma_{-K}\mathcal{B}_K + V_{k'}V_kV_{-k'}U_K\gamma_{-k'}^+\mathcal{B}_K^+) \\
& - (U_k^2U_{-K}V_K\gamma_{-K}^+\mathcal{B}_K^+ + U_k^2V_{-k'}U_K\gamma_{-k'}\mathcal{B}_K + U_k^2V_{-k'}V_K \\
& + U_kV_kV_{-k'}V_K\gamma_k\mathcal{B}_k \\
& + V_{k'}U_kV_{-k'}V_K\gamma_{k'}^+\mathcal{B}_k^+)\} \tag{4.72}
\end{aligned}$$

We again make the assumption that the contribution of the fourth order terms to the energy of the system is negligible, thus we drop fourth order terms in eq. (4.72) and also that all U_k s and V_k s are equal to obtain,

$$\begin{aligned}
H_{t-J} = \sum_{k,-k} J \left\{ -\frac{1}{4} \left[-V_k^3 U_K \gamma_{k'} \gamma_{-k} + U_k^3 V_K \gamma_k^+ \gamma_{-k'}^+ - U_K V_k^3 \gamma_k \gamma_{k'} - U_K V_k^3 \gamma_{-k'}^+ \gamma_k^+ \right. \right. \\
+ 2U_K V_k^3 \gamma_{-k}^+ \gamma_{-k'}^+ - U_k^2 V_k^2 \gamma_{k'}^+ \gamma_{-k}^+ + U_k^2 V_k^2 \gamma_k^+ \gamma_{-k}^+ - 2U_K V_k^3 \gamma_k \gamma_{-k'} \\
+ V_k^4 + 2U_k^2 V_k^2 \left. \right] + \frac{1}{4} V_k^2 - \frac{1}{4} + \frac{1}{4} V_k^2 + \frac{1}{4} V_k^2 - \frac{1}{4} V_k^4 \\
+ \frac{1}{4} U_K V_K \gamma_{k'}^+ \gamma_{k'}^+ + \frac{1}{4} U_K V_K \gamma_{-k'} \gamma_k \\
+ \left(-\frac{1}{4} U_K V_K + \frac{1}{4} U_K V_k^3 - \frac{1}{4} U_K V_K \right. \\
\left. + \frac{1}{4} U_K V_k^3 \right) \left((\mathcal{b}_k^+ \mathcal{b}_k^+ + \mathcal{b}_k \mathcal{b}_k) \right) \left. \right\} \\
- \sum_{kk'} t_{kk'} \left\{ 2U_K^2 V_k^2 + U_k^3 V_K \gamma_k^+ \mathcal{b}_k^+ + U_k^3 V_K \gamma_{k'} \mathcal{b}_k + U_K V_k^3 \gamma_k \mathcal{b}_k \right. \\
+ U_K^2 V_k^2 \gamma_{-k'}^+ \mathcal{b}_k^+ + U_k^3 V_K \gamma_{-k}^+ \mathcal{b}_k^+ + U_k^3 V_K \gamma_{-k} \mathcal{b}_k + U_K V_k^3 \gamma_{-k'} \mathcal{b}_k \\
\left. + U_K V_k^3 \gamma_{k'}^+ \mathcal{b}_k^+ \right\} \quad (4.73)
\end{aligned}$$

To diagonalize the Hamiltonian in eq. 4.73, we put the sum of the off-diagonal terms equal to zero and simplify the resultant expression to obtain the diagonalized Hamiltonian as;

$$H_{diag} = \sum_{k,-k} J \left\{ -\frac{1}{4} + \frac{3}{4} V_k^2 - \frac{1}{2} V_k^4 - \frac{1}{2} U_K^2 V_k^2 \right\} - \sum_{kk'} t_{kk'} \{ 2U_K^2 V_k^2 \} \quad (4.74)$$

To determine the values of U_K and V_k used for the diagonalization, we equate the off-diagonal term $\left(-\frac{1}{2} U_K V_K + \frac{1}{2} U_K V_k^3 \right) (\mathcal{b}_k^+ \mathcal{b}_k^+ + \mathcal{b}_k \mathcal{b}_k)$ to zero. Thus;

$$\left(-\frac{1}{2} U_K V_K + \frac{1}{2} U_K V_k^3 \right) (\mathcal{b}_k^+ \mathcal{b}_k^+ + \mathcal{b}_k \mathcal{b}_k) = 0 \quad (4.75)$$

Solving equation 4.75 and using equation 4.24, we obtain the values of U_k and V_k as; $U_k = \sqrt{2}$ and $V_k = 1$ (4.76)

4.4 Thermodynamic properties of high- T_c superconductors

i. Superconducting energy of the t-J system

Using equation 4.76 in equation 4.74 the magnitude of the ground state energy of the system is obtained as;

$$E_0 = (J + 4t) \quad (4.77)$$

We can express the energy of the system at any temperature, E as a function of temperature by multiplying the ground-state energy, E_0 by the thermal activation factor, $e^{-\frac{\Delta E}{kT}}$ (Khanna, 2008), where k is Boltzmann's constant and ΔE is the energy gap. The energy gap for superconductors is a very small quantity and it is generally 1% of the minimum energy of the system (Khanna, 2008). Thus $\Delta E = 0.01E_0$. So at any temperature T , the energy of the system is given as;

$$E = E_0 e^{-\frac{0.01E_0}{kT}} = E_0 e^{-\frac{E_0}{100kT}} \quad (4.78)$$

Substituting equation 4.77 in equation 4.78, we obtain the magnitude of energy of the system at any given temperature as;

$$E = (J + 4t). e^{-\left(\frac{J+4t}{100kT}\right)} \quad (4.79)$$

ii. Specific heat capacity of the t-J system

The specific heat capacity at constant volume c_v of the system is obtained by determining the first derivative of the energy of the system with respect to the temperature (Khanna, 2008). Hence, using equation 4.79, we calculate the magnitude of c_v as follows;

$$c_v = \frac{\partial E}{\partial T} = \frac{\partial}{\partial T} \left[(J + 4t) \cdot e^{-\left(\frac{J+4t}{100kT}\right)} \right] = \frac{(J + 4t)^2}{100kT^2} \cdot e^{-\left(\frac{J+4t}{100kT}\right)} \quad (4.80)$$

Hence, according to this model the superconducting specific heat capacity at constant volume is given as;

$$c_v = \frac{(J + 4t)^2}{100kT^2} \cdot e^{-\left(\frac{J+4t}{100kT}\right)} \quad (4.81)$$

iii. Entropy of the t-J system

Entropy s of the system is obtained by evaluating the integral given below ³⁵(Khanna & Kirui, 2002);

$$s = \int \frac{c_v dT}{T} \quad (4.82)$$

Where c_v is specific heat capacity at constant volume and T is the temperature of the system.

Substituting equation 4.81 in equation 4.82 we have;

$$s = \int \frac{\left[\frac{(J + 4t)^2}{100kT^2} \cdot e^{-\left(\frac{J+4t}{100kT}\right)} \right] dT}{T} = \left[\frac{(J + 4t)}{T} e^{-\left(\frac{J+4t}{100kT}\right)} - k \cdot e^{-\left(\frac{J+4t}{100kT}\right)} \right] \quad (4.83)$$

Thus the superconducting entropy by this model is given as;

$$s = \frac{(J + 4t)}{T} e^{-\left(\frac{J+4t}{100kT}\right)} - k \cdot e^{-\left(\frac{J+4t}{100kT}\right)} \quad (4.84)$$

iv. Transition temperature of the t-J system

Transition temperature of the superconducting state, T_c is calculated from the condition

that (Khanna and Kirui, 2002);

$$\left[\frac{\partial c}{\partial T} \right]_{T=T_c} = 0 \quad (4.85)$$

Substituting equation 4.81 in equation 4.85, we have;

$$\frac{\partial}{\partial T} \left(\frac{(J + 4t)^2}{100kT^2} \cdot e^{-\left(\frac{J+4t}{100kT}\right)} \right)_{T=T_c} = 0 \quad (4.86)$$

Evaluating the partial derivative in equation 4.86, we obtain;

$$\frac{(J + 4t)^2}{100k} \cdot e^{-\left(\frac{J+4t}{100kT}\right)} \cdot \left\{ -\frac{2}{T_c^3} + \frac{(J + 4t)}{100kT_c^4} \right\} = 0 \quad (4.87)$$

Solving equation 4.87, we obtain transition temperature of the t-J system as;

$$T_c = \frac{(J + 4t)}{200k} \quad (4.89)$$

CHAPTER FIVE

THE DIPOLE MEDIATED t-J MODEL OF HIGH-T_c SUPERCONDUCTIVITY: “THE t-J-d MODEL”

5.1 Introduction

In this chapter, a new model of high-T_c superconductivity, called the t-J-d model, is derived. The effective Hamiltonian of this model is obtained from the sum of the diagonalized t-J model and the diagonalized electronic dipole interaction Hamiltonian. Thus, the contribution of dipole vibration energy to the t-J model energy in the superconducting state is considered.

The interaction Hamiltonian of a dipole of dipole moment $P(\mathbf{R}, t)$ at the location \mathbf{R} interacting with an electron at position \mathbf{r} is given by (Heebok Lee et al, 1991);

$$H_{eq} = \sum_{k\sigma k'\sigma'q'\lambda} h_{k\sigma k'\sigma'q'\lambda} (b_{q\lambda}^+ + b_{q\lambda}) C_{k'\sigma'}^+ C_{k\sigma} \quad (5.1)$$

where $C_{k'\sigma'}^+$ and $C_{k\sigma}$ are the creation and annihilation operators for an electron with wave vector k and spin σ while $b_{q\lambda}^+$ and $b_{q\lambda}$ are the creation and annihilation operators for a collective dipole quantum with wave vector q and polarization λ . The constant $h_{k\sigma k'\sigma'q'\lambda}$ is defined as;

$$h_{k\sigma k'\sigma'q'\lambda} = r |P_x(0)| \left[\frac{\hbar}{2I_k N \omega_\lambda(q)} \right]^{\frac{1}{2}} (\xi_{q\lambda}(k - k')) D_d^{kk'} \delta_{k-k', q+G} \quad (5.2)$$

where G is a reciprocal vector, $\omega_\lambda(q)$ is the frequency of vibration of a dipole with polarization index λ at a generalized location q , I_k is the moment of inertia of the

oscillating dipole, $\xi_{q\lambda}$ is the λ^{th} component of the unit polarization vector ξ_q of the collective wave, N is the number of the oscillating dipoles in the crystal. $P(0)_x$ is the dipole moment in the x-direction at time $t=0$, i.e static state and $P = \alpha E$ where α is polarazability and E is the electric field. The dynamic matrix $D_d^{kk'}$ is defined as;

$$D_d^{kk'} = \int d^3r U_{k'\sigma'}(r) e^{-ik'r} \frac{e}{\epsilon|r-R|} U_{k\sigma}(r) e^{ikr} \quad (5.3)$$

where e is the electronic charge unit, ϵ is energy of an electron and $U_{k\sigma}(r) e^{ikr}$ is the Bloch state of the electron in the system.

5.2 Diagonalization of the dipole Hamiltonian, H_{eq}

By considering eq. (5.1), we express the quantum dipole operators as a product of two electron operators such that;

$$b_{q\lambda}^+ = C_{i\sigma}^+ C_{i\sigma'}^+ \quad (5.4)$$

And

$$b_{q\lambda} = C_{i\sigma} C_{i\sigma'} \quad (5.5)$$

Thus

$$(b_{q\lambda}^+ + b_{q\lambda}) = C_{i\sigma}^+ C_{i\sigma'}^+ + C_{i\sigma} C_{i\sigma'} \quad (5.6)$$

Substituting eq. (4.5) in eq. (5.6), we obtain;

$$(b_{q\lambda}^+ + b_{q\lambda}) = \mathcal{f}_{i\sigma}^+ b_i \mathcal{f}_{i\sigma'}^+ b_i + \mathcal{f}_{i\sigma} b_i^+ \mathcal{f}_{i\sigma'} b_i^+ \quad (5.7)$$

Carrying out the canonical transformation from the old operators $\hat{b}_{i\sigma}^+, \hat{b}_{i\sigma}$ and b_i^+, b_i to the new operators, $\gamma_{i\sigma}^+, \gamma_{i\sigma}$ and \hat{b}_i^+, \hat{b}_i respectively, we substitute eqs. (4.33)-(4.40) in eq. (5.7) to get;

$$\begin{aligned} (b_{q\lambda}^+ + b_{q\lambda}) &= (U_{i\sigma}\gamma_{i\sigma}^+ + V_{i\sigma}\gamma_{i\sigma'}) (U_i\hat{b}_i + V_i\hat{b}_i^+) (U_{i\sigma}\gamma_{i\sigma'}^+ - V_{i\sigma}\gamma_{i\sigma}) (U_i\hat{b}_i + V_i\hat{b}_i^+) \\ &+ (U_{i\sigma}\gamma_{i\sigma} + V_{i\sigma}\gamma_{i\sigma'}^+) (U_i\hat{b}_i^+ + V_i\hat{b}_i) (U_{i\sigma}\gamma_{i\sigma'} - V_{i\sigma}\gamma_{i\sigma}^+) (U_i\hat{b}_i^+ \\ &+ V_i\hat{b}_i) \end{aligned} \quad (5.8)$$

We now represent the particle spin up state with k and spin down with $-k$. The scattered particle spin states will be represented by k' and $-k'$ for spin up and spin down respectively. Eq. (5.8) becomes;

$$\begin{aligned} (b_{q\lambda}^+ + b_{q\lambda}) &= (U_k\gamma_k^+ + V_k\gamma_{-k}) (U_k\hat{b}_k + V_k\hat{b}_k^+) (U_k\gamma_{-k}^+ - V_k\gamma_k) (U_k\hat{b}_k + V_k\hat{b}_k^+) \\ &+ (U_k\gamma_k + V_k\gamma_{-k}^+) (U_k\hat{b}_k^+ + V_k\hat{b}_k) (U_k\gamma_{-k} - V_k\gamma_k^+) (U_k\hat{b}_k^+ \\ &+ V_k\hat{b}_k) \end{aligned} \quad (5.9)$$

Expanding the expressions in eq. (5.9);

$$\begin{aligned} \text{i. } & (U_k\gamma_k^+ + V_k\gamma_{-k}) (U_k\hat{b}_k + V_k\hat{b}_k^+) (U_k\gamma_{-k}^+ - V_k\gamma_k) (U_k\hat{b}_k + V_k\hat{b}_k^+) \\ &= [U_k^2\gamma_k^+\hat{b}_k + U_kV_k\gamma_k^+\hat{b}_k^+ + U_kV_k\gamma_{-k}\hat{b}_k + V_k^2\gamma_{-k}\hat{b}_k^+] \\ & [U_k^2\gamma_{-k}^+\hat{b}_k + U_kV_k\gamma_{-k}^+\hat{b}_k^+ - U_kV_k\gamma_k\hat{b}_k - V_k^2\gamma_k\hat{b}_k^+] \end{aligned} \quad (5.10)$$

We substitute eq. (4.56) in eq. (5.10) to obtain;

$$\begin{aligned} & (U_k\gamma_k^+ + V_k\gamma_{-k}) (U_k\hat{b}_k + V_k\hat{b}_k^+) (U_k\gamma_{-k}^+ - V_k\gamma_k) (U_k\hat{b}_k + V_k\hat{b}_k^+) \\ &= [U_k^2\eta_k + U_kV_k(\gamma_k^+\hat{b}_k^+ + \gamma_{-k}\hat{b}_k) + V_k^2(1 - \eta_{-k})] \end{aligned}$$

$$\left[U_k^2 \eta_{-k} + U_k V_k (\gamma_{-k}^+ \mathcal{b}_k^+ - \gamma_k \mathcal{b}_k) - V_k^2 (1 - \eta_k) \right] \quad (5.11)$$

Expanding eq. (5.11) we obtain;

$$\begin{aligned} & (U_k \gamma_k^+ + V_k \gamma_{-k}) (U_k \mathcal{b}_k + V_k \mathcal{b}_k^+) (U_k \gamma_{-k}^+ - V_k \gamma_k) (U_k \mathcal{b}_k + V_k \mathcal{b}_k^+) \\ &= U_k^4 \eta_k \eta_{-k} + U_k^2 U_k V_k \eta_k (\gamma_{-k}^+ \mathcal{b}_k^+ - \gamma_k \mathcal{b}_k) - U_k^2 V_k^2 \eta_k (1 - \eta_k) \\ &+ U_k^3 V_k \eta_{-k} (\gamma_k^+ \mathcal{b}_k^+ + \gamma_{-k} \mathcal{b}_k) + U_k^2 V_k^2 (\gamma_k^+ \mathcal{b}_k^+ + \gamma_{-k} \mathcal{b}_k) (\gamma_{-k}^+ \mathcal{b}_k^+ - \gamma_k \mathcal{b}_k) \\ &- U_k V_k^3 (1 - \eta_k) (\gamma_k^+ \mathcal{b}_k^+ + \gamma_{-k} \mathcal{b}_k) + U_k^2 V_k^2 \eta_{-k} (1 - \eta_{-k}) \\ &+ U_k V_k^3 (1 - \eta_{-k}) (\gamma_{-k}^+ \mathcal{b}_k^+ - \gamma_k \mathcal{b}_k) \\ &- V_k^4 (1 - \eta_{-k}) (1 - \eta_k) \end{aligned} \quad (5.12)$$

We assume that the lowest energy state of this system has all the occupation numbers η_k equal to zero and the contribution of the fourth order terms is negligible, then eq. (5.12) becomes;

$$\begin{aligned} & (U_k \gamma_k^+ + V_k \gamma_{-k}) (U_k \mathcal{b}_k + V_k \mathcal{b}_k^+) (U_k \gamma_{-k}^+ - V_k \gamma_k) (U_k \mathcal{b}_k + V_k \mathcal{b}_k^+) \\ &= -U_k V_k^3 (\gamma_k^+ \mathcal{b}_k^+ + \gamma_{-k} \mathcal{b}_k) + U_k V_k^3 (\gamma_{-k}^+ \mathcal{b}_k^+ - \gamma_k \mathcal{b}_k) - V_k^4 \end{aligned} \quad (5.13)$$

ii. The second expression in eq. (5.9) can now be expanded as follows;

$$\begin{aligned} & (U_k \gamma_k + V_k \gamma_{-k}^+) (U_k \mathcal{b}_k^+ + V_k \mathcal{b}_k) (U_k \gamma_{-k} - V_k \gamma_k^+) (U_k \mathcal{b}_k^+ + V_k \mathcal{b}_k) \\ &= [U_k^2 \gamma_k \mathcal{b}_k^+ + U_k V_k \gamma_{-k}^+ \mathcal{b}_k^+ + U_k V_k \gamma_k \mathcal{b}_k + V_k^2 \gamma_{-k}^+ \mathcal{b}_k] \\ & [U_k^2 \gamma_{-k} \mathcal{b}_k^+ - U_k V_k \gamma_k^+ \mathcal{b}_k^+ + U_k V_k \gamma_{-k} \mathcal{b}_k - V_k^2 \gamma_k^+ \mathcal{b}_k] \end{aligned} \quad (5.14)$$

Again we substitute eq. (4.56) in eq. (5.14) to obtain;

$$(U_k \gamma_k + V_k \gamma_{-k}^+) (U_k \mathcal{b}_k^+ + V_k \mathcal{b}_k) (U_k \gamma_{-k} - V_k \gamma_k^+) (U_k \mathcal{b}_k^+ + V_k \mathcal{b}_k)$$

$$\begin{aligned}
&= [U_k^2(1 - \eta_k) + U_k V_k(\gamma_{-k}^+ \mathcal{C}_k^+ + \gamma_k \mathcal{C}_k) + V_k^2 \eta_{-k}] \\
&\quad [U_k^2(1 - \eta_{-k}) - U_k V_k(\gamma_k^+ \mathcal{C}_k^+ - \gamma_{-k} \mathcal{C}_k) - V_k^2 \eta_k] \tag{5.15}
\end{aligned}$$

Expanding eq. (5.15), we obtain;

$$\begin{aligned}
&(U_k \gamma_k + V_k \gamma_{-k}^+)(U_k \mathcal{C}_k^+ + V_k \mathcal{C}_k)(U_k \gamma_{-k} - V_k \gamma_k^+)(U_k \mathcal{C}_k^+ + V_k \mathcal{C}_k) \\
&= U_k^4(1 - \eta_k)(1 - \eta_{-k}) - U_k^3 V_k(1 - \eta_k)(\gamma_k^+ \mathcal{C}_k^+ - \gamma_{-k} \mathcal{C}_k) - U_k^2 V_k^2 \eta_k(1 - \eta_k) + \\
&U_k^3 V_k(1 - \eta_{-k})(\gamma_{-k}^+ \mathcal{C}_k^+ + \gamma_k \mathcal{C}_k) - U_k^2 V_k^2(\gamma_{-k}^+ \mathcal{C}_k^+ + \gamma_k \mathcal{C}_k)(\gamma_k^+ \mathcal{C}_k^+ - \gamma_{-k} \mathcal{C}_k) - \\
&U_k V_k^3 \eta_k(\gamma_{-k}^+ \mathcal{C}_k^+ + \gamma_k \mathcal{C}_k) + U_k^2 V_k^2 \eta_{-k}(1 - \eta_{-k}) - U_k V_k^3 \eta_{-k}(\gamma_k^+ \mathcal{C}_k^+ - \gamma_{-k} \mathcal{C}_k) - \\
&V_k^4 \eta_{-k} \eta_k \tag{5.16}
\end{aligned}$$

We assume that the lowest energy state of this system has all the occupation numbers η_k equal to zero and the contribution of the fourth order terms is negligible, then eq. (5.16) becomes;

$$\begin{aligned}
&(U_k \gamma_k + V_k \gamma_{-k}^+)(U_k \mathcal{C}_k^+ + V_k \mathcal{C}_k)(U_k \gamma_{-k} - V_k \gamma_k^+)(U_k \mathcal{C}_k^+ + V_k \mathcal{C}_k) \\
&= U_k^4 - U_k^3 V_k(\gamma_k^+ \mathcal{C}_k^+ - \gamma_{-k} \mathcal{C}_k) \\
&\quad + U_k^3 V_k(\gamma_{-k}^+ \mathcal{C}_k^+ + \gamma_k \mathcal{C}_k) \tag{5.17}
\end{aligned}$$

Substituting eqs. (5.13) and (5.17) in eq. (5.9), we have;

$$\begin{aligned}
(b_{q\lambda}^+ + b_{q\lambda}) &= \{(U_k^4 - V_k^4) - U_k V_k^3(\gamma_k^+ \mathcal{C}_k^+ + \gamma_{-k} \mathcal{C}_k) + U_k V_k^3(\gamma_{-k}^+ \mathcal{C}_k^+ - \gamma_k \mathcal{C}_k) \\
&\quad - U_k^3 V_k(\gamma_k^+ \mathcal{C}_k^+ - \gamma_{-k} \mathcal{C}_k) + U_k^3 V_k(\gamma_{-k}^+ \mathcal{C}_k^+ + \gamma_k \mathcal{C}_k)\} \tag{5.18}
\end{aligned}$$

We now consider the electron operators $C_{k'\sigma'}^+ C_{k\sigma'}$ in eq. (5.1). Using eq. (4.5) we can express these operators as;

$$C_{k'\sigma'}^+ C_{k\sigma'} = \hat{f}_{j\sigma'}^+ b_j \hat{f}_{i\sigma'} b_i^+ \quad (5.19)$$

Using the inverse- transformed electron operators in eqs. (4.33) to (4.36) in eq. (5.19), we obtain;

$$C_{k'\sigma'}^+ C_{k\sigma'} = (U_{j\sigma} \gamma_{j\sigma}^+ - V_{j\sigma} \gamma_{j\sigma'}) (U_j \hat{b}_j + V_j \hat{b}_j^+) (U_{i\sigma} \gamma_{i\sigma'}^+ - V_{i\sigma} \gamma_{i\sigma}^+) (U_i \hat{b}_i^+ + V_i \hat{b}_i) \quad (5.20)$$

Representing the particle spin up state with k and spin down with $-k$, the scattered particle spin states will be represented by k' and $-k'$ for spin up and spin down respectively then eq. (5.20) becomes;

$$C_{k'\sigma'}^+ C_{k\sigma'} = (U_{k'} \gamma_{k'}^+ - V_{k'} \gamma_{-k'}) (U_{k'} \hat{b}_{k'} + V_{k'} \hat{b}_{k'}^+) (U_k \gamma_{-k} - V_k \gamma_k^+) (U_k \hat{b}_k^+ + V_k \hat{b}_k) \quad (5.21)$$

Expanding the expression in eq. 5.21, we obtain;

$$\begin{aligned} & (U_{k'} \gamma_{k'}^+ - V_{k'} \gamma_{-k'}) (U_{k'} \hat{b}_{k'} + V_{k'} \hat{b}_{k'}^+) (U_k \gamma_{-k} - V_k \gamma_k^+) (U_k \hat{b}_k^+ + V_k \hat{b}_k) \\ &= [U_{k'}^2 \gamma_{k'}^+ \hat{b}_{k'} - U_{k'} V_{k'} \gamma_{-k'} \hat{b}_{k'} + U_{k'} V_{k'} \gamma_{k'}^+ \hat{b}_{k'}^+ - V_{k'}^2 \gamma_{-k'} \hat{b}_{k'}^+] \\ & \quad [U_k^2 \gamma_{-k} \hat{b}_k^+ + U_k V_k \gamma_{-k} \hat{b}_k - U_k V_k \gamma_k^+ \hat{b}_k^+ - V_k^2 \gamma_k^+ \hat{b}_k] \end{aligned} \quad (5.22)$$

Substituting eq. (4.56) in eq. (5.22), we obtain;

$$\begin{aligned} & (U_{k'} \gamma_{k'}^+ - V_{k'} \gamma_{-k'}) (U_{k'} \hat{b}_{k'} + V_{k'} \hat{b}_{k'}^+) (U_k \gamma_{-k} - V_k \gamma_k^+) (U_k \hat{b}_k^+ + V_k \hat{b}_k) \\ &= [U_{k'}^2 \eta_{k'} - U_{k'} V_{k'} (\gamma_{-k'} \hat{b}_{k'} - \gamma_{k'}^+ \hat{b}_{k'}^+) - V_{k'}^2 (1 - \eta_{k'})] \\ & \quad [U_k^2 (1 - \eta_{-k}) + U_k V_k (\gamma_{-k} \hat{b}_k - \gamma_k^+ \hat{b}_k^+) - V_k^2 \eta_k] \end{aligned} \quad (5.23)$$

Expanding eq. (5.23) we get;

$$\begin{aligned}
& (U_{k'}\gamma_{k'}^+ - V_{k'}\gamma_{-k'}) (U_{k'}\mathcal{B}_{k'} + V_{k'}\mathcal{B}_{k'}^+) (U_k\gamma_{-k} - V_k\gamma_k^+) (U_k\mathcal{B}_k^+ + V_k\mathcal{B}_k) \\
&= U_{k'}^2 U_k^2 \eta_{k'} (1 - \eta_{-k}) + U_{k'}^2 U_k V_k \eta_{k'} (\gamma_{-k} \mathcal{B}_k - \gamma_k^+ \mathcal{B}_k^+) - U_{k'}^2 V_k^2 \eta_{k'} \eta_k \\
&\quad - U_{k'} V_{k'} U_k^2 (1 - \eta_{-k}) (\gamma_{-k'} \mathcal{B}_{k'} - \gamma_{k'}^+ \mathcal{B}_{k'}^+) \\
&\quad - U_{k'} V_{k'} U_k V_k (\gamma_{-k'} \mathcal{B}_{k'} - \gamma_{k'}^+ \mathcal{B}_{k'}^+) (\gamma_{-k} \mathcal{B}_k - \gamma_k^+ \mathcal{B}_k^+) \\
&\quad + U_{k'} V_{k'} V_k^2 \eta_k (\gamma_{-k'} \mathcal{B}_{k'} - \gamma_{k'}^+ \mathcal{B}_{k'}^+) - V_{k'}^2 U_k^2 (1 - \eta_{k'}) (1 - \eta_{-k}) \\
&\quad - V_{k'}^2 U_k V_k (1 - \eta_{-k'}) (\gamma_{-k} \mathcal{B}_k - \gamma_k^+ \mathcal{B}_k^+) \\
&\quad + V_{k'}^2 V_k^2 \eta_k (1 - \eta_{k'}) \tag{5.24}
\end{aligned}$$

For the lowest energy state, we now set the number operators $\eta_k = 0$. We also consider the effect of the fourth order terms to be negligible because their contribution to the energy of the system is too small. Thus eq. (5.24) yields;

$$\begin{aligned}
& (U_{k'}\gamma_{k'}^+ - V_{k'}\gamma_{-k'}) (U_{k'}\mathcal{B}_{k'} + V_{k'}\mathcal{B}_{k'}^+) (U_k\gamma_{-k} - V_k\gamma_k^+) (U_k\mathcal{B}_k^+ + V_k\mathcal{B}_k) \\
&= -V_{k'}^2 U_k^2 - U_{k'} V_{k'} U_k^2 (\gamma_{-k'} \mathcal{B}_{k'} - \gamma_{k'}^+ \mathcal{B}_{k'}^+) \\
&\quad - V_{k'}^2 U_k V_k (\gamma_{-k} \mathcal{B}_k - \gamma_k^+ \mathcal{B}_k^+) \tag{5.25}
\end{aligned}$$

We now substitute eqs. (5.18) and (5.25) in eq. (5.1) to obtain;

$$\begin{aligned}
H_{eq} &= \sum_{kk'} h_{kk'} \{ (U_k^4 - V_k^4) - U_k V_k^3 (\gamma_k^+ \mathcal{B}_k^+ + \gamma_{-k} \mathcal{B}_k) + U_k V_k^3 (\gamma_{-k}^+ \mathcal{B}_k^+ - \gamma_k \mathcal{B}_k) \\
&\quad - U_k^3 V_k (\gamma_k^+ \mathcal{B}_k^+ - \gamma_{-k} \mathcal{B}_k) + U_k^3 V_k (\gamma_{-k}^+ \mathcal{B}_k^+ + \gamma_k \mathcal{B}_k) \} [-V_{k'}^2 U_k^2 \\
&\quad - U_{k'} V_{k'} U_k^2 (\gamma_{-k'} \mathcal{B}_{k'} - \gamma_{k'}^+ \mathcal{B}_{k'}^+) \\
&\quad - V_{k'}^2 U_k V_k (\gamma_{-k} \mathcal{B}_k - \gamma_k^+ \mathcal{B}_k^+)] \tag{5.26}
\end{aligned}$$

Expanding eq. (5.26), we obtain;

$$\begin{aligned}
H_{eq} = \sum_{kk'} h_{kk'} \{ & -U_k^2 V_k^2 (U_k^4 - V_k^4) - (U_k^4 - V_k^4) U_{k'} V_{k'} U_k^2 (\gamma_{-k'} \mathcal{B}_{k'} - \gamma_{k'}^+ \mathcal{B}_{k'}^+) \\
& - (U_k^4 - V_k^4) U_k V_k^2 V_k (\gamma_{-k} \mathcal{B}_k - \gamma_k^+ \mathcal{B}_k^+) + U_k^3 V_k^3 V_{k'}^2 (\gamma_k^+ \mathcal{B}_k^+ + \gamma_{-k} \mathcal{B}_k) \\
& + U_k^3 V_k^3 U_{k'} V_{k'} (\gamma_k^+ \mathcal{B}_k^+ + \gamma_{-k} \mathcal{B}_k) (\gamma_{-k'} \mathcal{B}_{k'} - \gamma_{k'}^+ \mathcal{B}_{k'}^+) \\
& + U_k^2 V_k^4 V_{k'}^2 (\gamma_k^+ \mathcal{B}_k^+ + \gamma_{-k} \mathcal{B}_k) (\gamma_{-k} \mathcal{B}_k - \gamma_k^+ \mathcal{B}_k^+) \\
& - U_k^3 V_k^3 V_{k'}^2 (\gamma_{-k}^+ \mathcal{B}_k^+ - \gamma_k \mathcal{B}_k) \\
& - U_k^3 V_k^3 U_{k'} V_{k'} (\gamma_{-k}^+ \mathcal{B}_k^+ - \gamma_k \mathcal{B}_k) (\gamma_{-k'} \mathcal{B}_{k'} - \gamma_{k'}^+ \mathcal{B}_{k'}^+) \\
& - U_k^2 V_k^4 V_{k'}^2 (\gamma_{-k}^+ \mathcal{B}_k^+ - \gamma_k \mathcal{B}_k) (\gamma_{-k} \mathcal{B}_k - \gamma_k^+ \mathcal{B}_k^+) \\
& + U_k^5 V_k^2 V_{k'} (\gamma_k^+ \mathcal{B}_k^+ - \gamma_{-k} \mathcal{B}_k) + U_k^5 V_k U_{k'} V_{k'} (\gamma_k^+ \mathcal{B}_k^+ - \gamma_{-k} \mathcal{B}_k) (\gamma_{-k'} \mathcal{B}_{k'} \\
& - \gamma_{k'}^+ \mathcal{B}_{k'}^+) + U_k^4 V_k^2 V_{k'}^2 (\gamma_k^+ \mathcal{B}_k^+ - \gamma_{-k} \mathcal{B}_k) (\gamma_{-k} \mathcal{B}_k - \gamma_k^+ \mathcal{B}_k^+) \\
& - U_k^5 V_k^2 V_{k'} (\gamma_{-k}^+ \mathcal{B}_k^+ + \gamma_k \mathcal{B}_k) \\
& - U_k^5 V_k U_{k'} V_{k'} (\gamma_{-k}^+ \mathcal{B}_k^+ + \gamma_k \mathcal{B}_k) (\gamma_{-k'} \mathcal{B}_{k'} - \gamma_{k'}^+ \mathcal{B}_{k'}^+) \\
& - U_k^4 V_k^2 V_{k'}^2 (\gamma_{-k}^+ \mathcal{B}_k^+ + \gamma_k \mathcal{B}_k) (\gamma_{-k} \mathcal{B}_k \\
& - \gamma_k^+ \mathcal{B}_k^+) \} \tag{5.27}
\end{aligned}$$

The fourth order terms can be neglected because their contribution to the energy of the system is too small, then eq. (5.27) becomes;

$$\begin{aligned}
H_{eq} = \sum_{kk'} h_{kk'} \{ & -U_k^2 V_k^2 (U_k^4 - V_k^4) - (U_k^4 - V_k^4) U_{k'} V_{k'} U_k^2 (\gamma_{-k'} \mathcal{b}_{k'} - \gamma_{k'}^+ \mathcal{b}_{k'}^+) \\
& - (U_k^4 - V_k^4) U_k V_k V_{k'}^2 (\gamma_{-k} \mathcal{b}_k - \gamma_k^+ \mathcal{b}_k^+) + U_k^3 V_k^3 V_{k'}^2 (\gamma_k^+ \mathcal{b}_k^+ + \gamma_{-k} \mathcal{b}_k) \\
& - U_k^3 V_k^3 V_{k'}^2 (\gamma_{-k}^+ \mathcal{b}_k^+ - \gamma_k \mathcal{b}_k) + U_k^5 V_{k'}^2 V_k (\gamma_k^+ \mathcal{b}_k^+ - \gamma_{-k} \mathcal{b}_k) \\
& - U_k^5 V_{k'}^2 V_k (\gamma_{-k}^+ \mathcal{b}_k^+ \\
& + \gamma_k \mathcal{b}_k) \} \tag{5.28}
\end{aligned}$$

Equating the off-diagonal terms to zero, we obtain the diagonalized dipole Hamiltonian from eq. (5.28) as;

$$H_d = \sum_{kk'} h_{kk'} \{ -U_k^2 V_k^2 (U_k^4 - V_k^4) \} \tag{5.29}$$

The t-J-d Hamiltonian can now be expressed as the sum of the diagonalized t-J and dipole Hamiltonians by combining eq. (4.74) and eq. (5.29) to obtain the result below;

$$\begin{aligned}
H_{t-J-d} = \sum_{k,-k} J \left\{ -\frac{1}{4} + \frac{3}{4} V_k^2 - \frac{1}{2} V_k^4 - \frac{1}{2} U_k^2 V_k^2 \right\} - \sum_{kk'} t_{kk'} \{ 2U_k^2 V_k^2 \} \\
- \sum_{kk} h_{kk'} \{ U_k^2 V_k^2 (U_k^4 - V_k^4) \} \tag{5.30}
\end{aligned}$$

The Hamiltonian in eq. (5.30) can now be use to study the thermodynamic properties of high- T_c superconductors.

5.3 Thermodynamic properties of high- T_c superconductors in the t-J-d model

i. The superconducting energy of the t-J-d system

Substituting the values of U_k and V_k in eq. (5.30) we obtain the ground state energy of the t-J-d system as;

$$E_0 = (J + 4t_{kk'} + 6h_{kk'}) \quad (5.31)$$

The energy of the system, E at any temperature can be obtained by multiplying the ground-state energy, E_0 , by the thermal activation factor, $e^{-\frac{\Delta E}{kT}}$, where k is Boltzmann's constant and ΔE is energy gap which is generally 1% of the minimum value (Khanna, 2008) of the system energy ($\Delta E = \frac{E_0}{100}$). Thus;

$$E = (J + 4t_{kk'} + 6h_{kk'}) \cdot e^{-\left(\frac{J+4t_{kk'}+6h_{kk'}}{100kT}\right)} \quad (5.32)$$

ii. The specific heat capacity of the t-J-d system

The specific heat capacity at constant volume c_v of the system is obtained by determining the first derivative of the energy of the system with respect to the temperature (Khanna, 2008). Hence, using eq. (5.32), we have;

$$\begin{aligned} c_v &= \frac{\partial E}{\partial T} = \frac{\partial}{\partial T} \left[(J + 4t_{kk'} + 6h_{kk'}) \cdot e^{-\left(\frac{J+4t_{kk'}+6h_{kk'}}{100kT}\right)} \right] \\ &= \frac{(J + 4t_{kk'} + 6h_{kk'})^2}{100kT^2} \cdot e^{-\left(\frac{J+4t_{kk'}+6h_{kk'}}{100kT}\right)} \end{aligned} \quad (5.33)$$

The specific heat capacity of the superconducting system according to t-J-d system can now be expressed as;

$$c_v = \frac{(J+4t_{kk'}+6h_{kk'})^2}{100kT^2} \cdot e^{-\left(\frac{J+4t_{kk'}+6h_{kk'}}{100kT}\right)} \quad (5.34)$$

iii. Entropy of the t-J-d system

Entropy s of the system is obtained by substituting eq. (5.34) in eq. (4.82);

$$s = \int \frac{(J + 4t_{kk'} + 6h_{kk'})^2}{100kT^3} \cdot e^{-\left(\frac{J+4t_{kk'}+6h_{kk'}}{100kT}\right)} \cdot dT \quad (5.35)$$

Evaluating the integral in eq. (5.35) gives the superconducting entropy as;

$$s = \left[\frac{(J + 4t_{kk'} + 6h_{kk'})}{T} - k \right] \cdot e^{-\left(\frac{J+4t_{kk'}+6h_{kk'}}{100kT}\right)} \quad (5.36)$$

iv. Transition Temperature of the t-J-d system

By substituting eq. (5.34) in eq. (4.85), we evaluate the critical temperature of the superconducting state as follows;

$$\left[\frac{\partial}{\partial T} \left(\frac{(J + 4t_{kk'} + 6h_{kk'})^2}{100kT^2} \cdot e^{-\left(\frac{J+4t_{kk'}+6h_{kk'}}{100kT}\right)} \right) \right]_{T=T_c} = 0 \quad (5.37)$$

The result of eq. (5.37) is;

$$\frac{(J + 4t_{kk'} + 6h_{kk'})^2}{100k} \cdot e^{-\left(\frac{J+4t_{kk'}+6h_{kk'}}{100kT_c}\right)} \cdot \left\{ -\frac{2}{T_c^3} + \frac{(J + 4t_{kk'} + 6h_{kk'})}{100kT_c^4} \right\} = 0 \quad (5.38)$$

Solving eq. (5.38), we obtain transition temperature of the t-J-d system as;

$$T_c = \frac{(J + 4t_{kk'} + 6h_{kk'})}{200k} \quad (5.39)$$

CHAPTER SIX

RESULTS AND DISCUSSION

6.1 Numerical evaluation of the ground state energy

(a) The ground state energy of the t-J system

The magnitude of the ground state energy of the t-J system is given in eq. (4.77) as;

$$E_0 = (J + 4t_{kk'})$$

The experimental values of J and $t_{kk'}$ for the electron-doped LSCO nearest neighbor hopping are 0.13eV and 0.41eV respectively (Lee et al,2006). Using these values in the above equation gives the superconducting ground state energy of LSCO as $E_0 = 1.77eV$.

Experimental values of J and $t_{kk'}$ for the hole-doped YBCO are given as 0.17eV and 0.44eV, which on substituting in eq. (4.77), we obtain the ground state energy of YBCO as

$E_0 = 1.89eV$. High- T_c superconducting cuprates are either electron-doped or hole-doped, thus we expect their ground state energy to fall within the range 1.77eV to 1.89 eV.

(b)The ground state energy of the t-J-d system

The Magnitude of the ground state energy of the t-J-d system is given in eq. (5.31) as;

$$E_0 = (J + 4t_{kk'} + 6h_{kk'}). \text{ We need to evaluate the numerical value of } h_{kk'}. \text{ Eq. (5.2)}$$

gives the expression of $h_{kk'}$ as; $h_{k\sigma k'\sigma'q\lambda} = r|P_k(0)| \left[\frac{\hbar}{2I_k N \omega_\lambda(q)} \right]^{\frac{1}{2}} (\xi_{q\lambda}(k - k')) D_d^{kk'} \delta_{k-k',q+G}$. Taking the polarization vector $\xi_{q\lambda}(k - k')$ as unity (Heebok et al, 1991), then;

$$h_{k\sigma k'\sigma'q\lambda} = r|P_k(0)| \left[\frac{\hbar}{2I_k N \omega_\lambda(q)} \right]^{\frac{1}{2}} D_d^{kk'} \delta_{k-k',q+G} \quad (6.0)$$

The dynamic matrix $D_d^{kk'}$ can be expressed as (Heebok et al, 1991);

$$D_d^{kk'} = \frac{|P_k(0)||P_{k'}(0)|}{\sqrt{I_k I_{k'}}} \cdot e^{-iq(r|k|-r|k'|)} \cdot \frac{1}{\alpha} \delta_{k,k'} \quad (6.1)$$

In eq. (6.1), α is polarazability.

When the distance of the incident and scattered electron from the scattering centre are equal, then $r|k| = r|k'|$ and the exponential in eq. (6.1) reduces to 1, thus;

$$D_d^{kk'} = \frac{|P_k(0)||P_{k'}(0)|}{\sqrt{I_k I_{k'}}} \cdot \frac{1}{\alpha} \cdot \delta_{k,k'} \quad (6.2)$$

For $k = k'$ eq. 6.2 reduces to

$$D_d^{kk'} = \frac{|P_k(0)|^2}{I_k} \cdot \frac{1}{\alpha} \quad (6.3)$$

For an oxygen ion in a superconducting crystal (Heebok et al, 1991), $P_k(0) = 0.2e\text{\AA}$, where e stands for electronic units of force, $I_k = 5.2g/cm^2$ and $\alpha = 3.88\text{\AA}$. Substituting these values in eq. (6.3) we obtain;

$D_d^{kk'} = 0.019826e^2 \times 10^{40} J^2 / kgm$. The frequency of vibration of a single dipole $\omega_\lambda = 0.92 \times 10^{14} Hz$ (Heebok et al, 1991). If the electron interacting with the dipoles is at a distance averagely equal to a lattice constant away from the dipole, then $r = a = 3.85\text{\AA}$. When these values are substituted in eq. (6.0), the value of $h_{kk'}$ is obtained as;

$$h_{kk'} = 0.0041139 eV \quad (6.4)$$

Having calculated the value of $h_{kk'}$, we now obtain the ground state energy of the t-J-d system by substituting $h_{kk'}$ in eq. (5.31). For LSCO, $J=0.13eV$ and $t=0.41eV$ (Tsendin, 2001); the magnitude of the ground state energy of the electron-doped LSCO is obtained as

$E_0 = 1.7947eV$. For the hole-doped YBCO, $J=0.17eV$ and $t=0.44eV$ thus the ground state energy of YBCO is evaluated as $E_0 = 1.9547eV$. Thus, in the t-J-d model, the ground state energy of high- T_c superconducting cuprates is expected to fall in the range of $1.7947eV$ to $1.9547eV$ with small deviations.

A quick comparison of the t-J system and t-J-d system ground state energy reveals that the ground state energy of the t-J system is lower than the ground state energy of the t-J-d system. This increase is attributed to the electron-dipole interactions. As explained in chapter one of this thesis, the interaction of electrons with polarized oxygen ions (compound dipoles) causes dynamic perturbations on the crystal-field generated dipoles changing their magnitudes and directions. The dipoles then oscillate collectively generating lattice vibrations or phonons which are quantized energy. Inelastic Neutron Scattering (INS) experiments (Andrei, 2004) show that phonons are an essential part of high- T_c superconductivity for they are highly coupled to the charge carriers.

An electron-phonon interaction parameter called spectral function $\alpha^2F(\omega)$ characterizes the coupling strength between charge carriers and phonons. ARPES measurements (Andrei, 2004) performed in LSCO, YBCO, Bi2212 and Bi2201 show a kink in the dispersion at 55-75 meV confirming the fact that optical phonons of energy 55-75meV are coupled with charge carriers. Regardless of the origin of phonons in HTS, their energies are usually high thus the true ground state energy of the HTS can only be obtained if phonon energy is considered as it has been done in the t-J-d model. In this case, the coupling phonon energy added to the t-J system is $6h_{kk'} = 24.68meV$. A

detailed analysis of the transfer energy, t and its effect on the superconducting transition temperature is done in section 6.3 (a) of this thesis.

6.2 Graphical analysis of system energy

a. Variation of the system energy, E with temperature, T of the system.

To obtain the variation of the energy of the system with the temperature, experimental values $J=0.13\text{eV}$, $t=0.41\text{eV}$ for LSCO, $J=0.17\text{eV}$, $t=0.44\text{eV}$ for YBCO and the calculated value of $h_{kk'}$ is substituted in eqs. (4.79) and (5.32). The value of $h_{kk'}$ is applicable for both superconductors since it calculated using experimental parameters that govern general superconducting crystals. Figures 6.0 and 6.1 are thus obtained for the t-J model and the t-J-d models respectively.

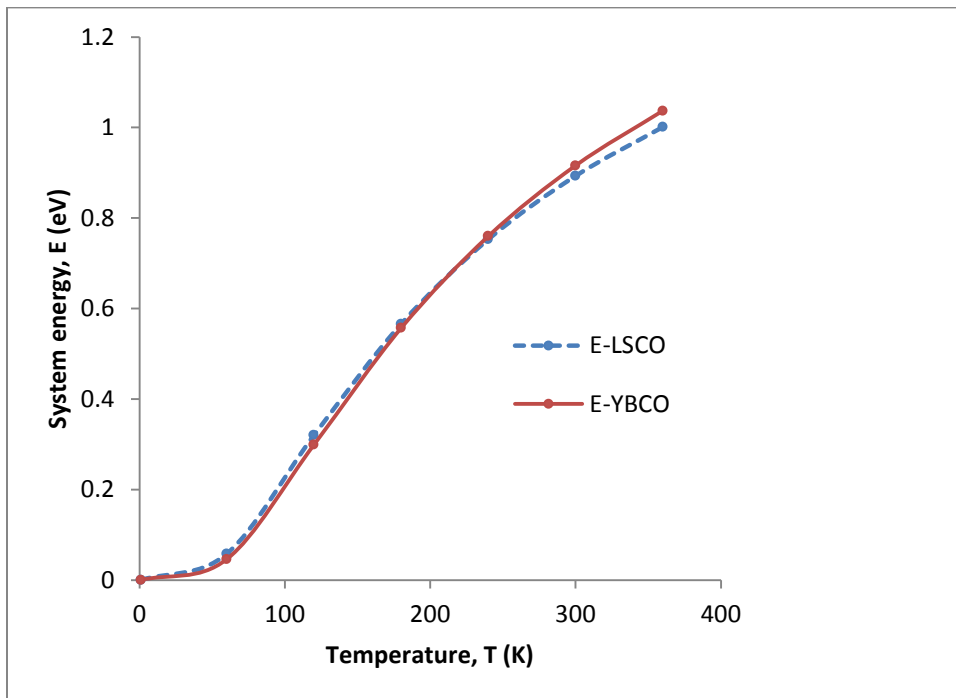


Figure 6.1 (a): Variation of system energy with temperature for the t-J model

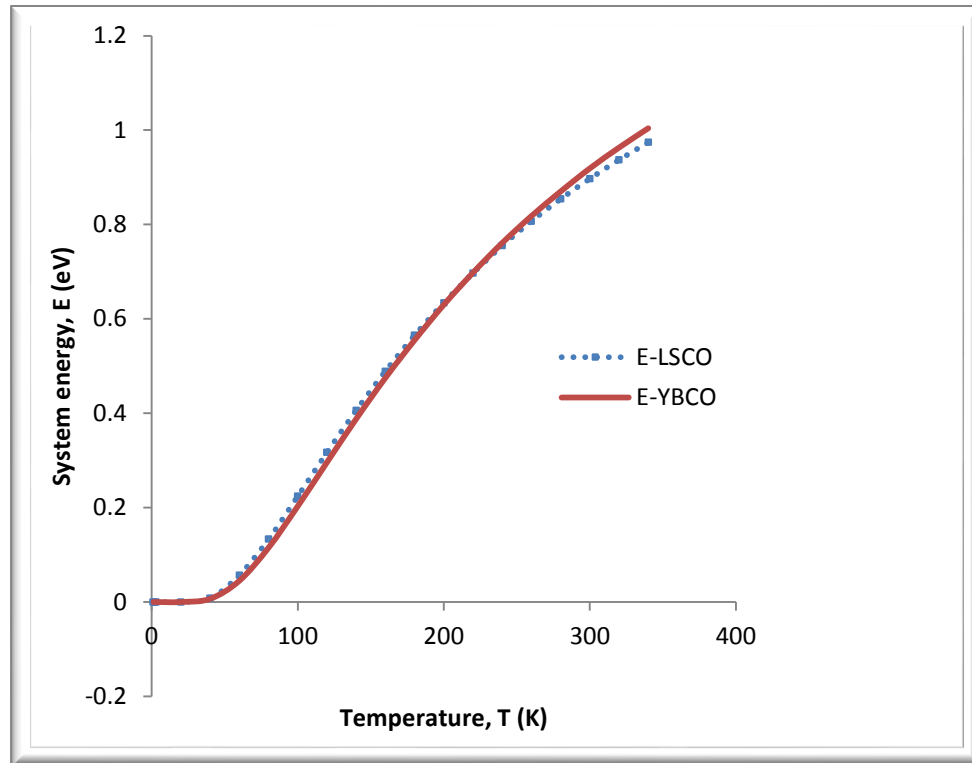


Figure 6.1 (b): Variation of system energy with temperature for the t-J-d model

For both LSCO and YBCO, both models show an exponential increase in the energy of the system as the temperature increases. The rate of increase of energy with temperature for LSCO (which has lower t) is lower than that of YBCO (which has higher t) in the temperature range of 0 K-220 K. However, at high temperatures approaching room temperature ($T > 220$ K), the trend is reversed with YBCO showing a lower rate of change of system energy. High- T_c superconductivity, being a low-energy process requires that the system energy should be kept as low as possible. Thus YBCO would be a better candidate for the construction of a room-temperature superconductor. At about 220 K, both LSCO and YBCO have common system energy of 0.70 eV. This energy could be an indicator of the transition point from the superconducting state to the normal state. When temperature is reduced below the transition temperature, energy of the superconductor

drops exponentially as is revealed in the graph. From these results, we can conclude that superconductors with lower transfer energy experience a low rate of change of energy with temperature at low temperatures and low rate of change of energy at high temperatures while the opposite is true for superconductors with high transfer energy.

Similar graphs were obtained by Danilo Gambacurta and Denis Lacroix (Danilo *et al.*, 2012) when studying the energy of small superconductors with a fixed number of particles (see Appendix E). Starting with a system of 10 particles whose energy was approximately -0.30 eV, increase in temperature from 0K to 5 K witnessed a corresponding exponential increase in energy in the positive y-axis. While Danilo used variational theory applied to low temperature small systems of particles, I have used the t-J-d theory applicable to high temperatures and can be generalized to large systems.

6.3 Numerical evaluation of the transition temperature

a. Numerical T_c of the t-J system

The critical temperature of the t-J system is given by equation 4.89. Substituting the values $J=0.13$ eV and $t=0.41$ eV for LSCO and $k= 8.63\times 10^{-5}$ eV/K, we obtain the numerical value of T_c for LSCO as $T_c = 102.5$ K. The experimental value of T_c for LSCO is 38 K (Andrei, 2004). The t-J model thus predicts a critical temperature value for LSCO that is 2.7 times higher than the present experimental value. It must be noted that LSCO was the first HTS discovered in 1987 with $T_c=38$ K. (Park, 2005, Appendix A). In the same year it was discovered that under moderate pressure, the T_c of LSCO increased to 52 K. Shortly afterward a higher T_c was obtained in YBCO (90 K) and even a higher

one in HgBaCaCuO (135 K). Research was shifted to the mercury based cuprates with much higher T_c and less has been done on LSCO. However the application of the t-J model reveals that higher T_c can be achieved in the LSCO.

Substituting $J=0.17\text{eV}$, $t=0.44\text{ eV}$ for YBCO (Tsendin, 2001) in eq. 4.89, $T_c = \frac{(J+4t_{kk'})}{200k}$ we get the numerical value of $T_c = 111.8\text{ K}$, which is higher than the current experimental value of 90 K (R. K. Puri et al, 2001) by 21.8 K. By applying the same calculations, one realizes that room temperature superconductivity ($T_c=300\text{ K}$) in LSCO is possible if the transfer energy is 1.262 eV and 1.252 eV in YBCO.

Since the lowest ever achieved experimental exchange energy for high- T_c superconductors is $J=0.13\text{ eV}$, we apply it together with experimental T_c values for various high- T_c superconductors in eq.4.89 to calculate transfer energies of t cuprates in the t-J model. The results are summarized in the table 3.0;

Table 3.0: A summary of transfer energy values of the t-J system for various high- T_c superconducting cuprates

Cuprate	Abbreviation	T_c (K)	Transfer energy, t (eV)
$\text{Bi}_2\text{Sr}_2\text{CuO}_6$	Bi2201	~12	0.0193
$\text{Nd}_{2-x}\text{Ce}_x\text{CuO}_4$	NCCO	24	0.0711
$\text{La}_{2-x}\text{Sr}_x\text{CuO}_4$	LSCO	38	0.13147
$\text{YBa}_2\text{Cu}_3\text{O}_{6+x}$	YBCO	93	0.3688
$\text{Bi}_2\text{Sr}_2\text{CaCu}_2\text{O}_8$	Bi2212	95	0.3774
$\text{Tl}_2\text{Ba}_2\text{CuO}_6$	Tl2201	95	0.3774
$\text{HgBa}_2\text{CuO}_4$	Hg1201	98	0.3904
$\text{Tl}_2\text{Ba}_2\text{CaCu}_2\text{O}_8$	Tl2212	105	0.4206
$\text{Bi}_2\text{Sr}_2\text{Ca}_2\text{Cu}_3\text{O}_{10}$	Bi2223	110	0.4422
$\text{Tl}_2\text{Ba}_2\text{Ca}_2\text{Cu}_3\text{O}_{10}$	Tl2223	125	0.5069
$\text{HgBa}_2\text{CaCu}_2\text{O}_8$	Hg1212	128	0.5241
$\text{TlBa}_2\text{Ca}_2\text{Cu}_4\text{O}_{11}$	Tl1224	128	0.5198
$\text{HgBa}_2\text{Ca}_2\text{Cu}_3\text{O}_{10}$	Hg1223	135	0.5500

Two very important observations can be made from Table 3.0. First, we observe that using the t-J model, the current critical temperature values of the various high- T_c superconducting cuprates can be achieved at transfer energy lower than the current experimental values. A good example is YBCO whose experimental transfer energy of 0.44 eV has been lowered to 0.3688 eV. This is a 19.3% decrease. For the electron-doped LSCO, t has been raised slightly from 0.13eV to 0.13147 eV. Secondly, the table shows that critical temperature increases with increase in transfer energy for high- T_c superconductors. It is, therefore, possible to achieve higher T_c by increasing t. Transfer energy; t can be increased by increasing onsite Coulomb repulsion energy U since

$J = \frac{2t^2}{U}$ (Park, 2005). The challenge that faces this approach is that for a given superconductor, U is increased by increasing charge carriers on a centre and these charges can only be increased to a certain maximum value beyond which stability will not be sustained. The second challenge is that for t-J system, the experimental ratio $\frac{J}{t}$ should be equal to a third (Jakub Jedrak, 2011). However, this can be overcome by increasing J proportionately.

b. Numerical T_c of the t-J-d system

The T_c formula for the t-J-d system is given in eq. 5.39; $T_c = \frac{(J+4t_{kk'}+6h_{kk'})}{200k}$. Substituting the J and t values of LSCO and the calculated $h_{kk'}$ value in eq. 6.4 ($h_{kk'} = 0.0041139$) we find T_c for LSCO as 103.98 K. We observe that the t-J-d system gives a transition temperature that is both higher than that of the t-J system (102.5 K) and the highest known experimental value of 38 K (Andrei, 2004).

On substituting the J and t values of YBCO in eq. 5.39, T_c for YBCO is 113.2 K. This T_c is higher than that of the t-J model (111.8 K) by 1.4 K. For $\text{Bi}_2\text{Sr}_2\text{CuO}_6$ whose first neighbor hoping energy is $t=0.27$ eV (Jakub Jedrak, 2011), T_c in the t-J-d model is found to be 71.5 K. Compared to the experimental value of 12 K, the t-J-d system T_c is almost six times the experimental value.

Using the experimental T_c values for various high- temperature superconducting cuprates in eq. 5.39, the corresponding transfer energies are calculated and summarized in the table 4.0

Table 4.0: A summary of transfer energy values of the t-J-d system for various high- T_c superconducting cuprates

Cuprate	Abbreviation	T_c (K)	Transfer energy, t (eV)
$\text{Bi}_2\text{Sr}_2\text{CuO}_6$	Bi2201	~ 12	0.0131
$\text{Nd}_{2-x}\text{Ce}_x\text{CuO}_4$	NCCO	24	0.0649
$\text{YBa}_2\text{Cu}_3\text{O}_{6+x}$	YBCO	93	0.3626
$\text{Bi}_2\text{Sr}_2\text{CaCu}_2\text{O}_8$	Bi2212	95	0.3712
$\text{Tl}_2\text{Ba}_2\text{CuO}_6$	Tl2201	95	0.3713
$\text{HgBa}_2\text{CuO}_4$	Hg1201	98	0.3842
$\text{Tl}_2\text{Ba}_2\text{CaCu}_2\text{O}_8$	Tl2212	105	0.4144
$\text{Bi}_2\text{Sr}_2\text{Ca}_2\text{Cu}_3\text{O}_{10}$	Bi2223	110	0.4360
$\text{Tl}_2\text{Ba}_2\text{Ca}_2\text{Cu}_3\text{O}_{10}$	Tl2223	125	0.5001
$\text{HgBa}_2\text{CaCu}_2\text{O}_8$	Hg1212	128	0.5136
$\text{TlBa}_2\text{Ca}_2\text{Cu}_4\text{O}_{11}$	Tl1224	128	0.5136
$\text{HgBa}_2\text{Ca}_2\text{Cu}_3\text{O}_{10}$	Hg1223	135	0.5439

Comparing the results of the t-J-d system to those of the t-J system, it is clear that the t-J-d system has lowered transfer/ hopping energy for all the enlisted high- T_c cuprates. Experimentally, low transfer energy is a prerequisite for the achievement of higher critical temperatures. Such a recommendation was made by Lee, Nagaosa and Wen (Lee et al, 2006) who stated that when $\gg J$, holes are strongly delocalized. There exists competition between the exchange energy J and the kinetic energy which is of the order of t per hole or xt per unit area, where x is the doping level. When $xt \gg J$ we expect the kinetic energy to win and the system would be a Fermi-liquid metal with a weak residual anti-ferromagnetic correlation, a situation that is not favorable for the superconducting process. When $xt \leq J$, however, the system would like to maintain the antiferromagnetic

correlation while allowing the hole to move as freely as possible. This is the case of a Mott insulator and it enhances high- T_c superconductivity. The variation of critical temperature of the superconducting cuprates with transfer energy is shown in figure 6.2 (Appendix).

6.4 Variation of Heat capacity, C_v with Temperature, T

Substituting the experimental values $J=0.13\text{eV}$, $t=0.41\text{eV}$ for LSCO, $J=0.17\text{eV}$, $t=0.44\text{eV}$ for YBCO, and the calculated value of $h_{kk'} = 0.0041139\text{eV}$ in eqs. (4.84) and (5.34), heat capacity is found to vary with temperature in the t-J and t-J-d models as shown in figure 6.3.

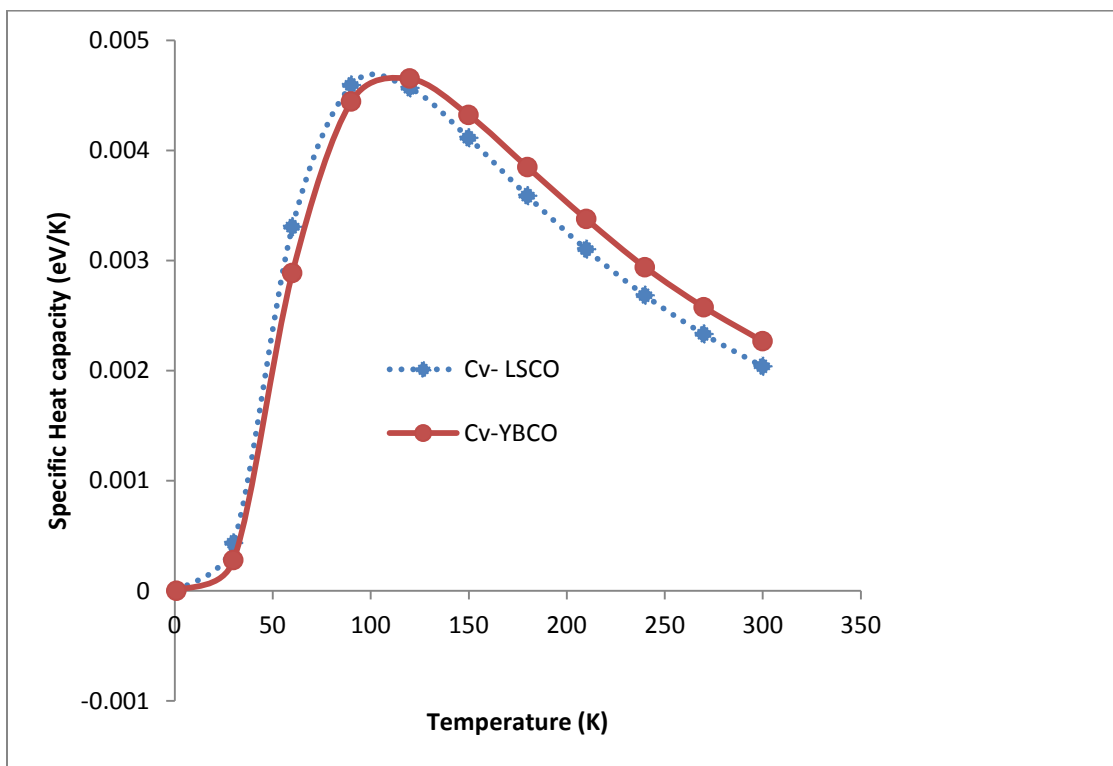


Figure 6.2(a): Variation of specific heat capacity with temperature for the t-J model

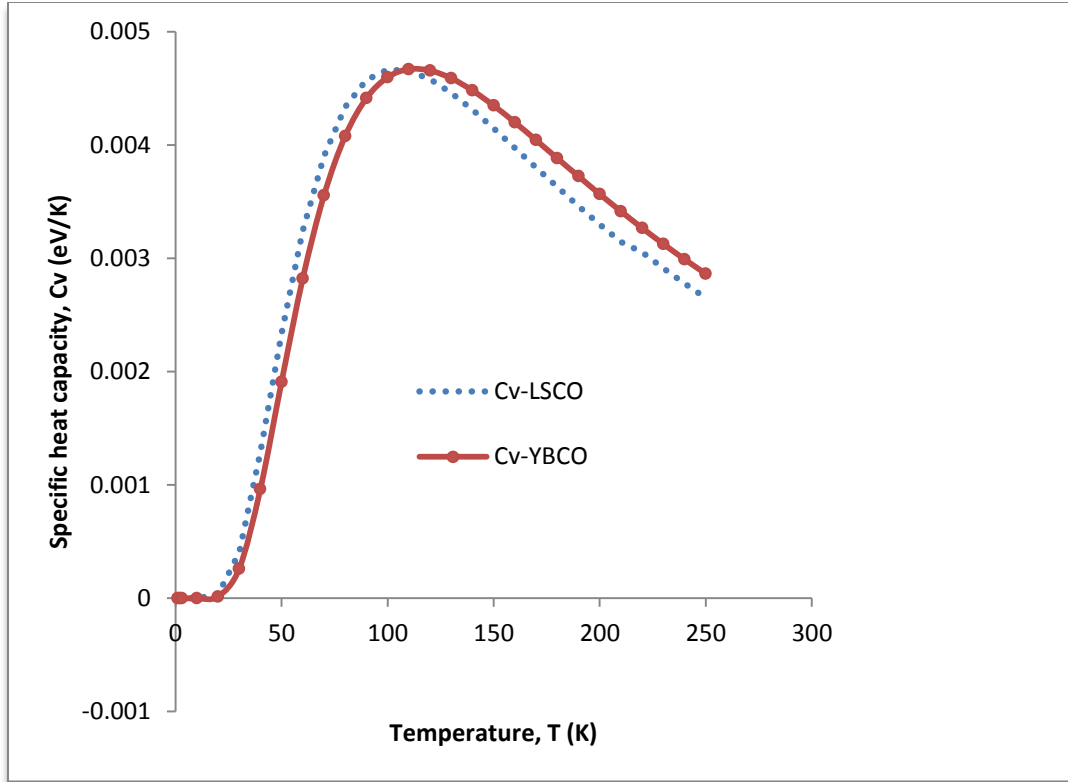


Figure 6.2 (b): Variation of specific heat capacity with temperature for the t-J-d model

For both LSCO and YBCO, the heat capacity is observed to drop exponentially with temperature from a given peak value which is constant for both LSCO and YBCO (regardless of the value of t). The maximum value of heat capacity for the cuprates is maintained at $4.7 \times 10^{-3} eV/K$.

At the peak or turning point of each graph, $\left[\frac{\partial c}{\partial T}\right]_{T=T_c} = 0$, hence the temperature corresponding to the peak is critical temperature of the superconductor. Clearly, T_c for LSCO is approximately 100 K which is higher than the experimental value of 38 K (Andrei, 2004). This value is approximately equal to the calculated value of 102.5 K. The

graph of YBCO gives $T_c = 110$ K which is also approximately equal to the calculated value of 111.8 K.

The shapes of the graphs obtained in this theory are in fine agreement with those obtained by Khanna and Kirui (Khanna et al, 2002) for the variation of heat capacity and temperature for the cuprates $Tl_2Ba_2Ca_2Cu_3O_{10}$ and $YBa_2Cu_3O_{7-\delta}$. In both cases heat capacity drops exponentially from a peak value and vanishes at $T=0$ K. In their theory; Anharmonic apical oxygen vibration in high- T_c superconductors, the peak of the graph gives $T_c = 255$ K for $YBa_2Cu_3O_{7-\delta}$ which is far above the experimental value making the t-J-d theory a better theory in the approximation of T_c in YBCO.

Volya, Brown and Zelevinsky studied thermodynamical properties of small superconductors with a fixed number of particles at very low temperature ranging from 0K to 5 K (Volya et al, 2001). They applied the Finite Temperature BCS (FT-BCS) approximations in the diagonalization of the quasi- particle pairing Hamiltonian for a small system of particles, $N=10$ particles. The results are shown in figure 6.4.

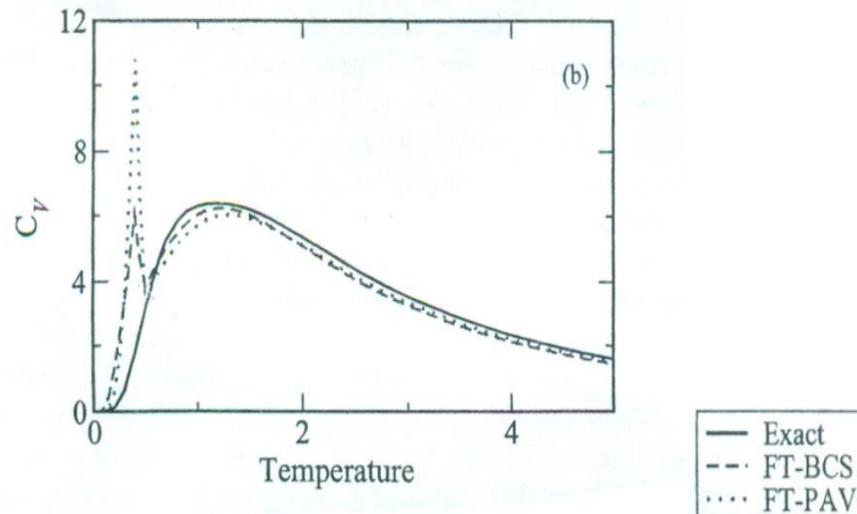


Figure 6.3: Evolution of energy with temperature obtained with FT-BCS, PAV (Danilo, 2012).

The shape of exact solution graph obtained for the variation of heat capacity, c_v with temperature perfectly agrees with that obtained in the t-J-d theory. A smooth curve with an exponential drop of c_v from a peak value is observed. The highest c_v obtained was approximately $4.5 \times 10^{-2} eV/K$ for $N=10$ particles, which is in agreement with the t-J-d results ($4.7 \times 10^{-3} eV/K$) for a one particle system, except that the t-J-d heat capacity is lower by a factor of 10^{-1} . If the number of particles in the t-J-d system is increased we expect a corresponding increase in c_v and the two results would thus agree. While Vyola's graph gives low $T_c=1$ K (peak temperature), the t-J-d system gives high- T_c for superconductors. It must also be noted that the FT-BCS theory suffers from the problem of overestimation of energy as it uses variational approach and a sharp super fluid- to-normal phase transition as the temperature increases.

6.5 Numerical C_v of the t-J and the t-J-d models

In the t-J model, the value of c_v by calculation is obtained as $6.65 \times 10^{-3} eV/K$ for LSCO using the calculated value of $T=T_c=102.5$ K in eq. 4.81, and $5.28 \times 10^{-3} eV/K$ for YBCO at $T=T_c=111.8$ K. In the t-J-d model, by using $T=T_c=103.98$ K for LSCO and $T=T_c=113.2$ K for YBCO in eq.5.34, the value of c_v is calculated as $6.39 \times 10^{-3} eV/K$ for LSCO and $5.0 \times 10^{-3} eV/K$. It is observed that for the same superconductor, c_v of the t-J-d model is lower than that of the t-J model. The reduction is attributed to the attractive energy between the electron and the dipole which enhances phonon-mediated pairing of electrons hence lowers heat per particle pair. In the derivation of ground state energy formula, we allowed all terms in the Hamiltonian to vanish and remained with the quasi particle excitation creation terms $\gamma_k^+ \gamma_{-k}^+$ so that only pairs of quasi particles could be excited. The minimum energy required to create such excitations is the exponential 2Δ (Khanna, 2008). Thus heat capacity will drop with increase in the energy that leads to the creation of quasi particles.

6.6 Variation of entropy, s with Temperature, T

Substituting the experimental values $J=0.13eV$, $t=0.41eV$ for LSCO, $J=0.17eV$, $t=0.44eV$ for YBCO, and the calculated value of $h_{kk'} = 0.0041139eV$ in eqs. (4.84) and (5.36), entropy is found to vary with temperature as shown below.

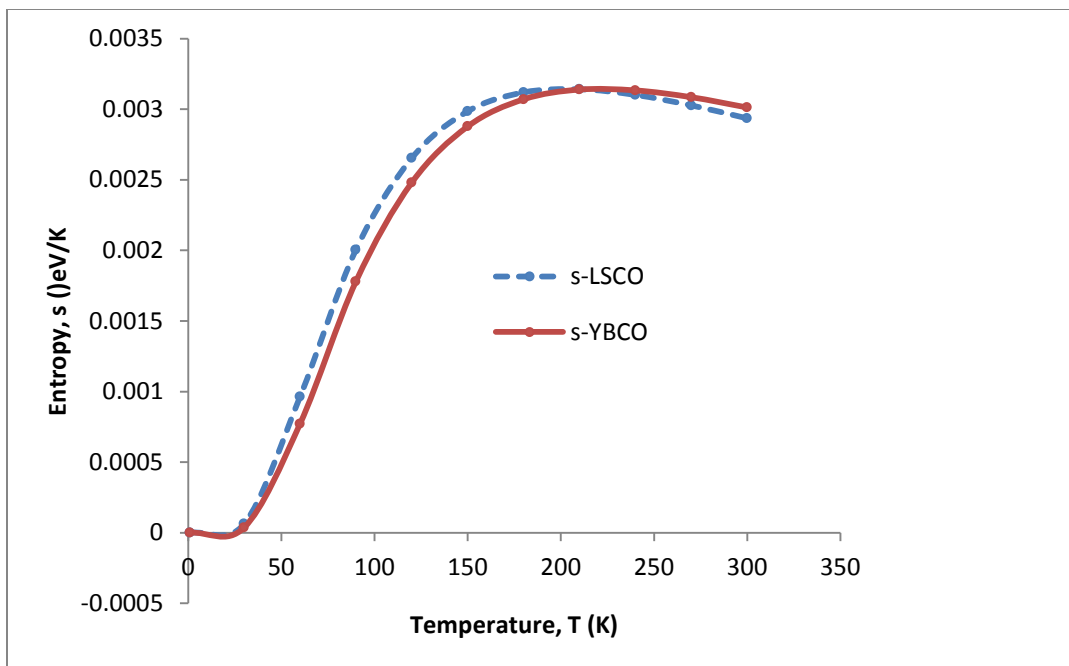


Figure 6.4(a): Variation of entropy with temperature for the t-J model.

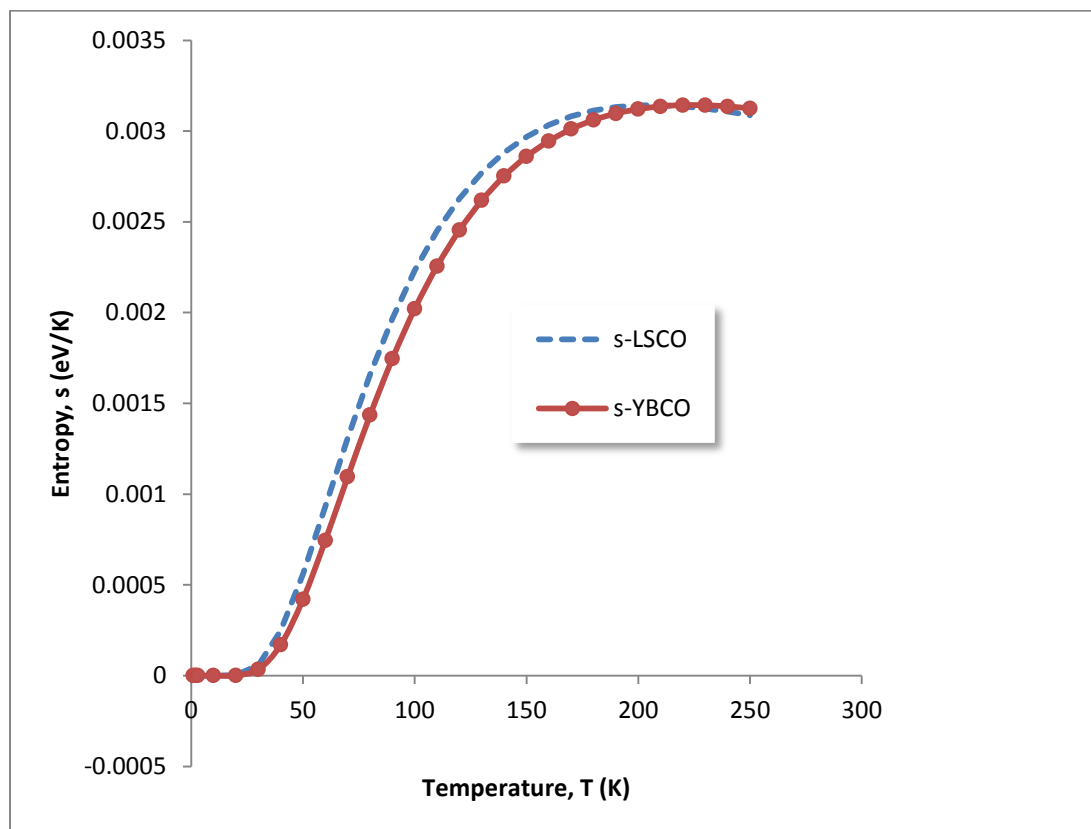


Figure 6.4 (b): Variation of entropy with temperature for the t-J-d model

The results presented shows exponential growth of entropy with temperature for both LSCO and YBCO in t-J and the t-J-d model. With small variation, the maximum entropy for LSCO and YBCO is approximately 3.13×10^{-3} eV/K in the t-J model and 3.15×10^{-3} eV/K in the t-J-d model.. At maximum entropy, critical temperature of LSCO is $T_c = 200$ K and that of YBCO is $T_c = 220$ K. We also note that the rate of increase of entropy with temperature of the system for LSCO is higher than that of YBCO. High- T_c superconductivity requires low entropy hence YBCO is better in building superconductors that can work at room temperature.

In their study of thermodynamic properties of small superconductors (Danilo et al, 2012), Danilo Gambacurta and Denis Lacroix applied the Finite Temperature Variation –After-Projection (FT-VAP) technique in minimizing free energy of superconducting state and calculated entropy of the system as; $s = -k_B \sum_i D_i^N \ln D_i^N$, where k_B is Boltzmann constant and D_i^N are the eigenvalues of the statistical operator in the Fock space composed by all the many body configurations with N particles. Variation of entropy with temperature graph was a smooth curve showing an exponential decrease of entropy with temperature from a maximum value of 0.125 eV/K (Appendix E/ Danilo et al, 2012). The shape of the graph is in agreement with t-J-d result. The maximum value of entropy in the FT-VAP theory is lower than the corresponding value of the t-J-d system as expected since the FT-VAP theory is dealing with very low temperatures (0 K-5 K) while the t-J-d theory is dealing with the whole range of temperature from low to high.

6.7 Numerical entropy of the t-J and the t-J-d models

The t-J model value of entropy at $T=T_c=102.5$ K for LSCO was calculated as $3.308 \times 10^{-3} eV/K$ and $2.58 \times 10^{-3} eV/K$ for YBCO at $T=T_c=111.8$ K. The t-J-d calculated value of entropy at $T=T_c=103.98$ K for LSCO was $1.278 \times 10^{-3} eV/K$ and $2.50 \times 10^{-3} eV/K$ for YBCO at $T=T_c=113.2$ K. Again one quickly notices that the t-J-d model has lower entropy as compared to the t-J model, a condition that is quite favorable for high- T_c superconductivity given that superconducting process is a high order process that require low entropy.

CHAPTER SEVEN

CONCLUSIONS AND RECOMMENDATIONS

7.1 CONCLUSIONS

The work covered in this thesis can be divided into two characteristic sections. In the first section, the t-J model Hamiltonian was diagonalized using Bogliubov-Volatin transformation and the thermodynamic properties of high- T_c superconductors, namely, energy, heat capacity, entropy and critical temperature in the t-J model were studied. The results obtained are in fine agreement with the FT-VAP study of thermodynamic properties of small superconductors (Danilo *et al.*, 2012). The t-J model has been found to predict transition in YBCO more accurately than the anharmonic apical oxygen theory (Khanna *et al.*, 2002) of high- T_c superconductivity. The t-J model, being a model that captures strong electronic correlations in HTS predicts the possibility of achieving more than double the experimental value of T_c for the electron-doped LSCO.

In the second section, the dipole interaction energy was included in the t-J model resulting in what is now referred to as the t-J-d model. As a proof of ARPES measurements (Andrei, 2004) that show high charge carrier coupling with phonon energy, the inclusion of phonon energy generated as a result of dipole oscillation has raised the ground state energy of the t-J model and the transition temperature of LSCO and YBCO. Due to attractive interaction energy between the charge carriers and the

dipoles the heat capacity and entropy of the t-J-d model is lower than that of the t-J model providing a better platform of high- T_c superconductivity.

Transfer energy for twelve categories of superconducting cuprates were calculated and it now evident that a linear relation between transfer energy and transition temperature exists. Careful application of this discovery can lead a rise in T_c of high- T_c superconductors. In summary, the theories developed in this research are of general validity and can be applied to any high- T_c superconductor in the analysis of thermodynamic properties.

7.2 RECOMMENDATIONS

The approach presented in this thesis pertaining to the development of new Hamiltonians of high- T_c superconductivity and the analysis of their thermodynamic properties is thorough and rigorous. However, it can be improved on in some ways, some of which are enlisted below;

- a In this thesis, emphasis was laid on first or nearest neighbor electron transfer energy. An extension can be made to second and third neighbor transfer energy with caution given that long-range electronic interaction destroys Cooper pair formation.
- b The effect of the on-site Coulomb energy, U , was not considered in this thesis. The inclusion of this energy in the developed theories will give more insight in the study of strong coupling when $U \gg t$ in the Heisenberg model and weak coupling when $U=0$ eV. It should be noted that an increase in on-site Coulomb energy reduces transfer energy (Belinicher et al, 1994, Appendix B).

- c Doping level is another paramount factor that can significantly alter the results if considered. Hole doping, for instance, affects the anti-ferromagnetic background of the superconductor because the movement of a hole creates a string of flipped spins (Demler, 2010) which results to an effective attraction between the holes.
- d The results obtained on the contribution of dipole energy to the superconducting state properties can be strengthened further by extending the one-particle study done in this research to the many particle system.

REFERENCES

- Aditya M. Vora. (2008) Modified Transition Temperature Equation for Superconductors. *Chin. Physica. Letters.* 25, 2162-2164.
- Alexandrov A.S, Samson J.H., Sica G. (2012). High Temperature Superconductivity from realistic Coulomb and Frohlich interactions. *Physical Review B.* 85, 104520.
- Alexandrov A.S , Kornilovitch P.E. (2002). High-temperature superconductivity and charge segregation in a model with strong long-range electron-phonon and Coulomb interactions, *Physical Letters A*, 299, 650-655.
- Anderson, P. W (1987). The resonating valence bond state in La_2CuO_4 and superconductivity, *Science.* 235, 1196-1198.
- Andrei Marouchkine, (2004). *Room-Temperature superconductivity*, Cambridge International Sciences Publishing, 7 Meadow Walk, Great Abington, Cambridge, U.K
- A. Volya, B.A Brown, V. Zelevinsky. (2001). Exact solution of the nuclear pairing problem. *Physics Letters B.* 509(1), 37-42.
- Bardeen J, Cooper L. N and Schrieffer J.R. (1957). Theory of superconductivity. *Physical Review.* 108, 1175-1204.
- Barnes, S.E, Maekawa S. (1976). A Jordan- Wigner transformation for the t-J and Hubbard models with holes. *Journal of Physics F.* 6, 1375.
- Baskaran G, Zou Z, Anderson P. W. (1987). The resonating valence bond state and high- T_c superconductivity- A mean field theory. *Solid State Communication.* 63, 973-976.

B.W. Rapando, Y.K. Ayodo, T.W. Sakwa, K.M. Khanna, A.Sarai. (2013). Transition Temperature of Hybridized Cuprate Systems, *International Journal of Physics and Mathematical Sciences*, 3(2), 104-109.

Corson J R, Orenstein J, Oh S, O'Donnell J, Eckstein J N. (2000). Nodal quasi-particle lifetime in the superconducting state of $\text{Bi}_2\text{Sr}_2\text{CaCu}_2\text{O}_{8+\delta}$. *Physical Review Letters*. 85(12), 2569.

Curro N J, Milling C. T, Haafe J. Slinchter P. C. (2000). Spin lattice relaxation and echo decay rates in the mixed state of $\text{YBa}_2\text{Cu}_3\text{O}_7$. *Physical Review B*, 62, 3473-3479.

Danilo Gambacurta, Denis Lacroix. (2012). Thermodynamical properties of small superconductors with a fixed number of particles. *Physical Review C*, 85, 1-4.

David Eichenberger, (2008). *Superconductivity and antiferromagnetism in the two-dimensional Hubbard model*, Ph.D Thesis, University of Fribourg (Suisse), Thesis no.1606.

David Halliday, Robert Resnick, (1966), *Physics Part I & II*, 3rd edition. Toppan Printing Company Ltd. London.

Emery, V.J. (1987). Theory of high-T_c superconductivity in oxides *Physical Review Letters*. 58, 2794-2797.

- Eugene Demler. (17th Nov. 2010). *Strongly Correlated systems in atomic and condensed matter physics*. Lecture notes for physics 284, Harvard University.
- Frohlich H. (1950). Theory of superconducting state I. The ground state at the absolute zero of temperature. *Physical Review*. 79, 845.
- Gunnarsson O. and Rösch O. (2006). Interplay between electron- phonon and Coulomb interactions in cuprates, *Physical Review B*, 73, 174521.
- G.J. Wu, S.L. Liu, X.B. Xu, J. Wu , H.M. Shao, (2004). The Paramagnetism Carried by Paramagnetic Ions and its Effect on Superconductivity in High T_c Superconductors, *Journal of Superconductivity*,17, 689-693.
- Heebok Lee and R.R Sharma. (1991). Dispersion relations and density of states of the collective oscillations of electronic dipoles in high- T_c superconductors. *Physical Review B*, 43, 7756.
- H. Oesterreicher, (2003). How ‘Musical’ Are High- T_c Superconductors and What Can Empirical Rules Tell About Their Origin?, *Journal of Superconductivity*, 16, 971-980.
- Hybertson, M. S. (1990). *Physical Review B*. 41, 11068.
- Jakub Jedrak. (2011). *Real-Space pairing in an extended t - J model*. PhD Thesis. Uniwersytet Jagielloński.
- Ju H. Kim, K. Kelvin, R. Wentzcovitch, (1991). Electron-phonon interactions in the high temperature superconductors, *Physical Review B*, 44, 5148-5165.

Kamerlingh H, Onnes, (1911), The superconductivity of mercury, *Leiden*

Communication.122b, 124C.

Kazuhiko Kuroki. (2011 December) *Computational Studies on High-Temperature*

Superconductivity. In the proceedings of Advanced Seminar, Osaka University IPC ,

Tokyo, Japan.

Kazushige Machida, Tsutomu Nishira, Tetsuo Ohmi, (1999). Orbital Symmetry of a Triplet

Pairing in a Heavy Fermion Superconductor UPt_3 , *Journal of Physical Society of*

Japan, 68, 334-3371.

K. M Khanna & M. S Karap Kirui. (2002). Anharmonic apical oxygen vibration in high- T_c

superconductors. *Indian Journal of Pure & Applied Physics*. 40, 887-895.

K.M.Khanna, (2008). *Superconductivity*, ISBN:9966-854-48-7, Moi University Press, Moi

University Eldoret, Kenya page ,26-37.

K. Park. (2005). Quantum Anti-ferromagnetism and High T_C Superconductivity; A close

connection between the t-J model and the projected BCS Hamiltonian. *Physical*

Review Letters. 95, 027001

K.D.Tsendin, D. V. Denisov. (2001). Theoretical possibility of increasing of superconducting

transition temperature in High Temperature superconductors by replacing Oxygen

with Chalcogens. *Journal of Optoelectronics and Advanced Materials*. 3, 549-552.

K. Miyake, S. Schmitz-Rink and C.M. Varma. (1986). Spin fluctuation mediated even parity

pairing in heavy fermion superconductors *Physical Review B*, 34(9), 6554-6556.

Kastner, M.A, Birgeneau R. J, Shirane G, Endoh Y. (1998). Magnetic, transport and optical properties of monolayer copper oxides *Reviews of modern physics*. 70, 897.

Lee, Sung.-Sik, Patrick.A Lee, (2005). U(1) Gauge theory of the Hubbard model: Spin-liquid states and possible application to K(BEDT-TTF)-2Cu-2(CN)-3. *Physical Review Letters*. 95, 036403.

L. Menon, D. Yu, P. F. Williams, S. Bandyopadhyaya, Y.Liu, B.Jayaram, (2001). Enhanced transition temperature in a quantum confined high- T_c superconductor, *Solid State Communications*, 117, 615-620.

Mark S. Hybertsen, E.B. Stechel, M. Schluter, D.R. Jennison, (1990). Renormalization from density-functional theory to strong-coupling models for electronic states in Cu-O materials, *Physical Review B*. 41, 11068-11072.

Mitake Miyazaki. (2005). Effects of Higher Hopping. *Journal of Superconductivity*. 18, 727-730.

Mishchenko A. S. and Nagaosa N. (2004). Electron-phonon coupling and a polaron in the t-J model: From the weak to the strong coupling regime *Physical Review Letters*. 93, 036402.

Miklos Gulacsi and Raymond Chan, (2011). High-Temperature Superconductivity: The Attractive U_p Regime, *Journal of Superconductivity*, 14, 651-658.

Meissner W and Oschenfeld R (1933), Meissner effect in superconductors.

Naturwissenschaften, 21, 787-788.

N.M Plakida, (2002). Superconductivity in the t-J model, *Condensed Matter Physics*, 5, 707-727.

Patrick A. Lee, Naoto Nagaosa. (2003). Collective modes in the superconducting ground states in the gauge theory description of the cuprates, *Physical Review B*. 68, 1 -19.

Patrick A. Lee, Naoto Nagaosa. (1992). Gauge theory of the normal state of high- T_c superconductors, *Physical Review B*, 46, 5621-5639.

Patrick Lee, Naoto Nagaosa, Xiao-Gang Wen. (2006). Doping a Mott insulator: Physics of high-temperature superconductivity. *Reviews of modern physics*. 78 (1), 78.

Pradeep Chaudhary , Anuj Nuwal, S. C Tiwari, R.K Paliwal, S. K Kakani. (2013). Polaronic Mechanism of Superconductivity in Cuprates. *International Journal of Superconductivity* 2013, 1-13.

Qiang Du, Max D. gunzburger, Janet S. Peterson. (1992). Analysis and approximation of the Ginzburg-Landau model of superconductivity, *SIAM Review*, 34, 54-81.

R. K. Puri ,V. K. Baabar. (2001). *Solid State Physics*; S Chard & Company Limited, Ramnagat New Delhi 1100s.

R.R. Sharma. (2001). Dipolon theory of energy gap parameters in high-temperature superconductors at zero temperature. *Physical Review B*, 63.

Sergei Sergeenkov, Marcel Ausloos. (1995). Field-Induced agind effects in inhomogeneous superconductors. *Physical Review B*. 52, 13526.

- Sulewsky, P.E, Fleury P. A Lyons K.B, Cheong S. W, Fisk Z (1990). Light scattering from quantum spin fluctuations in R_2CuO_4 ($R=La, Nd, Sm$). *Physical Review B*. 41. 225.
- Sung-Sik Lee and Patrick A. Lee. (2005). U1 Gauge Theory of the Hubbard Model: Spin Liquid States and Possible Application to $\kappa - (BEDTTTF)_2Cu_2(CN)_3$. *Physical Review Letters* 95, 1-4.
- Tifrea. (2003). Thermodynamic Properties of High-Temperature Superconductors in the Pseudogap Regime. *Journal of Superconductivity*. 16. P 993-999.
- Timusk T, Cao N Basov D N and Homes C C. (1996). *In spectroscopic Studies of Superconductors*, Edited by Ivan Bozovic and Dirk van der Marel, Proc. SPIE 2696 2.
- Th. A. Maier. (2004). On the nature of pairing in the two-dimensional t-J model. *Physical Review B*, 90. 359-361
- T.Sumaryada, Alexander Volya. (2006). *Thermodynamics of pairing in the mesoscopic system*, Bulletin of APS,DNP Meeting, October 2006, Vol.51, p 30.
- Varma,C.M. Schmitt-Rink (1987).Charge transfer excitations and superconductivity in ionic metals *Solid State Communication*. 62(10), 681-685.
- V.I Belinicher and A. L. Cherneysbev. (1994). Range of the t-J model parameters for CuO_2 planes: experimental data constraints. *Physical Review B*. 50, 18.

Wikipedia free encyclopedia. (2015). *The t-J model*. Retrieved on 25th January 2015 from <
<http://en.wikipedia.org/wiki/>>.

Whitten, Davis, Peck & Stanley. (2010). *Chemistry*, 9th edition. Mary Finch
Publishers.London.

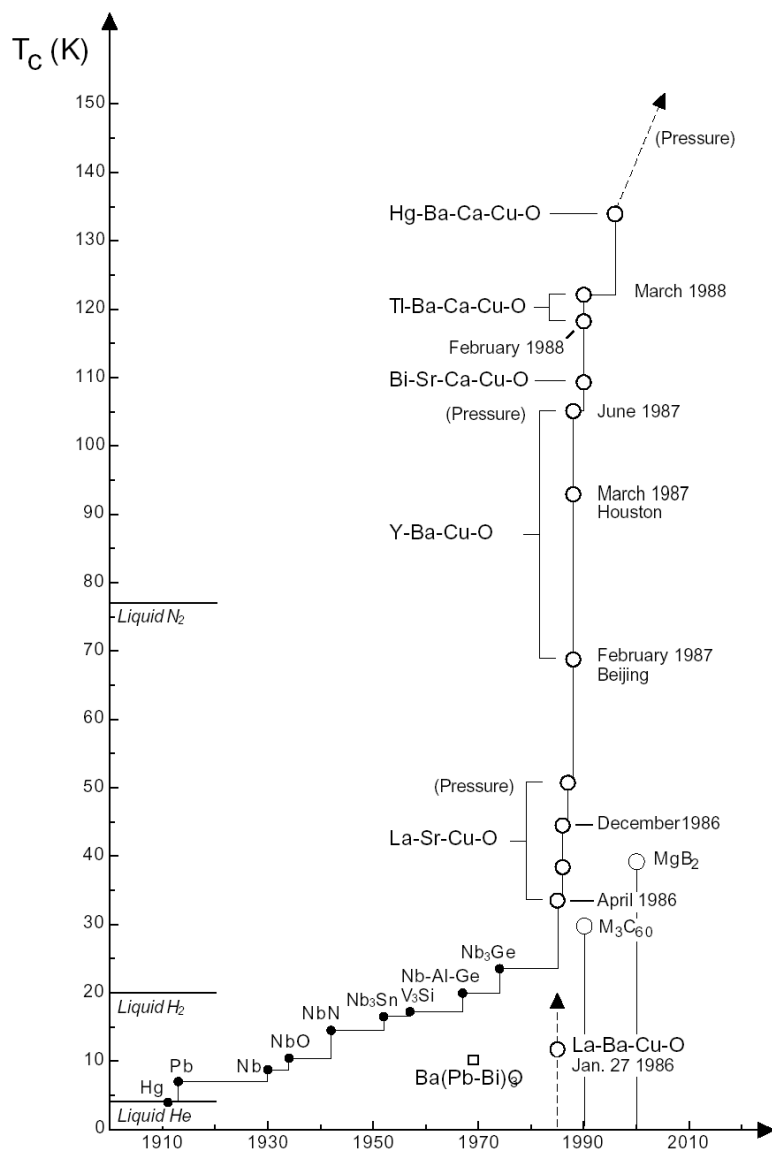
Y.K. Ayodo, T.W Sakwa, K.M. Khanna, B.W Rapando. (2011). The Prospects and
challenges of High Temperature Superconductors. *Journal of Science Technology
Education Management* . 4. 31-41.

Zaanen,J. (1985). *Physical Review Letters*. 55, 418.

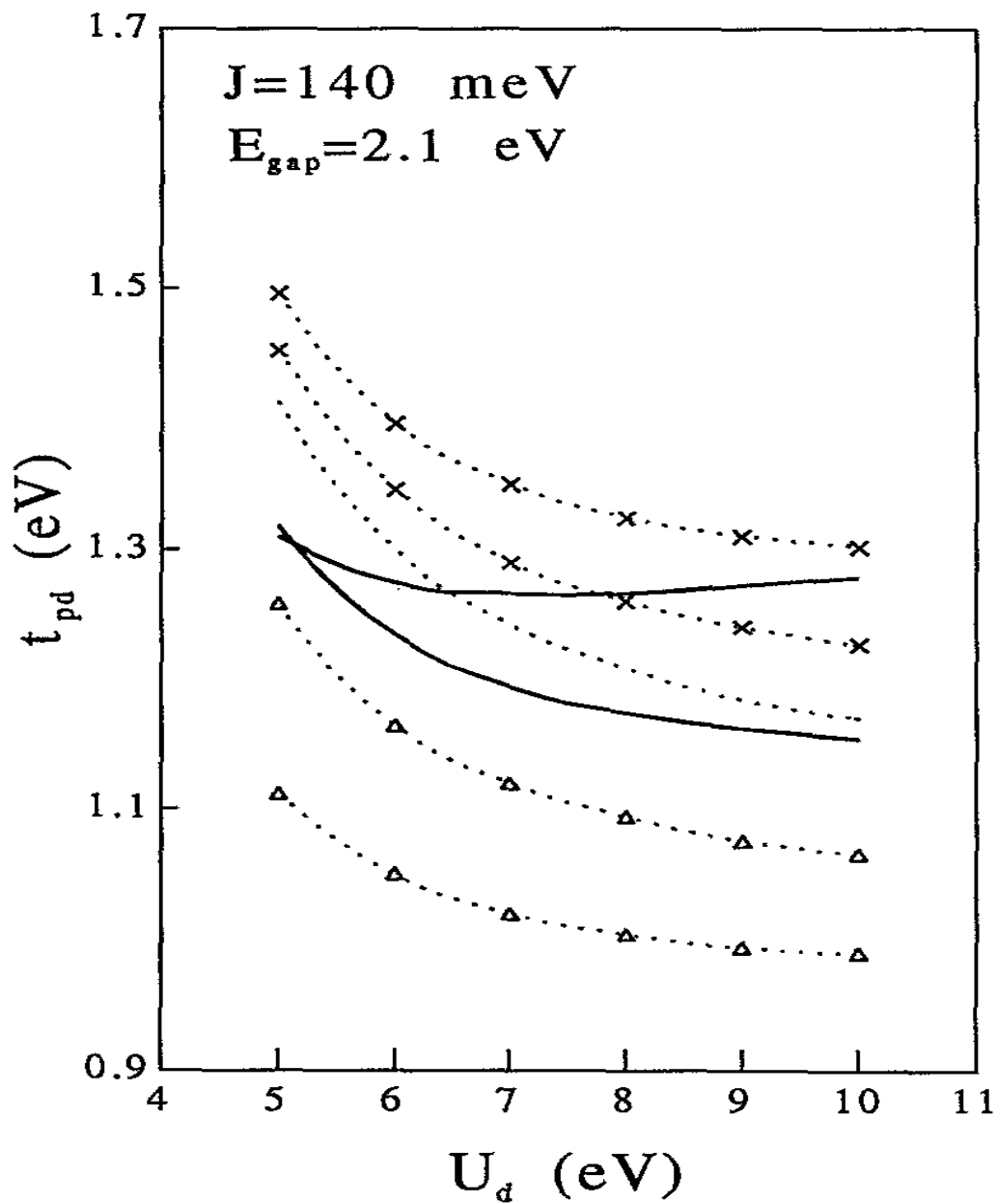
Zhang,F.C.,C.Gros,T.M.Rice and H.Shiba. (1988). A renormalized Hamiltonian approach to
resonant valence bond wave function. *Superconductivity ScienceTechnology*.1, 36-37.

APPENDICES

**Appendix I: CHRONOLOGICAL GROWTH OF T_c IN SUPERCONDUCTORS
(K. Park, 2005)**



Appendix II: VARIATION OF HOPING INTEGRAL t_{pd} WITH ON-SITE COULOMB REPULSION ENERGY, U_d FOR TRANSITIONS FROM P TO D LEVELS (BELINICHER *et al*, 1994)



Appendix III: DIPOLE STATISTICS IN CUPRATES

Due to	O _{1,1}		O _{1,2}	
	$E_z(\text{monopoles})$ [$e/(\text{\AA})^2$]	$E_z(\text{dipoles})$ [$e/(\text{\AA})^2$]	$E_z(\text{monopoles})$ [$e/(\text{\AA})^2$]	$E_z(\text{dipoles})$ [$e/(\text{\AA})^2$]
Bi at (0.000,0.285,0.0514)	0.232	0.003	0.190	0.003
Bi at (0.500,0.715,0.0514)	0.232	0.003	0.190	0.003
Bi at (0.000,0.215,0.4486)	0.019	-0.003	-0.021	-0.003
Bi at (0.500,0.785,0.4486)	0.019	-0.003	-0.021	-0.003
Sr at (0.000,0.773,0.1429)	0.254	-0.002	0.278	0.002
Sr at (0.500,0.227,0.1429)	0.254	-0.002	0.278	0.002
Sr at (0.000,0.727,0.3571)	-0.125	-0.002	-0.154	-0.002
Sr at (0.500,0.273,0.3571)	-0.125	-0.002	-0.154	-0.002
Ca at (0.000,0.750,0.2500)	-0.377	0.000	-0.364	0.000
Ca at (0.500,0.250,0.2500)	-0.377	-0.000	-0.364	0.000
Cu at (0.000,0.262,0.1973)	-0.101	-0.001	0.124	-0.001
Cu at (0.500,0.738,0.1973)	-0.101	-0.001	0.124	-0.001
Cu at (0.000,0.238,0.3027)	-0.252	-0.000	-0.290	-0.000
Cu at (0.500,0.762,0.3027)	-0.252	-0.000	-0.290	-0.000
O(1,1) at (0.250,0.500,0.1892)	0.000	0.010	-0.156	0.032
O(1,1) at (0.750,0.500,0.1892)	0.000	0.040	-0.104	0.022
O(1,1) at (0.250,0.000,0.3108)	0.254	0.008	0.364	0.021
O(1,1) at (0.750,0.000,0.3108)	0.237	0.006	0.289	0.007
O(1,2) at (0.250,0.000,0.2086)	0.130	-0.003	0.000	-0.001
O(1,2) at (0.750,0.000,0.2086)	0.087	-0.002	0.000	-0.004
O(1,2) at (0.250,0.500,0.2914)	0.304	-0.002	0.259	-0.000
O(1,2) at (0.750,0.500,0.2914)	0.241	-0.001	0.220	0.000
O(2) at (0.073,0.920,0.0522)	-0.099	-0.000	-0.086	-0.000
O(2) at (0.427,0.080,0.0522)	-0.099	-0.000	-0.086	-0.000
O(2) at (0.573,0.080,0.0522)	-0.096	-0.000	-0.084	-0.000
O(2) at (0.927,0.920,0.0522)	-0.096	-0.000	-0.084	-0.000
O(2) at (0.073,0.580,0.4478)	-0.008	0.000	0.010	0.000
O(2) at (0.427,0.420,0.4478)	-0.008	0.000	0.010	0.000
O(2) at (0.573,0.420,0.4478)	-0.008	0.000	0.009	0.000
O(2) at (0.927,0.580,0.4478)	-0.008	0.000	0.009	0.000
O(3) at (0.000,0.291,0.1239)	-0.191	0.015	-0.160	0.012
O(3) at (0.500,0.709,0.1239)	-0.191	0.015	-0.160	0.012
O(3) at (0.000,0.209,0.3761)	0.064	-0.019	0.084	-0.019
O(3) at (0.500,0.791,0.3761)	0.064	-0.019	0.084	-0.019
Net	-0.119	0.038	-0.051	0.061
Total		-0.081		0.010

**Appendix IV: TABLES OF
RESULTS FOR THE t-J-d MODEL**

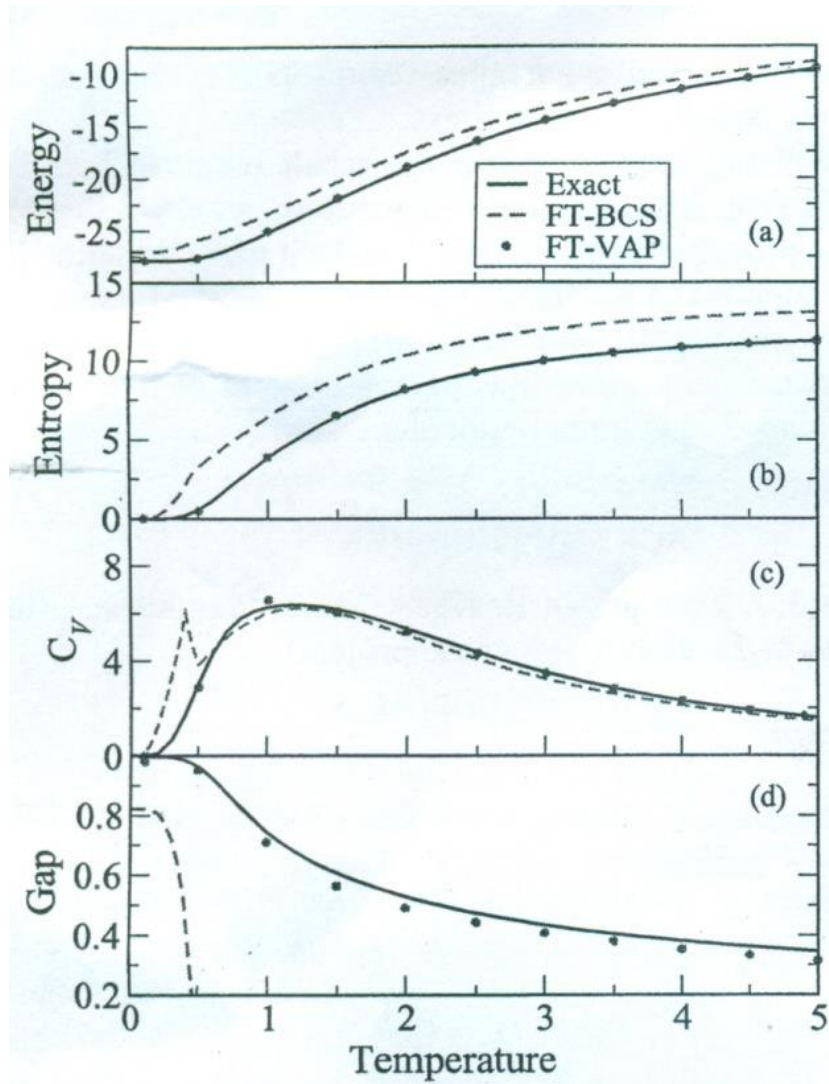
Table of results for variation of specific heat capacity with temperature		
T	Cv-LSCO	Cv-YBCO
1	0	0
2	0	0
3	0	0
10	3.47E-09	6.45E-10
20	2.85E-05	1.34E-05
30	4.05E-04	2.588E4
40	1.29E-03	9.61E-04
50	2.33E-03	1.91E-03
60	3.24E-03	2.82E-03
70	3.90E-03	3.55E-03
80	4.33E-03	4.08E-03
90	4.57E-03	4.41E-03
100	4.67E-03	4.60E-03
110	4.65E-03	4.67E-03
120	4.58E-03	4.66E-03
130	4.46E-03	4.59E-03
140	4.31E-03	4.48E-03
150	4.15E-03	4.35E-03
160	3.97E-03	4.20E-03
170	3.80E-03	4.04E-03
180	3.63E-03	3.88E-03
190	3.46E-03	3.72E-03
200	3.30E-03	3.57E-03
210	3.14E-03	3.41E-03
220	3.05E-03	3.27E-03
230	2.91E-03	3.13E-03
240	2.78E-03	2.99E-03
250	2.65E-03	2.86E-03

Table of results for variation of entropy with temperature		
T	s-LSCO	s-YBCO
1	0	0
2	0	0
3	0	0
10	1.67E-10	2.85E-11
20	2.73E-06	1.18E-06
30	5.83E-05	3.43E-05
40	2.47E-04	1.70E-04
50	5.59E-04	4.21E-04
60	9.32E-04	7.45E-04
70	1.31E-03	1.10E-03
80	1.66E-03	1.44E-03
90	1.97E-03	1.75E-03
100	2.23E-03	2.02E-03
110	2.45E-03	2.26E-03
120	2.63E-03	2.45E-03
130	2.77E-03	2.62E-03
140	2.88E-03	2.75E-03
150	2.97E-03	2.86E-03
160	3.03E-03	2.95E-03
170	3.08E-03	3.01E-03
180	3.11E-03	3.06E-03
190	3.13E-03	3.10E-03
200	3.14E-03	3.12E-03
210	3.14E-03	3.14E-03
220	3.14E-03	4.14E-03
230	3.12E-03	3.14E-03
240	3.11E-03	3.14E-03
250	3.09E-03	3.13E-03

Table of results for variation of temperature with energy		
T	E-LSCO	E-YBCO
1	0	0
2	0	0
3	0	0
20	5.47E-05	2.36E-05
40	7.91E-03	6.79E-03
60	5.70E-02	4.50E-02
80	1.33E-01	1.15E-01
100	2.24E-01	2.03E-01
120	3.17E-01	2.96E-01
140	4.06E-01	3.88E-01
160	4.89E-01	4.75E-01
180	5.65E-01	5.55E-01
200	6.34E-01	6.30E-01
220	6.97E-01	6.98E-01
240	7.55E-01	7.61E-01
260	8.07E-01	0.818
280	8.54E-01	0.87
300	8.97E-01	0.919
320	9.37E-01	0.963
340	9.74E-01	1.004

Appendix V: PREDICTIVE POWER OF FT-VAP (Danilo *et al*, 2012)

- (a) Energy
- (b) Entropy
- (c) Heat capacity
- (d) Average gap



Appendix VI: MATHCAD RESULTS

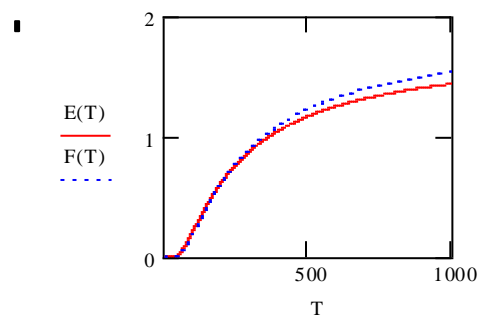
(a) Energy for the t-J model

$T := 1..1000$

$$E(T) := (0.13 + 4 \cdot 0.41) \cdot e^{\left[\frac{-(0.13 + 4 \cdot 0.41)}{0.00863T} \right]}$$

$$F(T) := (0.17 + 4 \cdot 0.44) \cdot e^{\left[\frac{-(0.17 + 4 \cdot 0.44)}{0.00863T} \right]}$$

T =	E(T) =	F(T) =
345	0.977	1.009
346	0.978	1.011
347	0.98	1.013
348	0.982	1.015
349	0.983	1.017
350	0.985	1.019
351	0.987	1.021
352	0.988	1.022
353	0.99	1.024
354	0.992	1.026
355	0.993	1.028
356	0.995	1.03
357	0.996	1.032
358	0.998	1.033
359	1	1.035
360	1.001	1.037



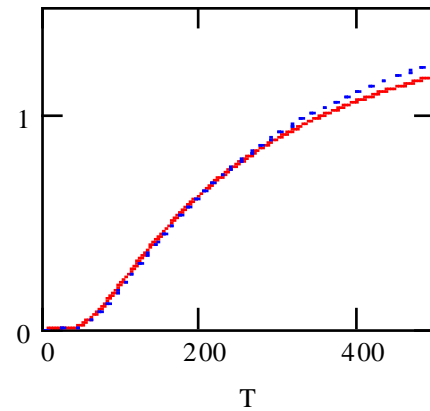
(b) Energy for t-J-d model

$$T := 1..500$$

$$E(T) := 1.7947 \cdot e^{\frac{-207.96}{T}}$$

$$F(T) := 1.9547 \cdot e^{\frac{-226.5}{T}}$$

T =	E(T) =	F(T) =
1	0	0
2	0	0
3	0	0
4	0	0
5	0	0
6	$1.59 \cdot 10^{-15}$	0
7	$2.248 \cdot 10^{-13}$	$1.732 \cdot 10^{-14}$
8	$9.215 \cdot 10^{-12}$	$9.888 \cdot 10^{-13}$
9	$1.655 \cdot 10^{-10}$	$2.298 \cdot 10^{-11}$
10	$1.669 \cdot 10^{-9}$	$2.846 \cdot 10^{-10}$
11	$1.105 \cdot 10^{-8}$	$2.231 \cdot 10^{-9}$
12	$5.342 \cdot 10^{-8}$	$1.241 \cdot 10^{-8}$
13	$2.026 \cdot 10^{-7}$	$5.301 \cdot 10^{-8}$
14	$6.351 \cdot 10^{-7}$	$1.84 \cdot 10^{-7}$
15	$1.71 \cdot 10^{-6}$	$5.41 \cdot 10^{-7}$
16	$4.067 \cdot 10^{-6}$	$1.39 \cdot 10^{-6}$



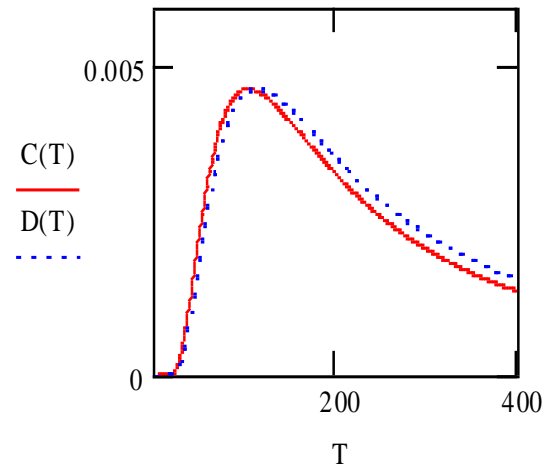
(c) Heat capacity for the t-J model

T := 1..500

$$C(T) := \left[\frac{(0.13 + 4 \cdot 0.41)^2}{0.00863 \cdot T^2} \right] \cdot e^{\frac{-(0.13 + 4 \cdot 0.41)}{0.00863 T}}$$

$$D(T) := \left[\frac{(0.17 + 4 \cdot 0.44)^2}{0.00863 \cdot T^2} \right] \cdot e^{\frac{-(0.17 + 4 \cdot 0.44)}{0.00863 T}}$$

T =	C(T) =	D(T) =
1	0	0
2	0	0
3	0	0
4	0	0
5	0	0
6	$1.439 \cdot 10^{-14}$	0
7	$1.396 \cdot 10^{-12}$	$1.175 \cdot 10^{-13}$
8	$4.165 \cdot 10^{-11}$	$4.879 \cdot 10^{-12}$
9	$5.681 \cdot 10^{-10}$	$8.609 \cdot 10^{-11}$
10	$4.494 \cdot 10^{-9}$	$8.368 \cdot 10^{-10}$
11	$2.397 \cdot 10^{-8}$	$5.282 \cdot 10^{-9}$
12	$9.524 \cdot 10^{-8}$	$2.415 \cdot 10^{-8}$
13	$3.022 \cdot 10^{-7}$	$8.631 \cdot 10^{-8}$
14	$8.041 \cdot 10^{-7}$	$2.543 \cdot 10^{-7}$
15	$1.86 \cdot 10^{-6}$	$6.426 \cdot 10^{-7}$
16	$3.843 \cdot 10^{-6}$	$1.434 \cdot 10^{-6}$



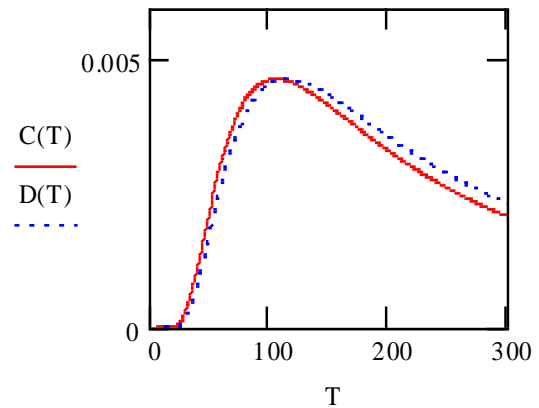
(d) Heat capacity for the t-J-d model

$$T := 1..300$$

$$C(T) := \left[\frac{[(0.13 + 4 \cdot 0.41 + 6 \cdot 0.0041139)^2]}{0.00863T^2} \right] \cdot e^{\frac{-(0.13 + 4 \cdot 0.41 + 6 \cdot 0.0041139)}{0.00863T}}$$

$$D(T) := \left[\frac{[(0.17 + 4 \cdot 0.44 + 6 \cdot 0.0041139)^2]}{0.00863T^2} \right] \cdot e^{\frac{-(0.17 + 4 \cdot 0.44 + 6 \cdot 0.0041139)}{0.00863T}}$$

T =	C(T) =	D(T) =
1	0	0
2	0	0
3	0	0
4	0	0
5	0	0
6	9.186·10 ⁻¹⁵	0
7	9.541·10 ⁻¹³	8.008·10 ⁻¹⁴
8	2.995·10 ⁻¹¹	3.5·10 ⁻¹²
9	4.251·10 ⁻¹⁰	6.427·10 ⁻¹¹
10	3.471·10 ⁻⁹	6.448·10 ⁻¹⁰
11	1.9·10 ⁻⁸	4.177·10 ⁻⁹
12	7.715·10 ⁻⁸	1.952·10 ⁻⁸
13	2.493·10 ⁻⁷	7.105·10 ⁻⁸
14	6.739·10 ⁻⁷	2.126·10 ⁻⁷
15	1.58·10 ⁻⁶	5.447·10 ⁻⁷
16	3.304·10 ⁻⁶	1.23·10 ⁻⁶



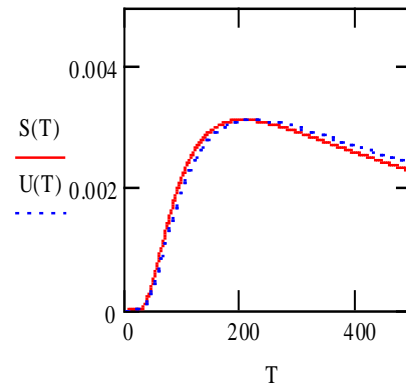
(e) Entropy for the t-J model

$$T := 1..500$$

$$S(T) := \left[\left[\frac{(0.13 + 4 \cdot 0.41)}{T} \right] \cdot e^{\frac{-(0.13 + 4 \cdot 0.41)}{0.00863T}} \right] - 0.0000863 e^{\frac{-(0.13 + 4 \cdot 0.41)}{0.00863T}}$$

$$U(T) := \left[\left[\frac{(0.17 + 4 \cdot 0.44)}{T} \right] \cdot e^{\frac{-(0.17 + 4 \cdot 0.44)}{0.00863T}} \right] - 0.0000863 e^{\frac{-(0.17 + 4 \cdot 0.44)}{0.00863T}}$$

T =	S(T) =	U(T) =
1	0	0
2	0	0
3	0	0
4	0	0
5	0	0
6	0	0
7	$4.764 \cdot 10^{-14}$	$3.676 \cdot 10^{-15}$
8	$1.624 \cdot 10^{-12}$	$1.745 \cdot 10^{-13}$
9	$2.492 \cdot 10^{-11}$	$3.463 \cdot 10^{-12}$
10	$2.19 \cdot 10^{-10}$	$3.74 \cdot 10^{-11}$
11	$1.285 \cdot 10^{-9}$	$2.597 \cdot 10^{-10}$
12	$5.569 \cdot 10^{-9}$	$1.295 \cdot 10^{-9}$
13	$1.914 \cdot 10^{-8}$	$5.014 \cdot 10^{-9}$
14	$5.485 \cdot 10^{-8}$	$1.591 \cdot 10^{-8}$
15	$1.359 \cdot 10^{-7}$	$4.307 \cdot 10^{-8}$
16	$2.995 \cdot 10^{-7}$	$1.025 \cdot 10^{-7}$



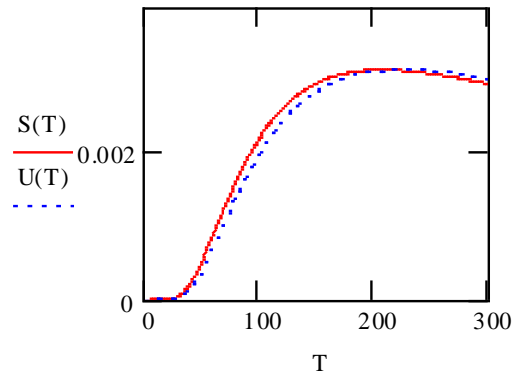
(f) Entropy for the t-J-d model

$$T := 1..300$$

$$S(T) := \left[\frac{((0.13 + 4 \cdot 0.41 + 6 \cdot 0.0041139))}{T} \right] \cdot e^{\frac{-0.13 + 4 \cdot 0.41 + 6 \cdot 0.0041139}{0.00863T}} - 0.0000863 e^{\frac{-0.13 + 4 \cdot 0.41 + 6 \cdot 0.0041139}{0.00863T}}$$

$$U(T) := \left[\frac{(0.17 + 4 \cdot 0.44 + 6 \cdot 0.0041139)}{T} \right] \cdot e^{\frac{-0.17 + 4 \cdot 0.44 + 6 \cdot 0.0041139}{0.00863T}} - 0.0000863 e^{\frac{-0.17 + 4 \cdot 0.44 + 6 \cdot 0.0041139}{0.00863T}}$$

T =	S(T) =	U(T) =
1	0	0
2	0	0
3	0	0
4	0	0
5	0	0
6	0	0
7	$3.21 \cdot 10^{-14}$	$2.474 \cdot 10^{-15}$
8	$1.152 \cdot 10^{-12}$	$1.236 \cdot 10^{-13}$
9	$1.839 \cdot 10^{-11}$	$2.553 \cdot 10^{-12}$
10	$1.668 \cdot 10^{-10}$	$2.846 \cdot 10^{-11}$
11	$1.004 \cdot 10^{-9}$	$2.028 \cdot 10^{-10}$
12	$4.449 \cdot 10^{-9}$	$1.034 \cdot 10^{-9}$
13	$1.558 \cdot 10^{-8}$	$4.076 \cdot 10^{-9}$
14	$4.534 \cdot 10^{-8}$	$1.314 \cdot 10^{-8}$
15	$1.139 \cdot 10^{-7}$	$3.605 \cdot 10^{-8}$
16	$2.54 \cdot 10^{-7}$	$8.684 \cdot 10^{-8}$



Appendix VII: Critical Temperature and transfer energy for t-J-d model.

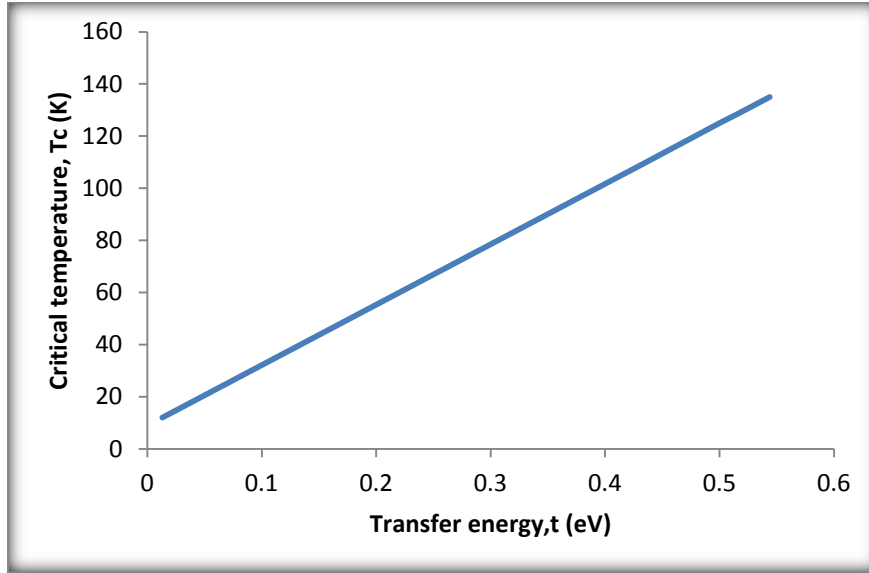


Figure 6.2: Variation of critical temperature with transfer energy.

Table of constants used

Quantity	Magnitude
Angstrom(Å)	1Å = 1.0×10 ⁻¹⁰ M
Electron charge(e)	e = 1.6×10 ⁻¹⁹ C
Electron mass(M _e)	M _e = 9.1×10 ⁻³¹ Kg
Electron-Volt (eV)	1eV = 1.6×10 ⁻¹⁹ J
Proton mass(M _p)	M _p = 1.673×10 ⁻²⁷ Kg
Reduced Planck's constant(ħ)	ħ = 1.055×10 ⁻³⁴ J _s
Exchange energy, (J)for LSCO	J= 0.13eV
Exchange energy, (J)for YBCO	J=0.17 eV
Bipolaron exchange energy for cuprates(J _p)	J _p =1eV
Boltzmann constant(k _B)	k _B = 8.63×10 ⁻⁵ eVK ⁻¹
On-Site Energy U, at maximum T _c	U = 1-2eV
Hopping energy t for Hole-doped Cuprates	t=0.44eV
Hopping energy t for electron-doped Cuprates	t=0.41eV
Hopping energy t for YBCO	t=0.609 eV
Superconducting order parameter of YBCO at T= 87.9K	Δ=0.00156 eV
Fermi energy of YBCO	E _f =0.23 eV